International Journal of Computer Science in Sport

Volume 10/2011/Edition 2

TABLE OF CONTENTS

Arnold Baca
Editorial 3

RESEARCH PAPERS

Minh Vu Huynh & Anthony Bedford
An Analysis of the Skills Acquisition Trainer for Badminton Program: Exploring the Effectiveness of Visual Based Training in Sport 5

Thorsten Dahmen & Dietmar Saupe
Calibration of a Power-Speed-Model for Road Cycling Using Real Power and Height Data 18

SCIENTIFIC REPORTS

Josef Wiemeyer & Regine Angert
Computer Methods to Assess Motor Imagery 37

Ihor Zanevskyy
Mathematical and Computer Model of Sport Archery Bow and Arrow Interaction 54

PROJECT REPORTS

Nina Schaffert & Klaus Mattes
Designing an Acoustic Feedback System for On-Water Rowing Training 71

Jürgen Perl & Daniel Memmert
Net-Based Game Analysis by Means of the Software Tool *SOCCER* 77

Jürgen Perl & Mark Pfeiffer
PerPot DoMo: Antagonistic Meta-Model Processing two Concurrent Load Flows 85

LETTER TO THE EDITOR

Robin R. Mellecker, Richard Coshott
Perspectives on Exergaming 93

Editorial

Arnold Baca

Department of Biomechanics, Kinesiology and Applied Computer Science,

ZSU, University of Vienna

Dear readers:

Welcome to the winter 2011 issue of the **International Journal of Computer Science in Sport (IJCSS).**

Two research papers, two scientific reports, three project reports and a "Letter to the Editor" have been included within this issue.

The investigations made by **Minh Vu Huynh** and **Anthony Bedford** evaluate the application of a software tool and its efficiency in predicting the level of badminton players as well as improving their anticipatory techniques.

Thorsten Dahmen and **Dietmar Saupe** discuss a parameter calibration model specifying the correlation of pedaling power and speed in road cycling.

Josef Wiemeyer and **Regine Angert** introduce a computer-aided selection test (CAST) for the assessment of visual and verbal components of motor imagery.

A mathematical model for the bow and arrow interaction in archery solved on the basis of Lagrange and Runge-Kutta methods is included in the contribution by **Ihor Zanevskyy**.

The paper by **Nina Schaffert** and **Klaus Mattes** presents an acoustic feedback system integrating boat acceleration and GPS data. It aims at the monitoring and control of the boat motion during on-water training sessions in rowing.

Jürgen Perl and **Daniel Memmert** illustrate a net-based implementation for the analysis of tactical behavior in game sports such as soccer.

In his second paper within this issue, **Jürgen Perl** demonstrates together with **Mark Pfeiffer** an approach combining two concurrent load flows based on the so-called PerPot model for the recognition of fatigue as well as recovery and the scheduling of long time training.

The issue concludes with a "Letter to the Editor" by **Robin R. Mellecker and Richard Coshott** giving an outlook on current applications and future scenarios for the field of active gaming.

If you have any questions, comments, suggestions and points of criticism, please send them to me.

Best wishes for 2012!

Arnold Baca, Editor in Chief
University of Vienna, arnold.baca@univie.ac.at

An Analysis of the Skills Acquisition Trainer for Badminton Program: Exploring the Effectiveness of Visual Based Training in Sport

Minh Vu Huynh & Anthony Bedford

The Royal Melbourne Institute of Technology, Australia

Abstract

This study examined the use of the Skills Acquistion Trainer for Badminton (SATB) software as a visual based training (VBT) method for a group of 41 participants. Using this program, we identified the athlete's skill level and awareness, and attempted to improve their overall in-game performance and decision making skills. Three different types of analyses were conducted on the SATB over the ten weeks of experimentation. Firstly, discriminant analysis was used to assess the accuracy that the SATB program had in classifying participants into the correct skill level groups. Secondly, a repeated measures ANOVA was carried out to examine the changes in score over the ten weeks of experimentation. Finally, a Pearson's correlation was carried out to examine the linear dependence between SATB variables and motor fitness constructs. The results from this study revealed three main findings: (1) the program was successful in predicting group membership among badminton players, with an accuracy of 87.8%, (2) players demonstrated a significant improvement on anticipatory techniques and (3) skill level was significantly correlated with SATB constructs. Overall, this study demonstrates the effectiveness of VBT in sport, and discusses the implications of perceptual skill acquisition and development.

KEYWORDS: BADMINTON, TRAINING, SKILLS ACQUISITION

Introduction

Badminton is the world's fastest racket sport, with a top speed of 421km/h. Because it is such a fast paced sport, the importance of swift decision making has become imperative for top level badminton players, and the need for athletes to train and improve their ability to instantaneously determine the best course of action has become essential. However, improving an individual's capacity for decision making is more complex and detailed (Macquet and Fleurance, 2007; Huynh and Bedford, 2010) than improving physical abilities such as strength or agility. In attempting to optimise an athlete's competency, the development of a training program that incorporates the improvement of reaction time and awareness in juxtaposition with physical performance would be ideal (Huynh and Bedford, 2010).

Typically, coaches and trainers place heavy emphasis on the movement execution component of the traditional training method (Blomqvist, Luhtanen and Laakso, 2001) and tend to overlook the significance of the cognitive processes of perception and decision-making. This is unfortunate considering that the quality of decision-making in a game situation is often as important as the execution of the motor skills (Blomqvist, Luhtanen and Laakso, 2001; Thomas, 1994). While it is essential that athletes continuously train and improve their physical

capabilities (Chin, Wong, So, Siu, Steininger and Lo, 1995; Fahlstrom, Lorentzon and Alfredson, 2002), it seems evident that the cognitive components of badminton must not be underemphasised when training athletes (Blomqvist, Luhtanen and Laakso, 2001). In developing and improving decision making, the ideal strategy would be to expose the athlete to all possible situations and scenarios that they may face. This allows them to retain certain responses within their subconsciousness; leading their bodies to instantaneously execute an appropriate action when similar situations arise (Hall, Schmidt, Durand and Buckolz, 1994).

In attempting to train and improve badminton players, Huynh and Bedford (2010) argue cognitive components of badminton must be considered. The authors suggest that in attempting to optimise skill proficiency, athletes need to incorporate a combination of both physical and cognitive aspects into their training program. They introduced a new visual based training (VBT) method of identifying and improving a badminton player's reaction time and awareness: the Skills Acquisition Trainer for Badminton (SATB). Utilising this program, the researchers stated that the badminton players were able to improve their reaction time, awareness and decision making skills by noticing the visual cues other players make when executing an action.

Previous research involving VBT has shown that the ability to detect and utilise advanced visual cues allows players to predict their opponent's actions more accurately. A classic example of this can be found in Abernethy and Russell's (1987) study regarding the differences between the ability of experts and novice to discriminate visual cues. The research suggested that novice badminton players were unable to detect information regarding advanced cue sources, which is the ability that provides experts with superior anticipatory skills. Specifically, the researchers stated that experts would utilise the visual cues from their opponent's *racket and arm placement* to predict stroke direction and speed, whereas novices were only capable of extracting advance information from the racket itself.

In a more recent study, Blomqvist, Luhtanen and Laakso (2001) compared the effects of two different forms of instructional training (traditional and visual based) on the knowledge and game performance of badminton players. They showed that by utilising a VBT method, they were able to improve the badminton knowledge, game understanding and serving skills of badminton players. The results of the study suggest that using a visual based style of training is highly effective in developing the cognitive aspects of a badminton player's game (e.g. their decision making skills). Participants in the traditional group (non-VBT) only improved their serving skills, suggesting that the traditional method of training is inadequate for optimising both physical and cognitive skills. Research regarding VBT and detecting visual cues for other sports has also shown similar results.

Renshaw and Fairweather (2000) utilised a visual based method to examine expertise among cricket players by assessing verbal discrimination when faced with five different types of bowling deliveries. They showed that expert batters were more successful than novices in identifying different types of deliveries made by an expert wrist-spin bowler. The overall detection rates in this study were significantly different between national, regional and club cricket players. National players correctly identified 63% of deliveries, regional players identified 56%, and club players correctly identified 48% of overall deliveries. However, when examining this discrimination capability for types of delivery, the authors found that batters were less able to discriminate deliveries that were similar in nature, regardless of expertise. Renshaw and Fairweather (2000) explained this poor discrimination ability due to the deliveries that were similar in nature to the legspin delivery (i.e. topspin and backspin). Similarly in badminton, the many different shot types used have similar appearances in

execution, and may generally only be differentiated during the last few milliseconds prior to the racket making contact with the shuttle.

In squash, the utilisation of VBT methods has also shown significant results for improving anticipatory skills. Abernethy, Wood and Parks (1999) demonstrate the way in which perceptual training can be used to detect visual cues in squash players. In their study, participants received one of three training methods for four weeks of experimentation: (1) perceptual and motor practice training, (2) supervised and motor practice training, and (3) just motor practice training. The perceptual training consisted of a series of instructions, video sequences and simulated practice. The supervised training consisted of reading racquet sport coaching manuals and watching videotape replays of top-level tennis matches. After the four weeks of training, participants were assessed on anticipatory skills using the temporal occlusion task devised by the author in a previous study (Abernethy, 1990). Overall, the researchers suggested that novices are able to acquire expert-like anticipatory skills using a training program that incorporates perceptual training in conjunction with motor practice.

These research studies lead us to predict that perceptual training early in an athletes skill development will prove beneficial for their anticipatory skills in the long run. However, this is not to say that VBT methods would be more efficient than, or that they should replace, the standard training regimines of physical training. In a practical sense, adapting a perceptual strategy which emulates an expert will not bring a novice to that level simply by forcing the model onto them (Abernethy and Russell, 1987). From a dynamic systems approach, these types of visual imagery training would be insufficient (Renshaw and Fairweather, 2000) unless coupled with a form of physical practice. Ideally, it is the combination of both visual training and motor practice that will enhance overall perceptual performance. Furthermore, with the digital age constantly developing, and the nature in which Gen-Z children are raised and taught through digital means (Mitchell, 2008; Tapscott, 2008; Howe and Strauss, 2008), the use of a VBT method to train athletes (e.g. the SATB program) should prove not only effective but also stimulating for athletes of the future.

Research in the field of digital learning has generally shown positive outcomes (Musgrove and Musgrove, 2004; Yelland and Lloyd, 2001; Riel and Schwarz, 2002) with many studies suggesting such methods to be beneficial and rewarding for children as young as five. Downes, Arthur and Beecher (2001) argue that the integration of digital learning in conjunction with traditional methods would provide a powerful framework for learning and development. The researchers reviewed the use of digital learning within a primary school environment for a group of students under eight years of age. They stated that a learning environment needs to be progressively layered so that children can actively investigate and satisfy their learning focus. Thus, the introduction of digital learning in early childhood allows for accurate interpretation of visual based imagery in other programs.

Daniels (2004) examined the use of technology to improve the writing skills of elementary school students. The researcher showed that over the duration of one year, the use of digital technology increased the proficiency rating of 5^{th} grade children from 16.7% to 54.3%. The author suggests that the improvement in writing skill was accredited to both digital learning and appropriate instructions from the educator. Despite the effectiveness of technology and digital learning, human guidance and intelligence in terms of facilitating the learning process should not be rendered redundant too hastily (Blahous, Dybdahl and Shaw, 1997). In a similar sense, when training athletes using visual based methods, the instructions and training of coaches in the traditional manner must still be reinforced.

In a similar study Nir-Gal and Klein (2004) examined the effect of digital learning on the cognitive performance on children aged 5 to 6. They indicated that children who engaged in adult-mediated computer activities improved the level of cognitive performance on measures of abstract thinking, planning ability, vocabulary, and visual-motor coordination. Additionally, the research revealed that children who were a part of the mediated group learned to use planning strategies more frequently than children in the control group (who alternatively relied on trial and error) to solve problems. Nir-Gal and Klein (2004) argued that, by utilising planning strategies, the students in the computer learning group were able to obtain a higher number of correct answers on various cognitive and motor tests, compared to students who only received verbal instructions. Ultimately, the researchers concluded that the integration of digital learning devices improved the awareness and decision making capabilities of students, as well as providing them with insight into their own learning processes.

These research studies demonstrate the effectiveness of visual based training and learning methods, particularly with the younger generation. The utilisation of a VBT method to acquire skills and knowledge has shown to be both rewarding and stimulating. As such, the SATB training program was designed to incorporate the visual stimulants and ease of use that appeal to the future generation of athletes. Using this program we will attempt to discriminate badminton players on skill level, with the focus of training the novice players to become aware of the visual cues which supply experts with their superior anticipatory techniques.

Striking a badminton shuttle requires precise prospective control of the interceptive action and must be prepared in advance to allow the body time to organize. Learning to anticipate moving objects is a difficult task and not easily mastered unless given an appropriate form of training. As such, the ability to anticipate approaching objects and when they will reach a desired goal or target is of particular importance in any fast paced sport. This leads us to believe that this type of research will be beneficial for improving the anticipatory skills of athletes of the future, due to their familiarity with digital technology.

The aim of the present study was firstly, to examine the accuracy of the SATB program in classifying participants into the correct skill level groups via discriminant analysis. The second task was to use a repeated measures ANOVA to examine whether participants were able to improve their anticipatory skills over the ten weeks of experimentation. Finally, a Pearson's correlation was carried out to examine the linear dependence between SATB variables and motor fitness variables. Using these outcomes, in conjunction with the physiological and biomechanical variables of the participants, we will assess the authenticity and accuracy of the SATB and comment on the overall effectiveness of the VBT approach to training badminton athletes.

Method

Participants

The participants for this study comprised of novice players (N = 15), intermediate players (N = 15), and expert players (N = 10). Participants were recruited from RMIT, badminton clubs, and the Australian Badminton Olympic team. All college students had prior experience in playing badminton, with most having played in high school round robins. In order to categorise participants into the appropriate skill level groups two factors were considered. Firstly, the participant's performance on a knowledge measures test (KMT) was used to evaluate their comprehension and awareness of badminton rules, strategies and techniques. The KMT used in

this study was a simplified version of McGee and Farrow's (1987) classic book "Test questions for physical education activities." Particpants were scored on how quickly and accurately they could differentiate shot types and rules utilised in badminton. Figure 1 and Figure 2 provide examples of the types of questions incorported in the KMT.

Measures

The SATB program that we recently introduced (Huynh and Bedford, 2010) is a VBT program which can be run from any compatible operating system. Its primary function is to assess participants' reponses as to measure their ability to estimate and predict shot types and direction in badminton. Participants would watch different clips of badminton rallies being played, with sequences running for 2 – 30s. This was followed by a still frame for 1 second after which participants would be asked to select the type of shot that was about to take place (e.g. drop shot) as well as the location that shot would be played (e.g. middle right). An example of this is shown in Figure 2 with the corresponding answer options.

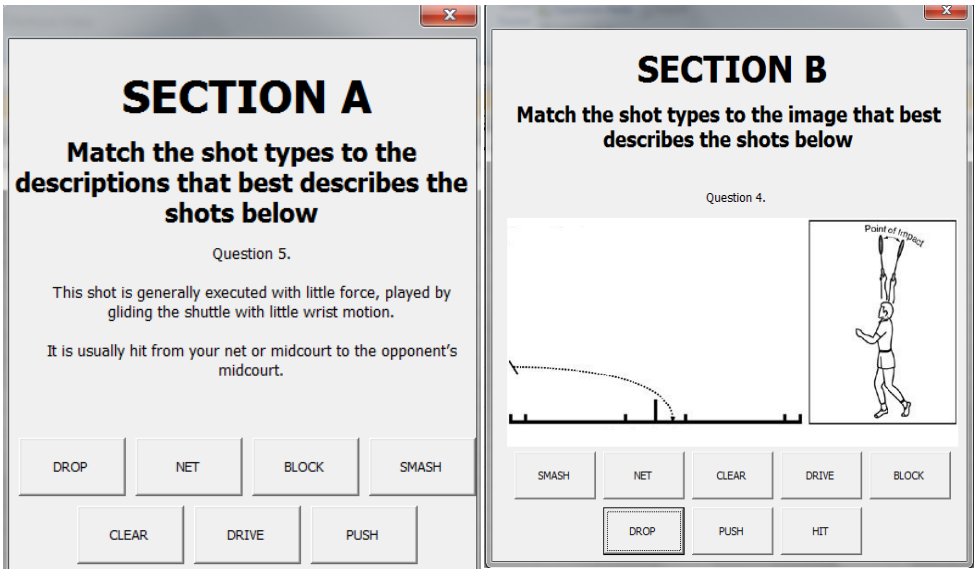

Figure 1. Sample questions used in the knowledge measures test for this study.

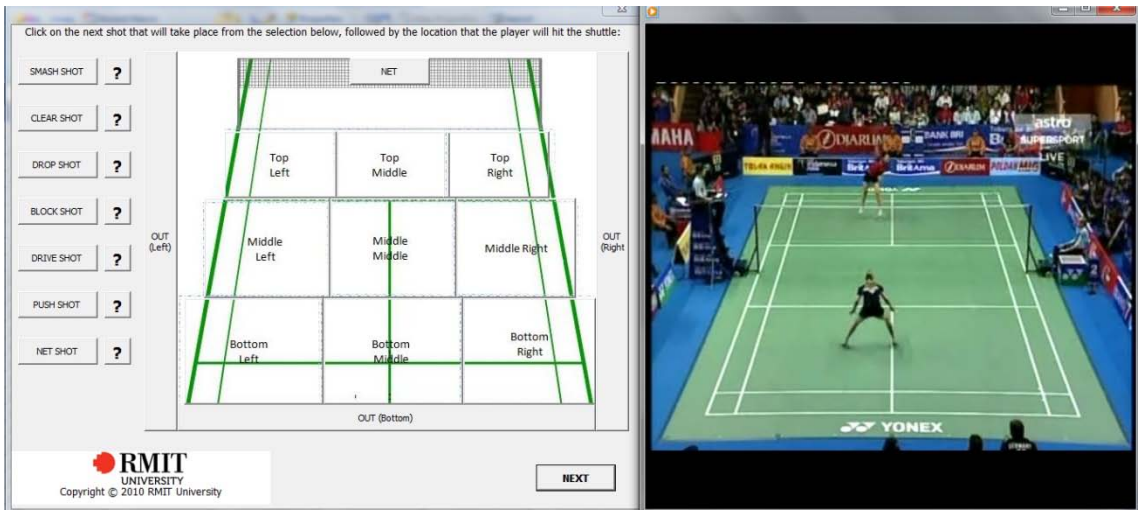

Figure 2. A screenshot of a sample question on the SATB.

Procedure

Participants were tested before and after the treatment period (the 10 weeks of experimentation using the SATB program) for shot type knowledge and speed using the KMT. Afterwards, participants were also administered the SATB once a week for ten weeks to examine their awareness, decision making and response time. Each sequence on the SATB was different, with varying lengths between 2-30s. Participants' performance in-game was also recorded on a weekly basis to determine if skills learnt could be applied in a live match. These video recordings were filmed at the Melbourne Sports and Aquatic Center (MSAC). Typically, these ran for an hour per week, with the researcher imitating various scenarios from the video sequences.

The SATB was based on a weighted system, with the assistance of experts' judgement and opinion (coaches and trainers who have played and taught for many years). Two points were awarded for the correct shot type response, one point for other possible shot types in that situation, and no points for any other shot types. Similarly, two points were given if participants chose the correct location the shuttle would land, one point if it was adjacent to the shuttle location, and no points for any other location selection. Participants were also timed from the point the rally sequence finishes to the point they had inputted their response to shot type and location in order to examine response time. As there were five questions per session, the maximum score a participant could acquire was 20, with an optimal time of 11.9s. Hence, the equation for the SATB score is given by:

$$SATB = \frac{11.9}{TIME} \times SCORE \qquad (1)$$

From equation 1, *TIME* is the combined time it took participants to answer all five questions regarding shot type and shuttle location. The value of 11.9 was based on Jorgensen, Garde, Laursens and Jensen's (2002) study "*Using mouse and keyboard under time pressure: preferences, strategies and learning*" (a click response time = 1.1±0.08 s), in conjunction with experts' opinion that it would take 2s to select both location and shot type. *SCORE* is the combined score of each correct response from the five questions. Therefore the maximum score an individual can acquire on the SATB is 20.

It is worth noting that the purpose of this type of training is not to replace the standard procedures of physical development, rather, to be integrated as an addition to their current training. As such, the current training tasks (e.g. on court traning) is different to the measuring task (the SATB). Participants would continue their regular on court training, whilst attempting the program on a weekly basis. This integrated style of training forms the basis of our new training program.

Results

The first task of this study was to apply discriminant analysis to the results collected from the SATB program and examine whether it was successful in categorising participants into the correct skill level groups. Skill level served as the dichotomous classification variable. The dependent variables in the analysis were represented by three different groups of factors: anthropometric factors, motor fitness factors and SATB factors. The anthropometric factors were height (cm), weight (kg), age (years), and experience (years); the motor fitness factors were 20m sprint (s), vertical jump (cm), and beep test (score); and the SATB factors were shot

type (score), court placement (score), and response time (s).

Results indicated discriminant analysis was effective in classifying ability level when using the SATB specific tests, however slightly less accurate when using the motor fitness tests. The motor fitness tests produced 73.2% (Wilks' Lambda = .36, $p < .001$) and SATB specific tests produced 87.8% (Wilks' Lambda = .19, $p < .001$) correct classifications, respectively. The means and standard deviations for the 20m sprint, beep test, and vertical jump tests are displayed in Table 1, with higher skill level participants displaying higher scores on the vertical jump and beep tests, and lower scores on the sprint tests. Table 2 indicates the accuracy of classification based on motor fitness constructs. In this model 73.2% of all three ability groups were classified correctly.

Table 1. Means and standard deviations for beginner, intermediate and advanced groups based on motor fitness. variables.

	Sprint test		Beep test		Vertical jump test	
	M	*SD*	*M*	*SD*	*M*	*SD*
Beginner	4.34	.37	7.74	1.98	58.67	9.31
Intermediate	3.86	.29	8.61	1.84	64.88	6.84
Advance	3.41	.19	9.82	1.25	64.01	6.61

Table 2. Classification results where 73.2% of original group cases correctly classified for the motor contructs.

		Predicted Group Membership			Total
		1	2	3	
Count	1. Beginner	11	4	0	15
	2. Intermediate	2	12	2	6
	3. Advanced	0	3	7	10
Count %	1. Beginner	73.3%	26.7%	0.00%	100.0%
	2. Intermediate	12.5%	75.0%	12.5%	100.0%
	3. Advanced	0.00%	30.0%	70.0%	100.0%

The means and standard deviations for the SATB specific tests: shot type, court placement and response time are displayed in Table 3. Once again, the scores are higher for those of a higher skill level when compared to those of a lower skill level. The timed score for the SATB response time reflects that a lower score is equated with higher ability on these tests. Table 4 displays the classification function coefficients for the beginner, intermediate and advanced groups, which enable derivation of the function scores for each skill level group. The values in Table 9 represent unstandardised classification coefficients. Table 10 indicates the accuracy of classification based on SATB specific constructs. The classification accuracy was 87.8% (Wilks' Lambda = .19, $p < .001$) correct classifications.

Table 3. Means and standard deviations for beginner, intermediate and advanced badminton athletes based on SATB variables.

	Shot type		Location		Time response	
	M	*SD*	*M*	*SD*	*M*	*SD*
Beginner	1.80	0.94	0.87	0.92	89.54	38.99
Intermediate	5.06	1.34	3.38	1.59	72.34	16.05
Advance	6.20	1.48	4.20	2.20	41.08	21.06

Table 4. Classification results where 87.8% of original grouped cases correctly classified for the SATB constructs.

		Predicted Group Membership			Total
		1	2	3	
Count	1. Beginner	14	1	0	15
	2. Intermediate	1	15	0	16
	3. Advanced	0	3	7	10
Count %	1. Beginner	93.3%	6.7%	0.0%	100.0%
	2. Intermediate	6.3%	93.8%	0.0%	100.0%
	3. Advanced	0.0%	30.0%	70.0%	100.0%

Our second task was to examine whether participants had improved their anticipatory skills over the ten weeks of experimentation, by utilising a repeated measures ANOVA. Assumptions of normality, homogeneity of variance and sphericity were met for all analyses. Results showed that differences between conditions were unlikely to have arisen by sampling error for the beginner ($F(9,81) = 59.19$, $p < .001$), intermediate ($F(9,81) = 79.2$, $p < .001$) and advanced ($F(9,81) = 88.88$, $p < .001$) groups. An overall effect size (partial η^2) showed that 81%, 84% and 91% of the variation in score can be accounted for by improvement over time across the three groups respectively. Figure 3 represents the change in score across the ten weeks of experimentation for the three skill level groups.

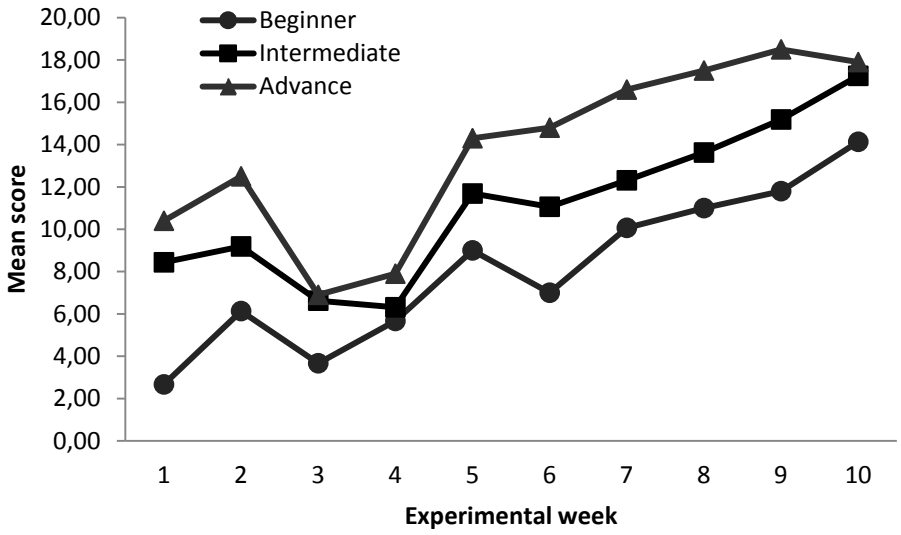

Figure 3. The change in score for the SATB for the three skill level groups across the ten week experimental period.

A second repeated measures ANOVA was carried out to examine the change in time across the ten weeks of experimentation. Results showed that differences between conditions were unlikely to have arisen by sampling error for the beginner ($F(9,81) = 31.11$, $p < .001$), intermediate ($F(9,81) = 39.93$, $p < .001$) and advanced ($F(9,81) = 15.22$, $p = .001$) groups. An overall effect size (partial η^2) showed that 69%, 73% and 63% of the variation in score can be accounted for by improvement over time across the three groups respectively. Figure 4 represents the change in time across the ten weeks of experimentation for the three skill level groups.

Our final analysis for this study was to carry out a Pearson's correlation to examine the linear dependence between SATB variables and motor fitness variables. Results indicated a strong positive correlation between skill level and the SATB factors of shot type and location type ($r = .80$, $p < .01$ and $r = .65$, $p < .01$ respectively). A similar strong negative correlation ($r = -.56$, $p < .01$) was observed for skill level and time, suggesting that the higher a participants skill level, the less time is required to select an answer. Table 5 summarises the Pearson's correlation.

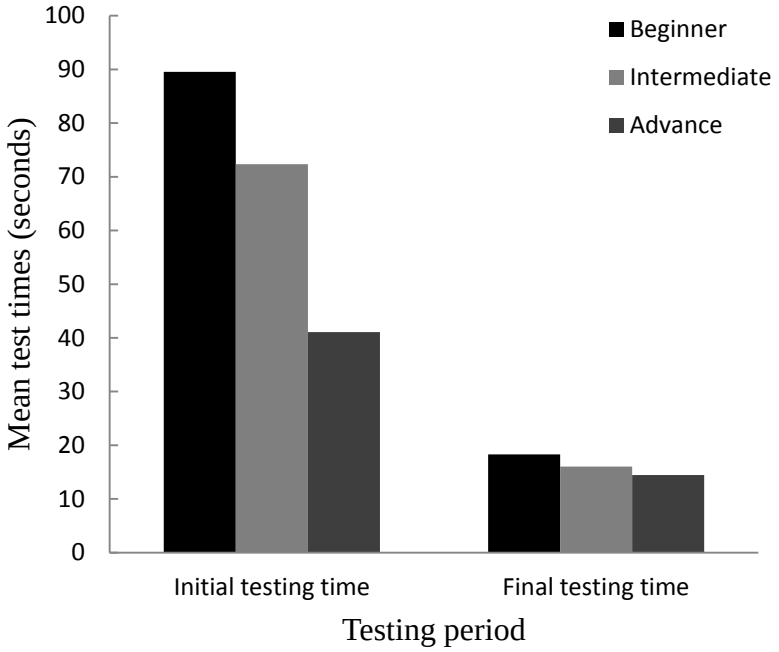

Figure 4. Mean time (s) on the SATB for the three skill level groups across the ten weeks of experimentation.

Table 5. Correlation results examining skill level across motor fitness and SATB specific constructs.

	Skill	Sprint	Beep	Vertical	Shot	Location	Time
1. Skill level	--	-.78*	.42**	.44**	.80**	.65**	-.56**
2. Sprint test		--	-.63**	-.45**	-.65**	-.47**	.50**
3. Beep test			--	.51**	.40*	.24	-0.19
4. Vertical test				--	.51**	.35*	-0.25
5. Shot type					--	.56**	-0.36*
6. Location						--	-0.39*
7. Time							--

Note: Correlations marked with a (*) were significant at p<.05; Correlations marked with (**) were significant at p<.01.

Discussion

The results from the present study aid our understanding of visual cue training and are consistent with previous research relating to skill acquisition (Huynh and Bedford, 2010; Blomqvist, Luhtanen and Laakso, 2001; Abernethy, Wood and Parks, 1999). As expected, participants in the intermediate skill level group out-performed beginners, in the same way that experts out performed intermediates, in both score and time during the initial SATB testing (in week one of experimentation).

The first goal of our study was to assess the authenticity and accuracy of the SATB as a VBT program. Utilising discriminant analysis, our results indicated that the program was successful in predicting group membership with an accuracy of 87.8%. We mentioned previously that minimal research has been carried out to examine the use of VBT methods in badminton,

despite some studies suggesting that cognitive performance is just as important as the execution of motor skills (Blomqvist, Luhtanen and Laakso, 2001; Huynh and Bedford, 2010; Thomas, 1994). These results will hopefully provide implications for coaches and trainers to utilise VBT methods in conjunction with traditional methods in developing training programs.

The second and main focus of our study was to observe whether we could utilise the SATB trainer to improve the anticipatory skills of badminton players over a duration of ten weeks. Our results suggest that the SATB program was effective in improving the overall time and responses relating to badminton scenarios. Specifically, we noticed that participants were more successful in selecting the correct shot type and destination if they had seen previous examples of the current player they were watching. Tong and Hong (2000) suggest that there are many different playing styles in badminton, varying from strength types to speed types, and by knowing your opponents playing style, you can successfully predict most of their shots. The results from this study are consistent with our previous findings (Huynh and Beford, 2010) that participants scored significantly higher in sessions where they had recognised an athlete's playing style from viewing them play in previous sessions.

The success of the SATB in training decision making and anticipatory skills is also consistent with the study by Blomqvist et al. (2001), who also reported an improvement in badminton knowledge, game undertanding and serving skill using a VBT method of training. The authors suggest that visual based learning tasks encourage participants to develop their tactical awareness, bringing cognitive aspects of their game to a conscious level. Similarly, the present study found that participants who used the SATB showed a consistent improvement in their ability to predict and react to the visual based sequences over the ten week period. Again, this provides further support for coaches and trainers to utilise VBT methods in future training programs.

The final task of our study was to examine the linear dependence between our SATB variables and the anthropometric variable of skill level using a Pearson's correlation. Results indicated a strong positive correlation between skill level and the SATB factors of shot type and location type from the analysis. Both correlations were significant, with shot type having a slightly larger correlation coefficient ($r = .80$, $p < .01$). These results suggest that participants were more likely to predict the correct shot type than to select the correct shuttle location on the SATB program. This was consistent across all three skill level groups. This can potentially be explained due to the level of skill possessed by the players in the sequences the participants viewed (all rallies were from top ranked national players from around the world). In the sequences, the athletes were capable of executing a variety of trick/fake shots that could land in almost any location. It was worth noting that even participants from the expert skill level group experienced difficulty assessing these type of shots. However, once participants become aware that a certain player was competent in executing these type of trick shots, and acquired knowledge of their playing style, they were more likely to select the correct location when viewing additional sequences involving that player. Further research regarding similar shot types and discriminating trick shots will be examined by the authors in a follow up study.

A related study by Abernethy et al. (1999) reported similar findings. While some insight was suggested into the acquirement of expert anticipatory skills via a VBT method, the design itself cannot ascertain definitive results regarding on court performance. The authors argue that perceptual training enhances anticipatory skill as assessed using video-based procedures, however, this does not speak directly to the third essential condition for the efficacy of visual-perceptual training, that of transferring these anticipatory skill gains to on court performance. The present study took this into consideration and examined the in-game performance of

participants following visual training. While the improvement in anticipatory skills for the intermediate and advanced group was not vast, the beginner group demonstrated exceptional improvement in both motor skills and responses (with greater speed and reaction time) to their opponents actions. No formal experiment was carried out to examine these on court changes, however, with these improvements in anticipatory skill being noted either by the coach/trainer or by the researcher when examining the video recordings of participant matches. Future research should study in game performance following VBT in more detail.

A number of points about the methodology should be noted. In their study Blomqvist et al. (2001) suggested that age and experience affected the outcomes of the experiment. The present study supported this notion with the results being skewed by participants who were in a lower skill level group yet possessing high anticipatory capabilities. These conditions were rare but did occur. The most common scenario was where participants classified as beginners because they had played minimal badminton and were not completely confident with their understanding of the rules (thus recieve a low score on the KMT) obtained exceptional anticipatory results on the SATB program because they were proficient in other racket sports (e.g. tennis). Care must be taken when interpreting these outcomes, as experts from other sports may affect the groups by being placed in the beginner or intermediate categories. The KMT would need to be modified for future studies to allow for such discrepancies.

It is worth noting that this type of two dimensional training is not a replacement for in game training. It is not designed to replicate exactly to a real in game situation. Instead, it is a means to train and develop cognitive skills whilst not on an actual court. Care needs to be taken when attempting to interpret these results as a substition for the traditional method of training.

Additional modifications would be required if attempting to apply the SATB program to other sports. Although this study can be extended, it is not applicable to invasion type games (e.g. soccer, hockey) due to differences in the number of players and the tactical aspects of evasion games (Blomqvist et al., 2001). The sports that would be applicable to this type of study would ideally be racket sports such as tennis and squash. The SATB program would need to be rewritten to allow utilisation for invasion games.

In summary, we examined and utilised the SATB as a VBT program to train and improve the anticipatory skills of badminton players. In addition, video recordings and feedback (from the coaches/trainers) were utilised to examine on court performance following the SATB training. Our results revealed a significant improvement in anticipatory capabilities for all skill level groups, in particular, beginners demonstrated the largest signs of improvement – both cognitively and physically. With the majority of coaches and trainers placing little emphasis on the cognitive aspects of training, these findings provide implications for traditional training regimes to be reviewed and modified, to allow for the inclusion of visual based development. Overall, the utilisation of a VBT method facilitates the acquisition of perceptual expertise, allowing athletes to train and improve off-court, and in a self paced manner.

References

Abernethy B., & Russel D.G. (1987). Expert-novice differences in an applied selective attention task. *Journal of Sport Psychology*, *9*, 326-345.

Abernethy, B. (1990). Anticipation in squash: Differences in advance cue utilization between expert and novice players. *Journal of Sport Sciences*, *8*, 17-34.

Blahous, E., Shaw, D., & Dybdahl, C. (1997). The impact of computers on writing: No simple answers. *Computers in the Schools*, *13*, 41-53.

Blomqvist, M., Luhtanen, P., & Laakso, L. (2001). Comparison of two types of instructions in badminton. *European Journal of Physical Education, 6, 139-155.*

Chin, M., Wong, A.S., So, R.C.H., Siu, O.T., Steininger, K., & Lo, D.T.L. (1995). Sports specific fitness testing of elite badminton players. *British Journal of Sports Medicine, 29*, 153-157.

Daniels, A. (2004). Composition instruction: Using technology to motivate students to write. *Information Technology in Childhood Education, Annual 2004*, 157-177.

Downes, T., Arthur, L., & Beecher, B. (2001). Effective Learning Environments for Young Children Using Digital Resources: An Australian Perspective. *Information Technology in Childhood Education, Annual 2001*, 139-153.

Fahlstrom, M., Lorentzon., & Alfredson, H. (2002). Painful conditions in the Achilles tendon region in elite badminton players. *American Journal of Sports Medicine, 30*, 50-54.

Howe, N., & Strauss, W. (2008). *Millennials & K-12 Schools*, LifeCourse Associates, 109-111.

Huynh, M., & Bedford, A. (2010). Skills acquisition in badminton: A visual approach to training. Proceedings of the 10th Australian Conference of Mathematics in Sport, 2010 July 5-7, Darwin, Australia.

Jorgensen, A.H., Garde, A.H., Laurens, B., & Jensen, B.R. (2002). Using mouse and keyboard under time pressure: Preferences, strategies and learning. *Behaviour & Information Technology, 21*, 317-319.

Macquet, A.C., & Fleurance, P. (2007). Naturalistic decision-making in expert badminton players. *Ergonomics, 50*, 1433-1450.

McGee, R., & Farrow, A. (1987). *Test questions for Physical Education Activities*. Champaign, II., Human Kinetics.

Mitchell, D. A. (2008). Generation Z striking the balance: Healthy doctors for a healthy community. *Aust Fam Physician, 37*, 665-667.

Musgrove, A., & Musgrove, G. (2004). Online learning and the younger student: Theoretical and practical applications. *Information Technology in Childhood Education, Annual 2004*, 213-225.

Nir-Gal, O., & Klein, P. S. (2004). Computers for cognitive development in early childhood: The teacher's role in the computer learning environment. *Information Technology in Childhood Education, Annual 2004*, 97-119.

Renshaw , I., & Fairweather, M. M. (2000). Cricket bowling deliveries and the discrimination ability of professional and amateur batters. *Journal of Sports Sciences, 18*, 951-957.

Riel, M., & Schwarz, J. (2002). School change with technology: Crossing the digital divide. *Information Technology in Childhood Education, Annual 2002*, 147-179.

Tapscott, D. (2008). Grown Up Digital: How the Net Generation is Changing Your World. McGraw-Hill, 15–16.

Thomas, K.T. (1994). The development of sport expertise: From Leeds to MVP legend. *Quest, 46*, 199-210.

Tong, Y.M., & Hong, Y. (2000). The playing pattern of world's top single badminton players. *Journal of Human Movement Studies, 38*, 185-200.

Yelland, N., & Llyod, M. (2001). Virtual kids of the 21st century: Understanding the children in schools today. *Information Technology in Childhood Education, Annual 2001*, 175-192.

Calibration of a Power-Speed-Model for Road Cycling Using Real Power and Height Data

Thorsten Dahmen & Dietmar Saupe

University of Konstanz

Abstract

The relationship between the pedaling power and the speed with road cycling can be described in the form of a dynamical system, that accounts for the inertia and several kinds of mechanical friction. Six out of twelve involved constant parameters are known or can be measured, whereas the determination of the remaining six parameters is prohibitive and depends on the specific cyclist, the bicycle, and the road surface. The sought six parameters occur in the model in only four terms with distinct dependency on power and speed. The parameters are combined to yield one coefficient per term. Using real power and speed measurements on a calibration track and a least squares fitting technique, we estimate these four coefficients. Although the interpretation of the distinct physical phenomena cannot be preserved completely, an experimental evaluation shows that our calibration improves the model speed estimation on both the calibration track and on other tracks with the same type of road surface. Moreover, we compare the significance of the parameters and show that, given precise measurements of a moderately varying slope, the calibration is accurate.

KEYWORDS: ROAD CYCLING, MATHEMATICAL MODEL, PARAMETER CALIBRATION

Introduction

As part of the Powerbike Project at the University of Konstanz, we design methods for data acquisition, modeling, analysis, optimization, and visualization of performance parameters in endurance sports with particular emphasis on competitive cycling (Dahmen, Byshko, Saupe, Röder, & Mantler, 2011). For accurate data acquisition in a laboratory environment, we developed a simulator system that provides a realistic cycling experience on real-world tracks and apply techniques of data processing and training control both online and offline.

The system is based on a Cyclus2 ergometer (RBM Elektronik-Automation GmbH, Leipzig, Germany) that allows to mount arbitrary bicycle frames to its elastic suspension. The eddy current brake, the force of which we control at a sampling rate of 2 Hz, guarantees non-slipping transmission of a braking resistance up to 3000 W. During a ride on the simulator, the applied brake force is computed in real-time as a function of various mechanical friction parameters, the current velocity, and the slope at the current position. A geo-referenced video of the cycling track is synchronized with the current position and the instantaneous performance parameters are monitored. The cyclist operates electronic push buttons on the handlebar to select gears which are simulated by an appropriate resistance control.

One of the major challenges regarding the analysis of performance data and the control of the ergometer brake of the simulator is to define a precise mathematical P-v-model, that describes

the relationship between the pedaling power P and the cycling speed v.

The model reduces the cyclist-bicycle system to a point mass moving forward along a one-dimensional path that is defined by its height as a function of distance. I.e., only forces that contribute to a torque in the crank are considered to have an effect on the cycling speed. Moreover, only the velocity component in the direction of the track, which we refer to as the speed v, is considered.

The model arises from an equilibrium of the propulsion that results from pedaling and resistance components including gravity, inertia, aerodynamic drag, mechanical rolling friction, and friction in the chain and in the bearings. An overview on the relationship between cycling power and speed, in particular aerodynamics and rolling resistance can be found in chapters 4–6 of Wilson, Papadopoulos, and Whitt (2004).

If the slope of a track and the masses of a cyclist and a bicycle are known, basic mechanical laws define the models for gravity and inertia very well. However, the aerodynamic and frictional resistance components rely on complex physical processes that involve a large number of parameters, which are individual and difficult to measure. Hence, simplifications of these processes are inevitable and the determination of the parameters can only be done empirically.

Existing techniques for the estimation of these model parameters can be divided into three categories: laboratory experiments, numerical simulations, and on-road experiments. In the following, we give references to the most prominent and state-of-the-art work related to the empirical determination of the resistance parameters.

As part of extensive research in the area of aerodynamics in sport (Nørstrud, 2008) most effort has been put into the determination of the aerodynamic friction parameters since on level ground and at high speed, aerodynamics clearly contribute the major part to the overall resistance and are very sensitive to the position of the cyclist, clothing, and the bicycle design (Lukes, 2005).

The most accurate parameters are derived from laboratory experiments, i.e., from wind tunnel tests. Reference values for aerodynamic drag parameters with high sensitivity to various positions and cycling equipment are given by García-López et al. (2008) and have been used to optimize the cyclist's position on the bicycle.

Recently, methods of computational fluid dynamics (CFD) have been validated using both drag and surface pressure measurements and were found to provide a better understanding of the flow field information and the origin of the drag force variations than wind tunnel experiments (Defraeye, Blocken, Koninckx, Hespel & Carmeliet, 2010a). A comparison of different CFD techniques applied to a scale model of a cyclist in a wind tunnel yielded that the steady Reynolds-averaged Navier-Stokes shear-stress transport k-ω model and low-Reynolds number modeling for the boundary layer provide the best results concerning three-component forces, moments, and surface pressure (Defraeye, Blocken, Koninckx, Hespel, & Carmeliet, 2010b). It is expected that this conclusion can be generalized to other high-speed applications of bluff-body shapes which arise in disciplines like swimming, skiing, or bob-sleighing, where related CFD techniques have been employed. Simulation results with higher spatial resolutions of individual body segments were presented by Defraeye, Blocken, Koninckx, Hespel, and Carmeliet (2011).

Tire drum testers and computer-controlled drive-train-testing systems, that measure torque and frictional heat using infrared sensors under various conditions, provide the means to examine

rolling resistance and transmission efficiencies in the laboratory (Lafford, 2000; Kyle & Berto 2001; Spicer, Richardson, Ehrlich, & Bernstein, 2000).

However, the technical complexities of these methods are impractical when the assessment of resistance parameters that match a specific cyclist, bicycle, and road surface is required and a mere transfer of established values from the literature is vague because the specific conditions can hardly be controlled or measured precisely. For this reason, on-road techniques were introduced.

Before portable power meters became available, the resistance was either directly measured while towing a cyclists over a flat road behind a motorcycle (di Prampero, Cortili, Mognoni, & Saibene, 1979; Capelli et al., 1993) or performing deceleration measurements (Candau et al., 1999) after which the data have to be fit to the model. Davies (1980) estimated pedaling power in the field assuming that it is equal to the power on an ergometer that causes the same metabolic costs which, however, introduced the physiological variability as an additional source of inaccuracy.

Recent studies have shown that rear-hub or crank-mounted power meters are sensitive enough to quantify the drafting effect (Edwards & Byrnes, 2007) and even measure the resistance parameters for rolling friction and aerodynamic drag when varying body position and tire pressure (Lim et al., 2011). For this purpose a cyclist rides on a smooth asphalt road of 200 m length several times with different but constant velocities in both directions. For each ride one obtains a data point that consists of the squared average velocity and the average resistance force. Then, the coefficients for aerodynamic drag respectively rolling resistance are computed from the slope respectively the intercept of a linear regression line of these data points.

Clearly, their protocol is limited by the ability of the riders to keep a constant speed and the availability of a long flat track that has the desired surface. Therefore, the experiments were performed on a road close to an airport and it was verified that the average power was the same for two rides with equal velocities but opposite directions. In addition, they used surveying equipment and found the roll of the road being less than 0.03% (It was confirmed by the authors that the corresponding inclination angle given in that paper was misprinted.)

In this contribution, we extend their approach in order to overcome the limitations mentioned above by measuring the slope of the track with a differential GPS device and fitting the whole dynamic P-v-model instead of the drag and rolling friction parameters only to the measured power and velocities as varying functions of the distance. Our view on the model is holistic in the sense that we focus on the accuracy of the P-v-relation rather than interpreting our results with respect to the underlying physical phenomena.

Thus, we present an accurate calibration method for the P-v-model that requires only knowledge of the slope profile and measurements of the pedaling power and the speed during rides with a road bicycle on a calibration track. The track may have a moderately varying slope and the cyclists is not required to keep a constant velocity. Furthermore, we perform a sensitivity analysis that reveals which parameters can be estimated accurately.

Our extension has an accuracy requirement regarding the slope of the track that is not provided by the current generation of gps-enabled bicycle computers. But we believe that due to the rapid advancement of navigation systems, in particular the development of the Galileo GNSS, our approach will become applicable without excessive technical equipment in future and hence could be the most accurate and feasible means to determine individual resistance parameters in cycling.

The following section introduces the P-v-model as adopted from (Martin et al., 1998). Subsequently, we present the calibration method and give details of the experimental setup for the rides before the results of the calibration are shown. Thereafter, a sensitivity analysis is performed in order to assess the robustness of our approach.

The Power-Speed-Model

Since the 1980s, mathematical models have been developed to describe the relationship between the pedaling power P and the cycling speed v. These models comprise a multitude of physical phenomena, but only since the advent of rear hub and crank-mounted power meters has it been possible to validate them as done by Martin et al. (1998). They compared outdoor power measurements of the SRM system on a flat road with different constant velocities to power predictions derived from the model, which accounted for over 97 % of the variation of cycling power.

The model equation can be derived from an equilibrium of forces, including the propulsive force F_p, the chain resistance force F_c, the inertial force F_i, the gravity force F_g, the rolling resistance force F_r, frictional resistance forces in the bearings F_b, and the air resistance force F_a:

$$\underbrace{\frac{P}{v}}_{F_p} - \underbrace{\frac{\zeta P}{v}}_{F_c} - \underbrace{\left(m + \frac{I}{r^2}\right)\dot{v}}_{F_i} - \underbrace{mgh'(x)}_{F_g} - \underbrace{mg\mu}_{F_r} - \underbrace{(\beta_0 + \beta_1 v)}_{F_b} - \underbrace{\frac{1}{2}c_d \rho A v^2}_{F_a} = 0\,, \tag{1}$$

subject to

$$x(t)|_{t=0} = 0 \text{ and } v(t)|_{t=0} = v_0\,. \tag{2}$$

The variables v, x, and t are speed, distance, and time, respectively. The other symbols denote parameters and are listed in Table 1.

Known or measurable constants			Specific, not easily measurable constants		
gravity constant	g	9.81 ms^2	chain friction	ζ	2.5 %
air density	ρ	1.2 kgm^3	rolling friction	μ	0.004
mass (cyclist + bike)	m	86.7 kg	bearing friction	β_0	0.091 N
inertia of	I	measured	bearing friction	β_1	0.0087 Nsm
wheels/crank/chain			shape coefficient	c_d	0.7
radius of the wheels	r	335.0 mm	frontal area	A	0.4 m^2
initial speed	v_0	measured	(cyclist and bike)		
Measurable functions of distance					
height profile	$h(x)$	measured			
pedaling power	$P(x)$	measured			

Table 1. Parameters of the P-v-model. Left column: Known or measurable constants and functions of the distance. Right column: The six sought coefficients ζ, μ, β_0, β_1, c_d, and A and literature values adopted from Martin et al. (1998).

We obtain an initial value problem, which has a unique differentiable solution $v(t)$ as output for any input pedaling power P that is a bounded, non-negative, and piecewise continuous

function of time[1]. For real data, a numerical solution can be found with the Runge-Kutta algorithm. In this paper, we use the ode45 function of Matlab.

We eliminate the time, which is irrelevant for our purposes, by dividing (1) by the speed $v = \dot{x}$ and obtain an ordinary differential equation for the speed v as a function of distance x:

$$\frac{P}{v^2} - \frac{\zeta P}{v^2} - \left(m + \frac{I}{r^2}\right) v'(x) - \frac{mgh'(x)}{v} - \frac{mg\mu + \beta_0}{v} - \beta_1 - \frac{1}{2} c_d \rho A v = 0\,, \qquad (3)$$

subject to

$$v(x)|_{x=0} = v_0\,. \qquad (4)$$

Besides the speed $v(x)$, the pedaling power $P(x)$, and the slope profile of the track $h'(x)$, the model contains 12 physical parameters, as listed in Table 1, which can be assumed to be constant. The values for g and ρ are well known physical constants. The mass of the cyclist and the bicycle m can be weighed with scales. The moment of inertia I of the wheels, the crank, and the chain is estimated experimentally as described in the appendix. The radius of the wheels r is defined by the size of the tires (700×25C corresponds to $r = 2105\,\text{mm} 2\pi \approx 335.0\,\text{mm}$). The initial speed v_0 can be measured with a bicycle computer (Garmin Edge 705). The height profile $h(x)$ is measured using a differential GPS device and the power $P(x)$ with an SRM Power Meter as described in the following section.

The remaining six parameters ζ, μ, β_0, β_1, c_d, and A, as given in the right half of Table 1, are constant, but they are difficult to estimate and, in addition, they are specific for the cyclist, the bicycle, or the track.

Parameter Calibration of the P-v-Model

The essential goal of this work is to determine an accurate P-v-model for realistic road cycling. Our approach is to take measurements of height profiles of specific cycling tracks and examine, to what extent the six unknown parameters can be determined by the measured speed and power data on these tracks.

Calibration Method

In the model equation (3), the six sought parameters occur in four terms, which differ in their dependency of the pedaling power P and the speed v. Therefore, only four compound coefficients can be estimated based on power and speed measurements. For notational convenience, we stack the four coefficients into the symbolic parameter vector $\boldsymbol{k}$ and the known or measurable constant parameters into a vector $\boldsymbol{\ell}$:

$$\boldsymbol{k} = \begin{pmatrix} k_1 \\ k_2 \\ k_3 \\ k_4 \end{pmatrix} = \begin{pmatrix} \zeta \\ mg\mu + \beta_0 \\ \beta_1 \\ \frac{1}{2} c_d \rho A \end{pmatrix} \text{and } \boldsymbol{\ell} = \begin{pmatrix} \ell_1 \\ \ell_2 \\ \ell_3 \\ \ell_4 \end{pmatrix} = \begin{pmatrix} g \\ m \\ v_0 \\ \frac{I}{r^2} \end{pmatrix}. \qquad (5)$$

We rewrite the model equation in terms of $\boldsymbol{k}$ and $\boldsymbol{\ell}$:

[1] We confine ourselves to the physically meaningful case, where $v(t) > 0$, i.e., the model does not cover cycling backwards or standing still.

$$\frac{P}{v^2} - \frac{k_1 P}{v^2} - (\ell_2 + \ell_4)v'(x) - \frac{\ell_1 \ell_2 h'(x)}{v} - \frac{k_2}{v} - k_3 - k_4 v = 0\,, \tag{6}$$

subject to

$$v(x)|_{x=0} - \ell_3 = 0\,. \tag{7}$$

In the following we interpret (6) as an implicit definition of the speed function

$$v\colon [0, L] \to \mathbb{R}_+, \tag{8}$$

$$x \mapsto v\big(x; \boldsymbol{k}, \boldsymbol{\ell}, h'(\cdot), P(\cdot)\big)\,, \tag{9}$$

where L is the length of the track.

Given a set of known or measured parameters $\boldsymbol{\ell}$, functions $h'(\cdot)$, $P(\cdot)$, and speed measurements $v_m(x)$ for a specific ride of a cyclist on the given track, our approach is to seek parameters $\boldsymbol{k}$, so that $v(x; \boldsymbol{k})$ is close to the speed measurement $v_m(x)$. Therefore, we define a cost function

$$J(\boldsymbol{k}) = \frac{1}{L}\int_0^L \big(\, v\big(x; \boldsymbol{k}, \boldsymbol{\ell}, h'(\cdot), P(\cdot)\big) - v_m(x)\big)^2 \,\mathrm{d}x$$

as the mean squared deviation of the modeled speed from the measurement over the length of the track. Then, we determine the estimated parameter vector $\widehat{\boldsymbol{k}}$ as being the argument of the minimum of $J(\boldsymbol{k})$:

$$\widehat{\boldsymbol{k}} = \arg\min_{\boldsymbol{k}} J\,(\boldsymbol{k})\,. \tag{10}$$

Such optimization problems can be solved numerically by gradient-based methods such as the Matlab function lsqcurvefit. In the next but one section we will derive an implicit, analytic formula for the gradient of J, which is beneficial for a robust and efficient implementation of such an optimization.

Data Acquisition on the Tracks

We acquire the coordinates of a 1048 m long asphalt cycling track besides the country road from Röhrnang to Liggeringen in south-west Germany (calibration track) using a differential GPS device (Leica GPS900). The sampling period is 1 s. The differential GPS device is attached to a road bicycle (Radeon RPS 9.0), which we push at walking speed along a lane on the cycling track, while we measure the distance by the rotation of the wheels with a common bicycle computer (Garmin Edge 705).

We use the time stamps of the differential GPS device and the bicycle computer to synchronize the distance and height measurements and obtain a precise height profile, the derivative of which with respect to the distance, $h'(x)$, is given in

Figure 1. We selected an only moderately varying profile on purpose, so that gravity does not predominate the resistance forces over those that involve the parameters to be determined. The differential GPS device indicates a 3D-coordinate quality with an error less than 1.8 cm for every measurement point.

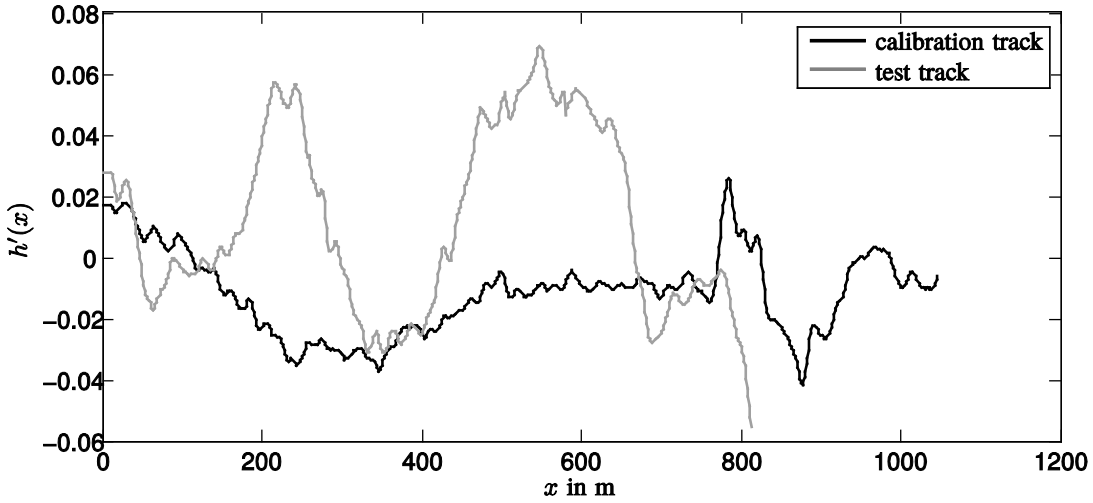

Figure 1. The slopes of the calibration track and the test track.

A cyclist cycles on the road bicycle on the calibration track five times forth and back while there is no wind. The speed is varied in a broad range and the cyclist keeps a constant upright sitting posture. The measured pedaling power $P(x)$, as shown in Figure 2, and the cycling speed $v_m(x)$, Figure 3, are measured by an SRM Power Meter (science edition). This data is used for calibration. The results are presented in the following section.

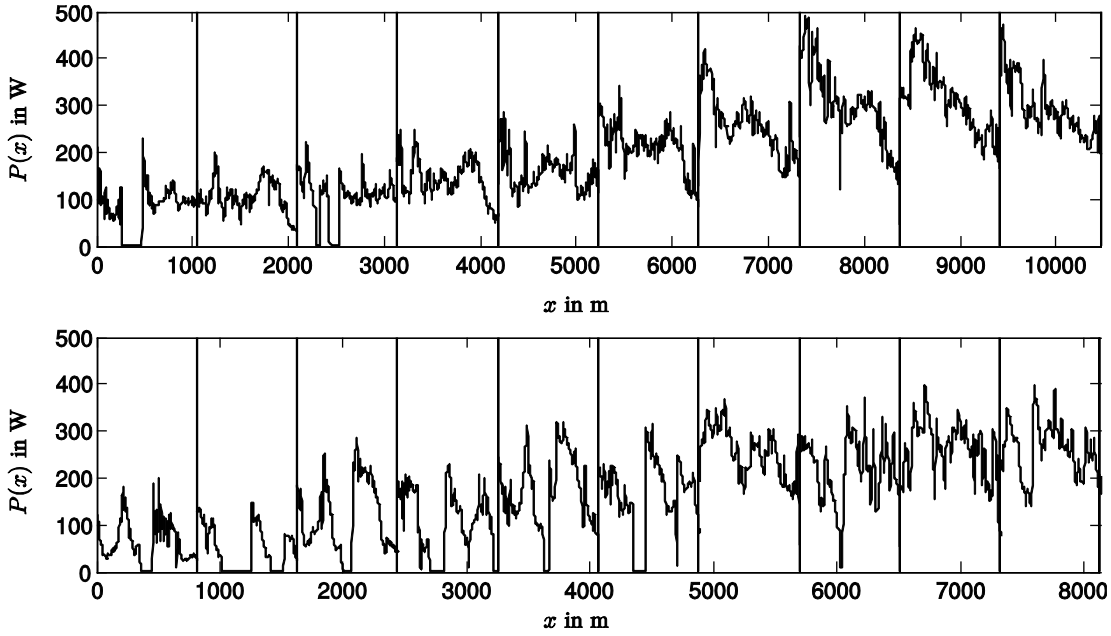

Figure 2. The measured pedaling power $P(x)$ on the calibration track (top) and the test track (bottom). The vertical lines indicate changes of direction at the ends of the track during which the data acquisition was interrupted.

In the same way, measurements are taken on an 813 m long asphalt cycling track in the same area between Allensbach and Kaltbrunn (test track), as depicted in

Figure 1, Figure 2, and Figure 4.

The height profile $h(x)$ is re-sampled on a regular 1 m grid and the smoothed slope $h'(x)$ is obtained using an adaptive-degree polynomial filter (Savitzky-Golay Filter) with a filter length

of 21 m (Barak, 1995).

Calibration Results

In order to demonstrate the results of our calibration approach, we first use the speed and power measurement data of the calibration track to obtain the parameter estimation $\widehat{\boldsymbol{k}}$ and compare the speed estimations $v(x;\widehat{\boldsymbol{k}})$ of the model to the speed estimation $v(x;\boldsymbol{k_{lit}})$, when using the literature values. For validation, we repeat the comparison on the test track, where we use the same calibrated parameters $\widehat{\boldsymbol{k}}$ in order to prove that they can enhance the model accuracy on other than the calibration tracks, too.

Rides on the Calibration Track

Figure 3 shows that the speed estimation of the P-v-model using parameters from literature, $v(x;\boldsymbol{k_{lit}})$, generally exceeds the measured speed $v_m(x)$. The speed estimation using the calibrated parameters $v(x;\widehat{\boldsymbol{k}})$ agrees better with the measured speed.

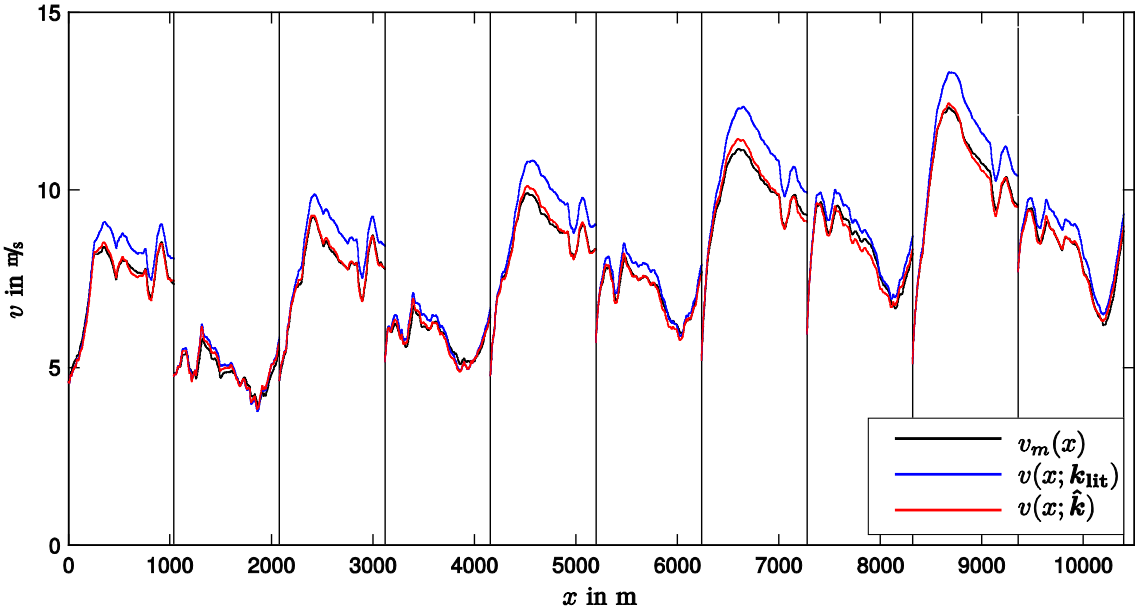

Figure 3. Rides on the calibration track: measured speed $v_m(x)$; speed estimation of the P-v-model, using literature parameters $v(x;\boldsymbol{k_{lit}})$; speed estimation using calibrated parameters $v(x;\widehat{\boldsymbol{k}})$.

The numerical values of the literature parameters $\widehat{\boldsymbol{k}}_{\boldsymbol{lit}}$ and the calibrated parameters $\widehat{\boldsymbol{k}}$ are given in Table 1. We observe that they deviate significantly from the original literature parameters and conclude that the relation to the original physical phenomena is partly lost.

$\boldsymbol{k}$	k_1	k_2	k_3	k_4	$\bar{e}(\boldsymbol{k})$	$\sigma_{e(x;\boldsymbol{k})}$	$\rho_{v_m(x),v(x;\boldsymbol{k})}$
$\boldsymbol{k_{lit}}$	2.5 %	3.41 N	0.0087 Nsm	0.168 kgm	0.45 ms	0.35 ms	0.9898
$\widehat{\boldsymbol{k}}$	0.3 %	4.22 N	0.076 Nsm	0.257 kgm	0.0073 ms	0.13 ms	0.9943

Table 2. Comparison between numerical values for the parameters $\boldsymbol{k}$ of the P-v-model as taken from literature, $\boldsymbol{k_{lit}}$, and as obtained by calibration, $\widehat{\boldsymbol{k}}$; the error function $e(x;\boldsymbol{k}) = v(x;\boldsymbol{k}) - v_m(x)$ is characterized by the mean error $\bar{e}(\boldsymbol{k})$, the standard deviation $\sigma_{e(x;\boldsymbol{k})}$, and the correlation coefficient $\rho_{v_m(x),v(x;\boldsymbol{k})}$.

However, the mean error $\bar{e}(\boldsymbol{k}) = \frac{1}{L}\int_0^L e\,(x, \boldsymbol{k})\,\mathrm{d}x$, the standard deviation $\sigma_{e(x;\boldsymbol{k})}$ and the correlation coefficient $\rho_{v_m(x),v(x;\boldsymbol{k})}$ in Table 2 clearly indicate, that the accuracy of the P-v-dynamics has improved. Note, that the residual of the cost function J can be expressed in terms of the mean error $\bar{e}(\boldsymbol{k})$ and the standard deviation $\sigma_{e(x;\boldsymbol{k})}$ as

$$J(\boldsymbol{k}) = \bar{e}^2(\boldsymbol{k}) + \sigma^2_{e(x;\boldsymbol{k})}\,. \tag{11}$$

In the next section, we demonstrate that the impact of the parameters k_1 and k_3 on the speed estimation is very small. Thus, small variations in the estimated speed can result in a considerable change of the parameter estimations $\hat{k}_1$ and $\hat{k}_3$. The parameter estimations $\hat{k}_2$ and $\hat{k}_4$ are more robust. The significant increase in k_4, which is related to the areal resistance coefficients c_d and A contributes the major part to the improvement of the P-v-model accuracy.

Validation Rides on the Test Track

In Lim et al. (2011) the experiments were repeated several times on the same level road in order to obtain empirical standard deviations for the estimated parameters and to show that changes of the experimental conditions have a significant effect on the estimations. As we, in addition, make use of measurements of the slope profile, we validate our method on a different cycling track with a road surface that has similar properties as the calibration track. Using the solution coefficient vector $\widehat{\boldsymbol{k}}$, we calculate a model estimation for the speed $v(x;\widehat{\boldsymbol{k}})$ of the rides on the test track and compare it to the measured speed as depicted in Figure 4.

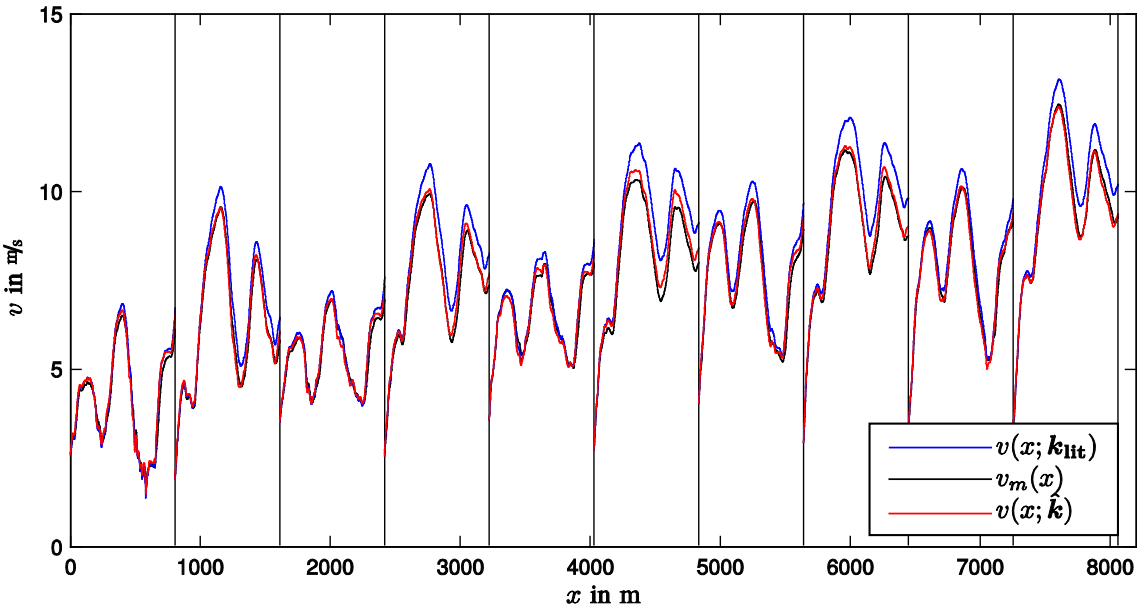

Figure 4. Rides on the test track: measured speed $v_m(x)$; speed estimation of the P-v-model, using literature parameters $v(x;\boldsymbol{k}_{lit})$; speed estimation using calibrated parameters $v(x;\widehat{\boldsymbol{k}})$.

As indicated by the error measures in Table 3, also on the test track, the match between the measured speed $v_m(x)$ and the speed estimation of the P-v-model $v(x;\boldsymbol{k})$, using the calibrated parameters $\widehat{\boldsymbol{k}}$ instead of the literature values $\boldsymbol{k}_{lit}$, is significantly better.

$\boldsymbol{k}$	$\bar{e}(\boldsymbol{k})$	$\sigma_{e(x;\boldsymbol{k})}$	$\rho_{v_m(x),v(x;\boldsymbol{k})}$
$\boldsymbol{k_{lit}}$	0.432 ms	0.350 ms	0.9958
$\widehat{\boldsymbol{k}}$	0.038 ms	0.163 ms	0.9978

Table 3. Error measures for the rides on the test track: absolute mean error of the speed $\bar{e}(\boldsymbol{k})$; standard deviation $\sigma_{e(x;\boldsymbol{k})}$; correlation coefficient $\rho_{v_m(x),v(x;\boldsymbol{k})}$.

The Sensitivity of the Model in Terms of the Parameters in k

The influence of the four parameters in $\boldsymbol{k}$ on the model speed estimation is very different. Experience shows that – for a well lubricated chain – the term with the parameter k_1 in (6) is negligible. The terms with the parameters k_2, k_3, and k_4 depend on the speed only. Figure 5 depicts how these coefficients contribute to the total resistance force which is directly proportional to their contribution to the acceleration $\dot{v}(x)$.

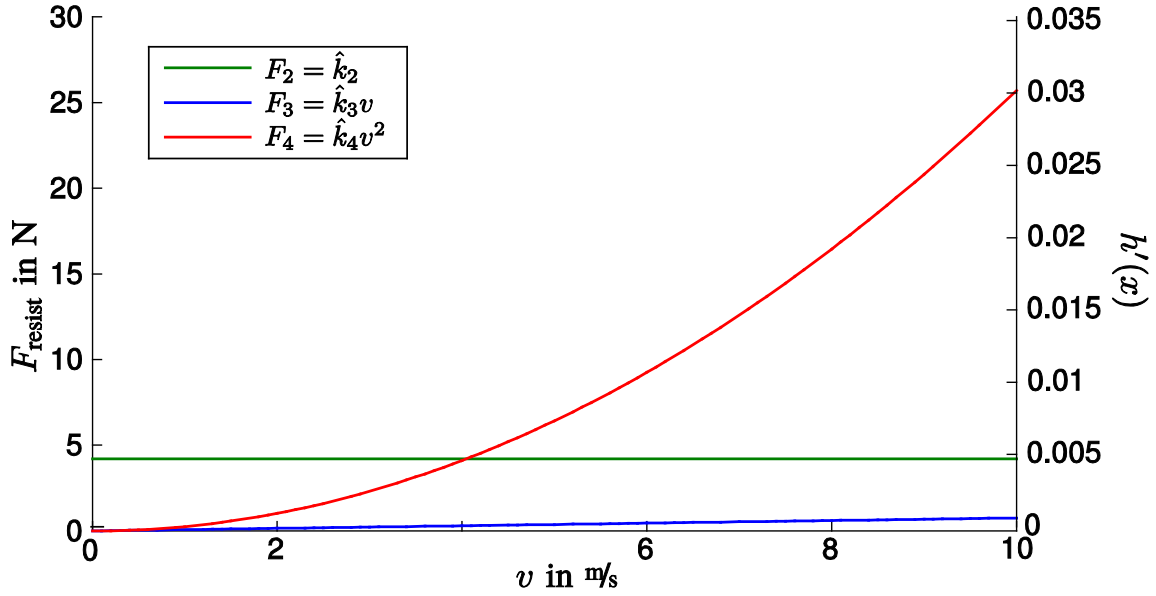

Figure 5. The contributions of the terms with the parameters k_2, k_3, and k_4 on the total resistance force F_{resist}. At $v = 4.05$ ms, the influence of k_4 becomes larger than the influence of k_2. The coefficient k_3 plays a minor role. The right ordinate axis indicates the slope $h'(x)$, that causes an equivalent resistance force.

For $v < 4.05\,ms$ the coefficient k_2 contributes the largest share to the total resistance force whereas for higher velocities, k_4 is dominant. The coefficient k_3 is in fact negligible for all practical purposes.

The right ordinate axis indicates the contribution of the slope $h'(x)$ to the resistance force. Its influence can easily exceed the influence of the other resistance components. Therefore, the slope of the calibration track may vary, but its magnitude should be moderate and it must be measured with high accuracy to ensure a successful parameter calibration. Note that the limitation on the magnitude of the slope only refers to the calibration track. Once the parameters have been determined, the model can be applied to steep tracks, if precise slope data are available for the track. In this situation the gravity component just becomes more influential.

However, these simple considerations are rather static and do not allow us to fully grasp how

changes in the parameters $\boldsymbol{k}$ affect the model output speed $v(x;\boldsymbol{k})$. Therefore, we make use of a local method of sensitivity analysis and compute the partial derivatives of the model estimation output $\frac{\partial v(x;\boldsymbol{k})}{\partial \boldsymbol{k}}$. Eventually, the quantities

$$s_{k_i}(x) = \frac{k_i}{v}\frac{\partial v(x;k_i)}{\partial k_i} \tag{12}$$

quantify the sensitivity of the model output $v(x;k_i)$ with respect to the parameters k_i, since they give the relative change of the model output speed $v(x)$, due to a relative change in the parameters in $\boldsymbol{k}$. In case the effect is small, we conclude, that the minimum $J(\widehat{\boldsymbol{k}})$ cannot be pronounced and hence the calibration method is not robust with respect to the considered parameter.

Besides, the partial derivatives are very beneficial in the implementation of our calibration method, because they are required for the computation of the gradient of our cost function

$$\frac{\partial}{\partial \boldsymbol{k}}\big(J(\boldsymbol{k})\big) = \frac{2}{L}\int_0^L \big(v(x) - v_m(x)\big)\frac{\partial v}{\partial \boldsymbol{k}}\,\mathrm{d}x\,. \tag{13}$$

The result facilitates gradient-based numerical optimization to solve (10).

In order to derive the partial derivatives, we make use of the theorem of implicit functions and define a function $\boldsymbol{f} = (f_1, f_2)^T$ to be equal to the left-hand side of (6):

$$\begin{aligned}&\boldsymbol{f}(v(x;\boldsymbol{k}), v'(x;\boldsymbol{k});\boldsymbol{k},\boldsymbol{\ell},h'(\cdot),P(\cdot))\\ &= \begin{pmatrix} \frac{P}{v^2} - k_1\frac{P}{v^2} - (\ell_2+\ell_4)v'(x) - \frac{\ell_1\ell_2 h'(x)}{v} - \frac{k_2}{v} - k_3 - k_4 v \\ v(x)|_{x=0} - \ell_3 \end{pmatrix}.\end{aligned} \tag{14}$$

Furthermore, let

$$\boldsymbol{F}(\boldsymbol{k}) := \boldsymbol{f}(v(x;\boldsymbol{k}), v'(x;\boldsymbol{k});\boldsymbol{k},\boldsymbol{\ell},h'(\cdot),P(\cdot)) \quad \forall\, \boldsymbol{k} \in \mathbb{R}_+^4. \tag{15}$$

Then,

$$\boldsymbol{F}(\boldsymbol{k}) \equiv \boldsymbol{0} \quad \forall\, \boldsymbol{k} \in \mathbb{R}_+^4, \tag{16}$$

and all derivatives clearly vanish:

$$\frac{d\boldsymbol{F}}{d\boldsymbol{k}} = \boldsymbol{0}. \tag{17}$$

We apply the chain rule for differentiation and obtain

$$\frac{d\boldsymbol{F}}{d\boldsymbol{k}} = \frac{\partial \boldsymbol{f}}{\partial v}\frac{\partial v}{\partial \boldsymbol{k}} + \frac{\partial \boldsymbol{f}}{\partial v'}\frac{\partial v'}{\partial \boldsymbol{k}} + \frac{\partial \boldsymbol{f}}{\partial \boldsymbol{k}} = 0 \tag{18}$$

The partial derivatives $\frac{\partial \boldsymbol{f}}{\partial v}$, $\frac{\partial \boldsymbol{f}}{\partial v'}$, and $\frac{\partial \boldsymbol{f}}{\partial \boldsymbol{k}}$, can be computed from (14). We obtain four nonlinear, first-order differential equations with four initial values whose solutions are the sought derivatives $\frac{\partial v}{\partial k_i}$:

$$\left(-\frac{2P}{v^3}+\frac{2k_1P}{v^3}+\frac{\ell_1\ell_2}{v^2}h'(x)+\frac{k_2}{v^2}-k_4\right)\frac{\partial v}{\partial k_i}-(\ell_2+\ell_4)\frac{\mathrm{d}}{\mathrm{d}x}\left(\frac{\partial v}{\partial k_i}\right)-\mathcal{K}_i=0 \qquad (19)$$

with

$$\left.\frac{\partial v}{\partial k_i}\right|_{x=0}=0 \quad \text{and} \quad \mathcal{K}_i=\begin{cases}\dfrac{P}{v^2} & \text{for } i=1\\ \dfrac{1}{v} & \text{for } i=2\\ 1 & \text{for } i=3\\ -v & \text{for } i=4\end{cases}. \qquad (20)$$

Again, the solutions can be computed with the Runge-Kutta method.

Figure 6 depicts the relative sensitivities of the model estimation speed $v(x;\widehat{\boldsymbol{k}})$ with respect to the calibration parameters in $\boldsymbol{k}$. All sensitivities are negative, since the parameters characterize resistances.

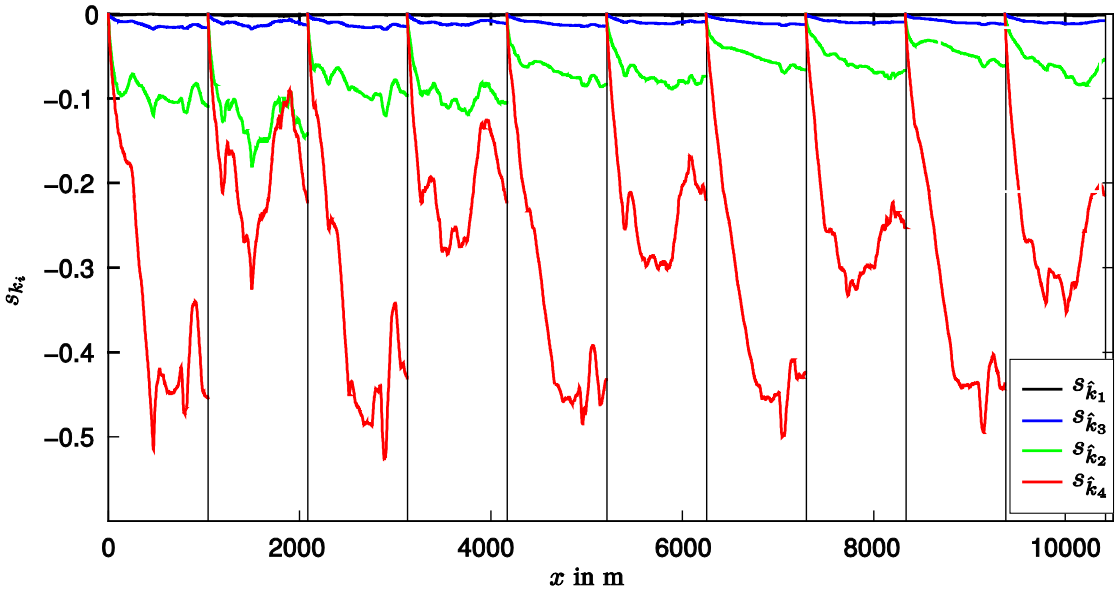

Figure 6. The relative parameter sensitivities s_{k_i}, defined in (12). The sensitivity s_{k_1} is so insignificant, that it almost coincides with the abscissa.

The graph confirms our previous assumption that the influence of the parameters k_1 and k_3 is very small and we conclude that on the one hand, our estimation method cannot be robust, but on the other hand an accurate estimation of the insensitive parameters k_1 and k_3 is not essential for a precise model speed estimation, either.

At the beginning of each ride, the sensitivity of every parameter vanishes, because the initial speed is solely defined by $\ell_3 = v_0$. In the course of each ride, the parameters gain influence. The moment of inertia determines how fast this influence is gained and demands a minimum length of the track for a sensible calibration. In particular with high velocities, k_4 is the most influential parameter and hence, its estimation is the most robust.

The method of computing partial derivatives and sensitivities can be applied in other contexts, as well, e.g., to quantify the influence of the known or measurable parameters $\boldsymbol{\ell}$, as

demonstrated in the appendix.

Limitations

Our calibration method estimates parameters to determine an holistic model that defines the relationship between pedaling power and cycling speed if power and height data are provided. However, there are limitations concerning both the model and the calibration method, which we discuss in this section.

The model itself contains several simplifications. Reducing the cyclist-bicycle system to a point mass neglects that we deal with a multi-segmental unit. The P-v-model does not consider relative movements and internal forces within that unit except of the resulting pedal force. The effects of, e.g., braking or pumping[2] on the cycling speed are omitted.

Furthermore, as only the speed of the point mass along a one-dimensional path is modeled, centripetal forces and gyroscopic effects in curves are discounted.

The holistic approach ensures that conditions like air density, road surface properties, or the shape of the cyclist-bicycle system are implicitly accounted for with respect to their impact on the speed. On the one hand, this is an advantage of our approach. On the other hand it is not possible to compute the compound parameters as functions of individual measurements of these conditions.

The calibration method is limited by the accuracy of the power meter, as discussed in and the differential gps device. In presence of obstacles close to the track like vegetation or settlements, the gps signal quality is degraded. The calibration track may have a moderately varying slope, however, the parameter sensitivity decreases with the magnitude of that slope.

Some of the limitations mentioned above like braking and pumping are less relevant in terms of road cycling time trials, in particular if the primary focus is on optimizing the distribution of the physical performance rather than the skillfulness of a cyclist on a specific track.

Regarding the simulator, additional limitations coincide with limitations of the simulator itself: The simulation speed is defined by the rotation of the ergometer flywheel which can only be accelerated by pedaling and not by braking or pumping at all. Though having an elastic suspension that allows for a sway pedal stroke, steering and centripetal forces are not simulated and the flywheel axis is fixed so that there are no gyroscopic effects. As the ergometer is non-motorized, we focus on cycling tracks without steep descents where braking is less relevant.

For these reasons, we consider our model and calibration method to be appropriate with respect to the available measurement devices and in particular to the application in cycling simulators.

Conclusions

The standard P-v-model has six constant physical parameters, the values of which cannot be easily determined by direct measurements. However, they can be substituted by four symbolic coefficients, which can be estimated given the profile of a track and simultaneous measurements of the pedaling power and the speed on the same track, in order to obtain an accurate P-v-model which is specific for the cyclist, the bicycle, and the road surface.

The calibration method should be carried out on moderately varying calibration tracks and a

[2] Pulling the cyclist's center of mass down and pushing it up again while passing a summit.

precise measurement of the slope profile as, e.g., with a differential GPS device is essential for a successful calibration. Furthermore, the accuracy is obtained at the cost of partly losing the physical interpretation of the parameters.

Yet, we demonstrated, that not only are the calibrated parameters valid on the track on which they have been estimated, but they can also improve the speed estimation on other tracks with the same road surface properties.

In fact, only two out of the four parameters have a significant influence in the P-v-model. The parameter that originates from the aerodynamic drag coefficients is dominant for velocities higher than 4 ms.

Outlook

The results of the parameter calibration will be used in future for the control of the braking force of the simulator and for the analysis of outdoor power and speed data for the following purposes.

In spite of the high accuracy of the differential GPS-device, it remains difficult to precisely measure the slope, since the GPS signal quality is disturbed by trees, buildings, or other obstacles on the roadside, so that the differential correction cannot be performed. Therefore, we plan to fuse the height measurements obtained from the differential GPS device with an estimation of the slope that can be computed by resolving the model equation (6) for $h'(x)$. It has been proven in many practical examples, where position data is aided by inertial navigation systems, that the Kalman smoother is the optimal linear estimator for this application.

Furthermore, a computer program is currently being developed, that allows to change any parameter of the P-v-model and visualize the effects on all the other parameters to explore any specific real scenario interactively.

Another major research question within the context of the Powerbike project is the computation of an optimal pacing strategy that assists the athlete to complete a specific course in minimal time. Mathematically, this can be formulated as an optimal control problem, where pedaling power is the control variable to be optimized, time to complete the course is the cost functional, and the P-v-model is the mechanical part of the dynamical system.

In addition, a physiological endurance model, limiting the admissible pedaling power according to the energy reserves of the cyclist, is required. Such whole-body bio-energetic models have been reviewed by Morton (2006).

An analytical treatment of the optimization problem for synthetic and piecewise constant slope profiles, and a simplified mechanical and physiological model has been presented by Gordon (2005). A numerical implementation of this approach, that accounts for varying slopes and mechanical inertia, has been implemented and tested on our simulator (Wolf & Dahmen, 2010). Yet, we believe, that a refinement of the physiological model and the methods for estimating its parameters is necessary, before the system can be used to train strategies in practice.

Therefore, we plan to use lactate measurements and spiroergometry for the calibration of the physiological model and to design real-time feedback and a model predictive control for time trials both on the simulator and in the field. For the optimization of group training in cycling a related model-predictive control uses a model for the cyclist's power demand according to the position within the group and the heart rate as physiological stress indicator (Le, 2010).

All these applications rely on the accuracy of the P-v-model, whereas the physical interpretation of the parameters is less important. Therefore, we consider the parameter calibration as an important basis element that will improve the accuracy of the results in various future applications.

References

Barak, P. (1995). Smoothing and differentiation by an adaptive-degree polynomial filter. *Analytical Chemistry*, *67*(17), 2758–2762.

Candau, R. B., Grappe, F., Ménard, M., Barbier, B. Millet, G. Y., Hoffman, M. D., Belli, A.R., & Rouillon, J. D. (1999). Simplified deceleration method for assessment of resistive forces in cycling. *Medicine & Science in Sports & Exercise*, *31*(10), 1441–1447.

Capelli C., Rosa G., Butti F., Ferretti G., Veicsteinas A., & Prampero P. E. di. (1993). Energy cost and efficiency of riding aerodynamic bicycles. European Journal of Applied Physiology and Occupational Physiology, *67*(2), 144–149.

Dahmen, T., Byshko, R., Saupe, D., Röder, M., & Mantler, S. (2011). Validation of a model and a simulator for road cycling on real tracks. *Sports Engineering*, *2*(14), 95–110.

Dahmen, T. (2010). Kalibrierung eines Leistungs-Geschwindigkeits-Modells für Rennradfahrten mit realen Leistungs- und Höhendaten [Calibration of a performance veolcity model for road cycling based on real performance and altitude data]. In J. Wiemeyer, D. Link, R. Angert, B. Holler, A. Kliem, N. Roznawski, D. Schöberl, & M. Stroß (Eds.), Sportinformatik trifft Sporttechnologie [Sports Informatics meets Sports Technology]. 8. Symposium of the dvs Section Sports Informatics, 15.–17. September, Darmstadt, 235–239.

Davies, C. T. (1980). Effect of air resistance on the metabolic cost and performance of cycling. *European Journal of Applied Physiology and Occupational Physiology*, *45*(2), 245–254.

Defraeye T., Blocken B., Koninckx E., Hespel P., & Carmelietd J. (2010a). Aerodynamic study of different cyclist positions: CFD analysis and full-scale wind-tunnel tests. *Journal of Biomechanics*, *43*(7), 1262–1268.

Defraeye T., Blocken B., Koninckx E., Hespel P., & Carmelietd J. (2010b). Computational fluid dynamics analysis of cyclist aerodynamics: Performance of different turbulence-modeling and boundary-layer modeling approaches. *Journal of Biomechanics*, *43*(12), 2281–2287.

Defraeye T., Blocken B., Koninckx E., Hespel P., & Carmelietd J. (2011). Computational fluid dynamics analysis of drag and convective heat transfer of individual body segments for different cyclist positions. *Journal of Biomechanics*, *44*(9), 1695-1701.

Edwards, A. G., & Byrnes, W. C. (2007). Aerodynamic Characteristics as Determinants of the Drafting Effect in Cycling. *Medicine & Science in Sports & Exercise*, *39*(1), 170–176.

García-López, J., Rodríguez-Marroyo J. A., Juneau, C.-E., Peleteiro J., Martínez A., & Villa, J. G. (2008). Reference values and improvement of aerodynamic drag in professional cyclists. *Journal of Sports Sciences*, *26*(3), 277–286.

Gordon, S. (2005). Optimizing distribution of power during a cycling time trial. *Sports Engineering*, *8*(2), 81–90.

Gressmann, M. (2002). Fahrradphysik und Biomechanik. Technik – Formeln – Gesetze [Technique – Formula – Law]. (7. Edition). Delius Klasing Verlag.

Kyle, R., & Berto, F. (2001). The mechanical efficiency of bicycle derailleur and hub-gear transmissions. *Human Power*, 52, 3–11.

Lafford, J. (2000). Rolling resistance of bicycle tires. *Human Power*, *50*, 14–19.

Le, A. (2010). Sensor-based training optimization in professional cycling by model predictive control. Shaker Verlag GmbH, Germany.

Lim, A. C., Homestead, E. P., Edwards, A. G., Carver, T. C., Kram, R., & Byrnes, W. C. (2011). Measuring changes in aerodynamic/rolling resistances by cycle-mounted power meters. *Medicine & Science in Sports & Exercise*, *43*(5), 853–860.

Lukes, R. A., Chin, S. B., Haake, S. J. (2005). The understanding and development of cycling aerodynamics. *Sports Engineering*, *8*(2), 59–74.

Martin, J. C., Milliken, D. L., Cobb, J. E., McFadden, K. L., & Coggan, A. R. (1998). Validation of a mathematical model for road cycling power. *Journal of Applied Biomechanics*, *14*(3), 276–291.

Morton, R. H. (2006). The critical power and related whole-body bio-energetic models. *European Journal of Applied Physiology*, *96*(4), 339–354.

Nørstrud H. (Ed.). (2008). *Sport Aerodynamics*. (1st ed.). Springer.

Spicer, J. B., Richardson C. J. K., Ehrlich, M. J. & Bernstein J. R. (2000). On the efficiency of bicycle chain drives. *Human Power*, *50*, 3–9.

Wilson, D. G., Papadopoulos, J., & Whitt, F. R. (2004). *Bicycling Science 3rd Ed.*. The MIT Press, USA.

Wolf, S., & Dahmen, T. (2010). Optimierung der Geschwindigkeitssteuerung bei Zeitfahrten im Radsport [Optimization of velocity control at time trial in road cycling]. In J. Wiemeyer, D. Link, R. Angert, B. Holler, A. Kliem, N. Roznawski, D. Schöberl, & M. Stroß (Eds.), *Sportinformatik trifft Sporttechnologie* [Sports Informatics meets Sports Technology]. 8. Symposium of the dvs Section Sports Informatics,, 15.–17. September, Darmstadt, 235–239.

Appendix

The Accuracy of the Power Meter Devices

In Dahmen (2010), an SRM Power Meter V, professional edition with four strain gauges, was used for which the manufacturer claims an accuracy of ± 2 %. For the experiments in this paper, we used a SRM Power Meter IIV, scientific edition, with 8 strain gauges and an accuracy of 0.5 %. However, a perfect reference for pedaling power does not exist and inquiries on the manufacturer's calibration method revealed that the accuracies of power meters have not been evaluated scientifically.

In order to compare the calibrations of our two SRM Power Meters, we perform a step test ranging from $80 - 300$ W on a Cyclus2 ergometer and computed the averages of the SRM power measurements during each step, as depicted in Figure 7.

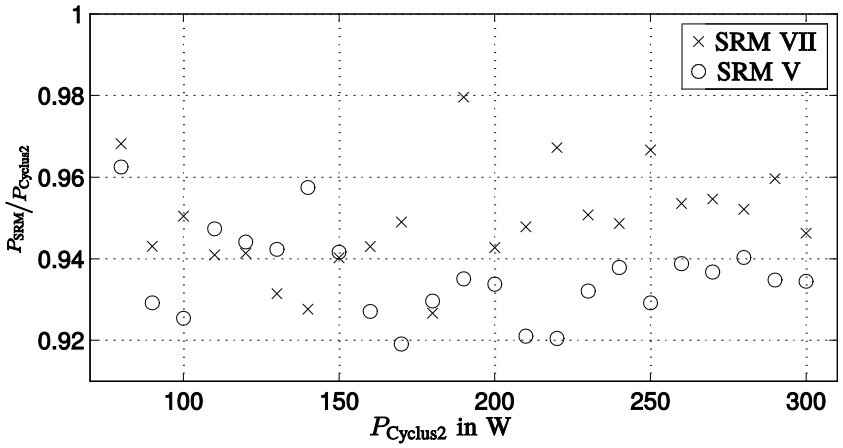

Figure 7. Comparison of power measurements of an SRM Power Meter IIV and an SRM Power Meter V. Both devices were used to measure the power during a step test on a Cyclus2 ergometer (power range: $80 - 300$ W, step duration 30 s, cadence 80 rpm. The SRM measurement power P_{SRM} divided by the nominal power of the Cyclus2, P_{Cyclus2} for each step is plotted versus P_{Cyclus2}. For the Cyclus2 ergometer, the manufacturer claims an accuracy of ± 2 % for $P > 250$ W and $\pm 5\ W$ for $P < 250$ W. All devices were either new or recently calibrated by the manufacturer.

In fact, we had expected, that the SRM power meters display a slightly larger power since they measure the sum of the power absorbed by the ergometer brake, the frictional resistance of the ergometer mechanics, and the frictional resistance of the chain and the crank of the bicycle, whereas the nominal power of the ergometer should be equal to the power absorbed by the ergometer brake only. However, we observe that both SRM devices measure significantly less power than the nominal power during each step. Moreover, particularly with a nominal power above 200 W, we detect that the power measurements of the Power Meter VII exceed those of the Power Meter V.

We conclude that the determination of the parameters of the P-v-model with our method is affected by the lack of a reliable calibration method of power meters. Even if model estimations and measurements match well, we have to be aware of a possible additional error regarding the unknown true pedaling power.

Estimation of Wheel, Crank, and Chain Inertia

The moments of inertia of a bicycle wheel can be determined by hanging up the wheel in a horizontal position and having it oscillate around its axis, Gressmann (2002).

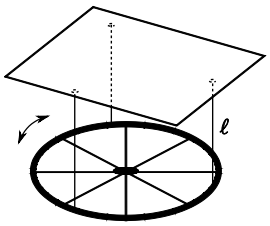

Figure 8. Setup of a pendulum experiment for the determination of the wheel inertia.

For this purpose, we fasten three equally long pieces of string to three equally spaced points on the rim, as sketched in Figure 8. The other ends of the pieces of string are fixed to a horizontal board above the wheel, so that the pieces of string are vertical when the system is at rest. The inertia I_w of this physical pendulum is

$$I_w = \frac{T^2 mg\ell}{4\pi^2}, \tag{21}$$

where T is the oscillation period, ℓ is the length of the pieces of string. With the wheel oscillating, we measure the time for 20 periods and compute a momentum of $I_{wf} = 0.14\ \text{kgm}^2$ for the front wheel an and $I_{wr} = 0.16\ \text{kgm}^2$ for the rear wheel.

The inertia of the crank is composed of the inertia of the pedals I_p, of the crank arm I_a, of the chainrings I_c, and of the SRM Power Meter I_{SRM}. Each component can be approximated by a primitive geometric form rotating around the center of the crank axis: (pedal – point mass, crank arm – solid cylinder, chainrings – rings, SRM – solid disk).

We measure the weights and the sizes of each component and compute the individual moments of inertia. Their sum yields the total inertia of the crank $I_c = 0.02\ \text{kgm}^2$.When the cyclist does not pedal ($P = 0$), only the wheels and not the crank contribute to the inertia. The resulting moment of inertia I of the wheels, the crank, and the chain is

$$I = \begin{cases} I_{wf} + I_{wr} & \text{for } P = 0 \\ I_{wf} + I_{wr} + \gamma^2 I_c + r_s^2 m_{ch} & \text{for } P > 0\,, \end{cases} \tag{22}$$

with γ being the transmission ratio, r_s is the radius of the rear sprocket wheel currently used by the chain, and m_{ch} is the mass of the chain.[3] The transmission ratios in the experiments can be reconstructed from the measured cadence f_c:

$$\gamma = \frac{v}{f_c r_w}. \tag{23}$$

The details of these computations for our experiments are omitted since this is straightforward and the inertia only has a negligible impact in the P-v-model.

Sensitivities and Partial Derivatives of the Speed With Respect to ℓ

The sensitivities s_{l_i} of the speed estimation of the model with respect to the parameters in $\boldsymbol{\ell}$ can be derived in analogy to the derivation of the sensitivities s_{k_i}. First, we derive the differential equations for $\frac{\partial v}{\partial \ell_i}$, which correspond to (20):

$$\left(-\frac{2P}{v^3} + \frac{2k_1 P}{v^3} + \frac{\ell_1 \ell_2}{v^2} h'(x) + \frac{k_2}{v^2} - k_4\right)\frac{\partial v}{\partial \ell_i} - (\ell_2 + \ell_4)\frac{d}{dx}\frac{\partial v}{\partial \ell_i} - \mathcal{L}_i = 0\,, \tag{24}$$

where

$$\left.\frac{\partial v}{\partial \ell_i}\right|_{x=0} = \begin{cases} 0 & \text{for } i = 1,2,4 \\ 1 & \text{for } i = 3 \end{cases} \quad and \quad \mathcal{L}_i = \begin{cases} \frac{m}{v} h'(x) & \text{for } i = 1 \\ v'(x) + \frac{g}{v} h'(x) & \text{for } i = 2 \\ 0 & \text{for } i = 3 \\ v'(x) & \text{for } i = 4 \end{cases}. \tag{25}$$

Then, we define the sensitivities of the model estimation speed with respect to the parameters in $\boldsymbol{\ell}$ in analogy to (12):

[3] During the rides for the calibration experiments, gear changes were avoided, not to disturb the power measurement.

$$s_{\ell_i}(x) = \frac{\ell_i}{v}\frac{\partial v(x;\ell_i)}{\partial \ell_i}. \tag{26}$$

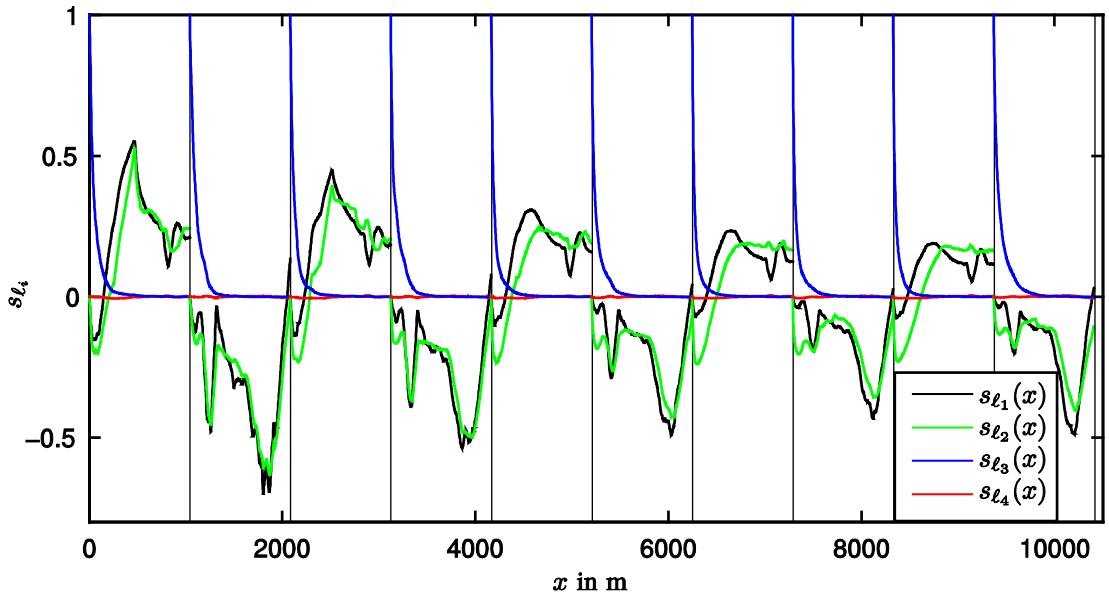

Figure 9. Sensitivities s_i of the model estimation speed $v(x;\widehat{\boldsymbol{k}})$ with respect to the parameters in $\boldsymbol{\ell}$.

Figure 9 depicts the sensitivities s_{ℓ_i} for the rides on the calibration track. At the beginning of each ride, the initial speed ℓ_3 is dominant because for $x = 0$ the speed is solely defined by the initial speed v_0. However, its influence decreases rapidly and after 200 m the sensitivity with respect to the gravity factor $g = \ell_1$ and to the mass $m = \ell_2$ reveal the largest impact on $v(x;\widehat{\boldsymbol{k}})$. The moment of inertia of the wheels, the crank, and the chain, which is represented by ℓ_4 is negligible.

Figure 6 and Figure 9 allow a direct comparison of the sensitivities of all parameters of the *P*-v-model.

Computer Methods to Assess Motor Imagery

Josef Wiemeyer & Regine Angert

Institute of Sport Science, Technische Universität Darmstadt

Abstract

Motor imagery plays an important role in motor control and learning. Motor imagery can be assessed on three levels: subjective experience, motor behaviour, and physiological measures. In this paper we propose a computer-aided selection test (CAST) which enables researchers to analyse the procedure of reconstructing mental representations. The two versions of the CAST (pictures vs. verbal items) allow a thorough procedural analysis of motor imagery. The added value of the developed CAST, e.g., assessing cognitive time, corrections, and order of selection, is demonstrated using the data of an experiment in motor learning.

KEYWORDS: MOTOR IMAGERY, MOTOR REPRESENTATIONS, MOTOR LEARNING, MOTOR CONTROL, TEST

Introduction

Motor learning in sport is a complex dynamic process leading to more or less permanent changes in motor memory. From a formal perspective, this dynamic process can be devided into distinct stages. Numerous models (overview: Müller, 1995; Schmidt & Lee, 2005) propose that there is an initial cognitive stage of motor learning where explicit mental processes like mental imagery play an important role. The term ‘imagery’ denotes a “perception-like process in the absence of any external stimulus input” (Munzert, Lorey, & Zentgraf, 2009, p.307). Farah (1984) has proposed a component model of imagery. According to this model a mental image can be generated either by retrieval from long-term memory or a perceptual encoding process. This image is accessible to cognition and can be detected or inspected, e.g. described, rotated or matched with long-term memory. Imagery can pertain to different objects like three-dimensional cubes or human movements. In early experiments using three-dimensional drawings of cubes of different spatial orientation, Shepard and Metzler (1971) found that speed of recognition is linearly related to angle of rotation indicating that the participants perform mental rotations of the cubes. Kosslyn, Digirolamo, Thompson, and Alpert (1998) showed that different neural mechanisms are involved in the mental rotation of cubes versus hands. The authors found a “substantial activation in motor areas for the hands task, including primary motor cortex M1, premotor cortex, and the posterior parietal lobe” (Kosslyn et al., 1998, p.157). This experiment, among others (Munzert, Lorey & Zentgraf, 2009), clearly confirm the close relationship of motor imagery and motor preparation. Therefore, it is not surprising that motor imagery also plays an important role in motor learning. Furthermore there are gender differences in visual and motor imagery in favour of males (e.g., Hoyek et al., 2009).

The purpose of the present paper is to introduce and discuss an approach to computer-assisted assessment of motor imagery. First the basics of motor imagery are addressed. After discussing existing methods for assessing motor imagery we introduce our own method based on computer programs.

Motor Imagery and Internal Representation of Movement

According to Farah (1984) imagery comprises a set of procedural components (encoding, generation, detection and inspection) operating on representations in the information processing system. The term 'representation' denotes a "formal system for making explicit certain entities or types of information, together with a specification of how the system does this" (Marr, 1982, p.20). The structure of a representation can be described by (complete) sets of represented and representing elements and the relations within and between the sets (Dalenoort, 1990, Wiemeyer, 2001b; see Figure 1). When applying the term 'representation' to the human information processing system, different levels (e.g., central nervous system and cognitive system), codes (e.g., vision and proprioception), functions (e.g., planning and execution), and temporal dynamics (e.g., short versus long term stability) are distinguished (Wiemeyer, 2001b). The term 'internal representation' means that the representation is located within the human organism, e.g., the central nervous or the cognitive system. Examples for external representations are Hard disks or DVDs.

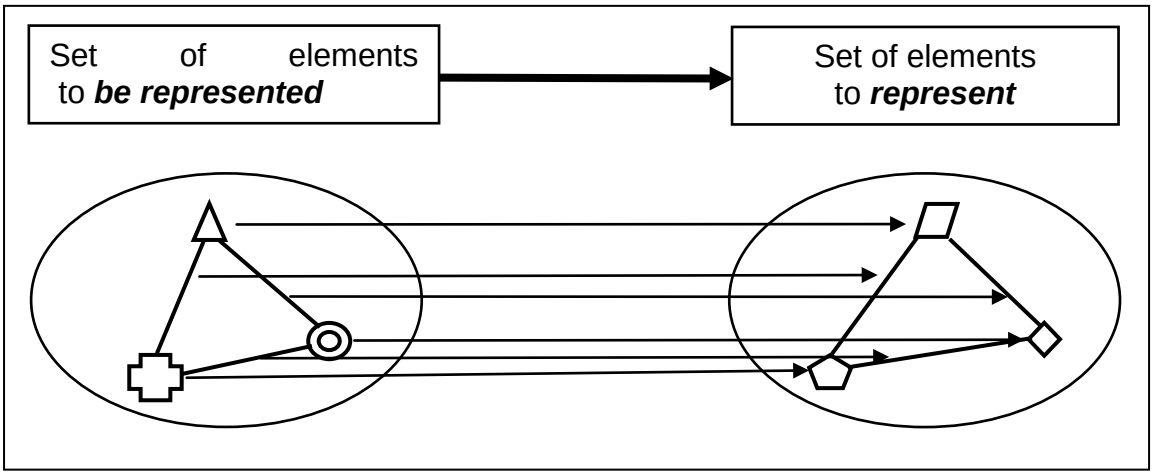

Figure 1. Representation as relation of two sets (from Wiemeyer, 2001b, p.2).

Motor imagery can be considered as an explicit process operating on representations of movements. The term 'explicit' denotes the fact that participants are (at least partly) aware of motor imagery and are therefore able to report about their representations.

Motor imagery is a cognitive correlate of motor learning (cf. Blischke, 1988, p.3; also Daugs, Blischke, Olivier, & Marschall, 1989; Hoyek et al., 2009; Munzert, Lorey, & Zentgraf, 2009). One important function of motor imagery is a kind of individual prescription or plan for the subsequent execution of the respective movement. Motor imagery is a structured conceptual representation which can function as an organisational framework for movement planning and execution. Although the term 'imagery' implies primarily visual aspects of internal representations further perceptual, motor and cross-perceptual components have to be considered:

- Acoustic or auditory components (e.g., sound caused by own movements)
- Proprioceptive components comprising tactile, vestibular, and kinaesthetic information (e.g., position information from sensors located in the joints)
- Verbal components (e.g., names for actions and movement segments)
- Abstract cross-modality reference concepts (e.g., the concept 'backward somersault')

Recent findings in movement science and neurophysiology (e.g., Schack & Mechsner, 2006;

Munzert, Lorey & Zentgraf, 2009) confirm the important role of anticipated sensory consequences for the cognitive control of motor learning. Visual representations of space seem to play an important role particularly in the beginning of motor learning (e.g., Kovacs & Shea, 2006; Panzer et al., 2007). As movements are changes of the body and body parts in space and time, timing aspects also play an important role (e.g., Hoyek et al., 2009). Concerning representation of space and time, there are well-known gender differences in favour of males, particularly in mental rotation (Linn & Petersen, 1985; Voyer, Voyer, & Bryden, 1995; Hoyek et al., 2009).

In the course of motor learning the structure of motor imagery can change in numerous ways. These changes extend to elements or their relations (Wiemeyer, 2001a). For instance, particular elements can be eliminated or sharpened. Another option is to integrate elements into higher-order structures or abstract rules (e.g., Zimmer & Körndle, 1988).

We can distinguish four types of changes (Wiemeyer, 2001a):

- It is common sense that at the beginning of the learning process knowledge is only crude and non-specific because the learner is lacking specific motor experience. The components of representations may become increasingly differentiated, specific and concrete as learning proceeds and subjective experiences increase. One important finding is that motor control becomes increasingly effector-dependent (e.g., Park & Shea, 2005).
- As a further result of learning abstractions may occur. Schmidt (1975), e.g., assumes that during learning we establish rules for producing and evaluating our movements. In our studies of learning gymnastic and skiing skills we actually found ‘if - then’ and ‘the more - the less’ rules.
- The relative significance of particular components may change. Müller (1995) states, that in the beginning of learning cognitive processes like imagery, perception, attention, anticipation and transformation with a strong emphasis on spatial aspects are very important, whereas in later stages adaptations of the motor system may gain primary importance.
- In the course of learning the formation of information units may take place, e.g., new action couplings (e.g., Gröben, 1997) and upward integration of basic units with downward constraints (Zimmer & Körndle, 1988).

One important means to enhance motor imagery often used in practice is applying rhythmic aids like instruments, voice or music. The rationale is to add a connecting link between actions and operations required for the respective motor skill and to convey additional information concerning timing and dynamics of the skill (Karageorghis & Priest, 2008). In an experiment, Effenberg (2005) showed that sonified information as “additional convergent auditory information can enhance perception accuracy … [and] reproduction accuracy of sports movements” (p.58), respectively. When hearing the sonification of a Force curve of countermovement jumps (CMJ) subjects were able to both better estimate and reproduce CMJs compared to the non-sonification condition.

Assessing Motor Imagery – Research Options

Of course, the actual structure of motor imagery is not accessible directly. As a consequence research can only try to reconstruct the structure of motor imagery based on the observable behaviour of the participants.

In principle psychological phenomena like motor imagery can be assessed on three levels: subjective experience, overt behaviour, or physiological responses. Because many physiological responses are either difficult to measure (e.g., central nervous system: electroencephalography [EEG], positron emission tomography [PET], functional magnetic resonance imaging [fMRI], or transcranial magnetic stimulation [TMS], see Munzert, Lorey, & Zentgraf, 2009 for a review) or only indirectly related to motor imagery (e.g., peripheral responses: heart rate or skin conductance), many research projects in motor learning concentrate on behaviour and reports. This does not mean that physiological measures are not valuable. Munzert, Lorey, and Zentgraf (2009) document the important contributions of neurophysiological studies to the basic understanding of motor imagery. One important finding is that imagery, planning, and execution of movements share similar neural representations:

> ... overlap of neural representations is not just found between motor imagery and motor execution. It also emerges when other cognitive motor processes such as movement observation, action planning, and action verbalization are compared with motor execution. (Munzert, Lorey, & Zentgraf, 2009, p.309)

However, these kind of studies can only contribute partly to the functional structure of motor imagery. In this regard behavioural measures and (verbal) reports may deliver more information about the functional significance of motor imagery.

Figure 2 illustrates that two general approaches can be applied to assess motor imagery at the behavioural or subjective level: either tests or asking questions. As can be seen in Figure 2, performance tests can be applied in order to assess the execution of the particular movement. The quality of execution can be measured by means of a centimeter-gram-second (cgs) or scoring system. The idea is that the quality of movement execution somehow corresponds to the structure of motor imagery.

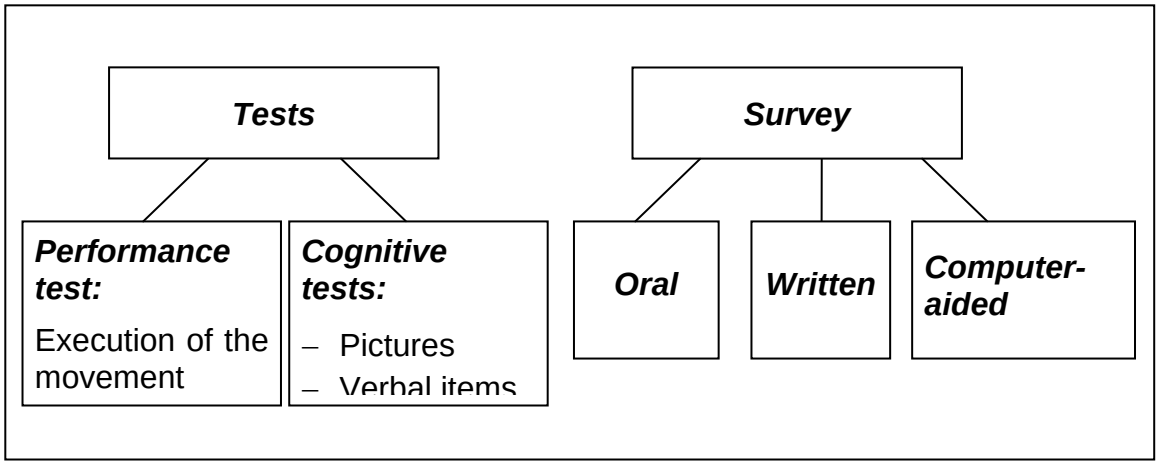

Figure 2. Research options of assessing motor imagery (according to Wiemeyer, 2001b, p.8).

A second test option is to use pictures and/or verbal items. The participant has to select and arrange these items in the correct way. An example of a cognitive drag-and-drop recognition test is illustrated in Figure 3.

As can be seen in Figure 3 the participant has to select the appropriate pictures (left part of the figure) and arrange them in the correct order. The test can also contain pictures that are not relevant to the respective skill in order to increase the validity of the test.

Surveys can be performed as oral, written or computer-aided procedures. The method proposed

by Schack (2001) is an example for a sophisticated computer-aided procedure. First, concepts have to be sorted according to similarity (split paradigm). Then a multi-stage data processing is performed in order to establish the individual structure of the motor imagery. This so-called 'structure-dimensional analysis' (SDA) comprises a cluster analysis, a factor analysis, and the analysis of inter- and intra-individual invariances.

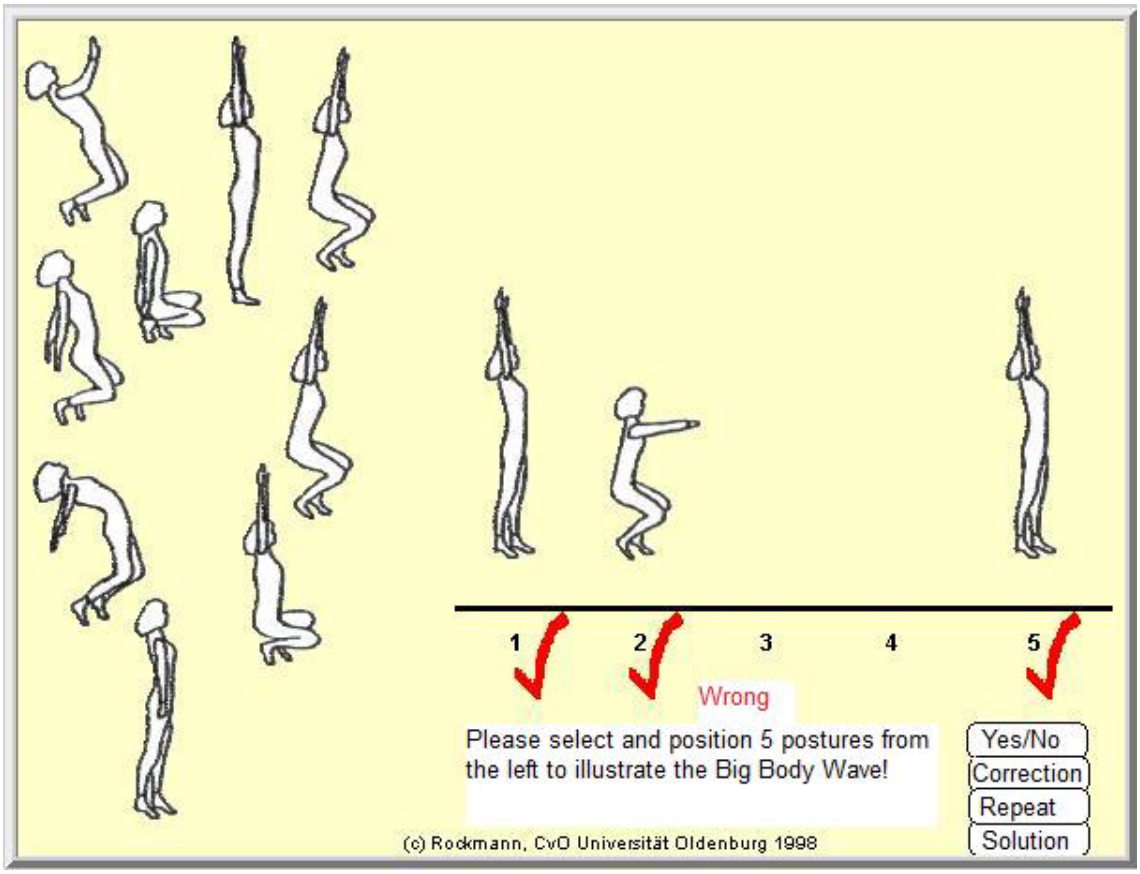

Figure 3. Example of a picture selection test (adapted from Rockmann, 1998).

Computer-Aided Selection Tests (CAST)

The current procedures for assessing motor imagery share one problem: The process of (re)construction of motor imagery is neglected. This means a considerable loss of information, because it may be very important to know how much time elapses for deliberating (cognitive time), which time is needed for just executing the decision (motor time), if and how often wrong decisions are corrected, which elements of the movement are reconstructed first (e.g., primacy and recency effects) etc. Therefore we developed a computer-aided selection test (CAST) paradigm that allows for assessing this information. According to Figure 2, the CAST is a cognitive test using pictures or verbal items.

The basic principle is to show visual or text material from which the correct components are selected by drag and drop actions. The software notes, which component is selected, how long it takes to drag the component to the target area, which corrections are made and saves all the relevant information in a text file for latter analysis. There are two versions of the CAST: a visual and a text version. In the next section both versions are described in detail.

CAST-P (visual version)

Figure 4 shows a screenshot of the computer-aided picture selection test (CAST-P).

The participant has to select the appropriate pictures from the selection areas (Figure 4, lower part) and to drag them to the correct target fields (Figure 4, upper part). Table 1 shows a part of the protocol generated by the CAST-P software.

- The test was started at 12.55 and was finished at 13.00.
- Test duration was 313.8 seconds, i.e., 5:13.8 minutes.
- In tact (T) 1 picture 2 ('P2') was selected from selection field (SF) 7 after 6.7 s and positioned in target field (TF) 1 after 7.5 s.
- The whole picture selections in the first tact (T1) were cancelled after 29.7 minutes.
- The final selection shows no errors in tacts 1, 3, and 5, but two, two and four errors in tacts 2, 4, and 6 , respectively. Therefore, 17 of 25 pictures (68%) were correctly selected.

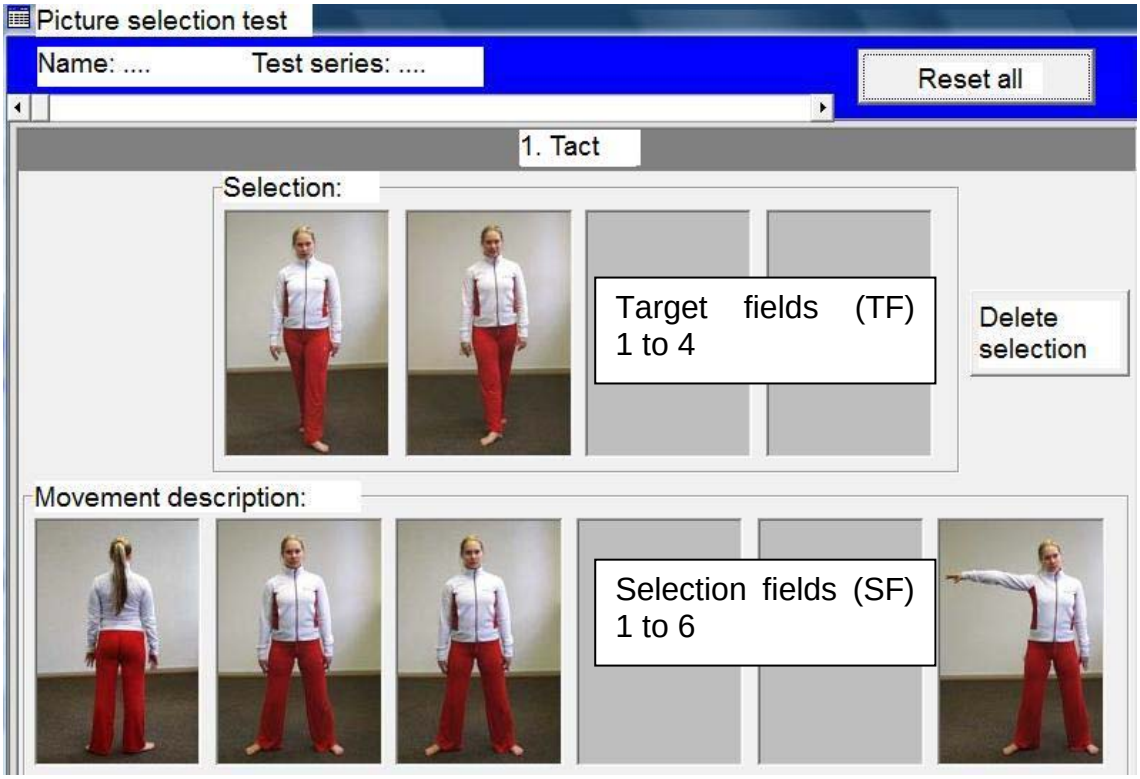

Figure 4. GUI of the CAST-P. Upper part: target fields; lower part: selection fields. The task is to select the pictures from the lower part and to drag them to the correct target fields in the upper part.

In general, the software notes and stores the following data:

- Starting and finishing date and time.
- Time of picture selection (mouse click)
- Time of picture positioning (release of mouse button)
- Time of cancellations and corrections
- Positioning of the picture in the wrong tact
- Final selection

Based on these data the following data can be calculated:

- Total time for test completion
- Partial times for test parts (tacts)
- Motor time as the difference of picture selection and picture positioning
- Cognitive time as difference of positioning the previous picture and selecting the next one
- Order of tact and picture selection
- Number and distribution of corrections
- Number and distribution of errors

The application of CAST allows a fine-grained procedural analysis of the motor imagery (re)construction. Based on existing models we expect that in the course of motor learning the quality of selections will increase, while the corrections, cognitive time and total test time will decrease.

Table 1. Selection from an original protocol file; Legend: P – picture ID, T – tact, SF – selection field, TF – target field.

Protocol		**Explanation**
1. General information		
Starting time:	03.04.2011 12:55:00	
Subject: ...		
...		
Test finished at:	03.04.2011 13:00:21	
2. Procedural information		
P2 / T1 / SF7 selected after:	6.7 s.	Picture 2 chosen from selection field 7
P2 / T1 / TF1 positioned after:	7.5 s.	Picture 2 dropped to target field 1
...		
P1 / T1 / TF3 reset after:	18.3 s.	Selection TF 3: cancelled
...		
Tact 1 reset after:	29.7 s.	Whole tact 1: cancelled
...		
Tact 1 complete after:	78.3 s.	Completion of T1: after 78.3 s
Whole test complete after: 313.8 s.		Completion of test: after 313.8 s
3. Final result		
Final selection:		
Tact 1: SF1 = P1 / SF3 = P2 / SF5 = P3 / SF6 = P4 / SF7 = P5		Tact 1: correct

Tact 2: SF1 = P6 / **SF3 = P9** / SF5 = P8 / **SF7 = P7**	Tact 2: P9 & P7 – mixed up
Tact 3: SF1 = P10 / SF3 = P11 / SF5 = P12 / SF7 = P13	Tact 3: correct
Tact 4: **SF1 = P20** / SF3 = P15 / **SF5 = P22** / SF7 = P17	Tact 4: 2 errors (wrong pictures)
Tact 5: SF1 = P18 / SF5 = P19	Tact 5: correct
Tact 6: SF1 = P20 / **SF3 = P23** / SF5 = P22 / **SF7 = P21** / **SF9 = P43** / **SF11 = P26**	Tact 6: 4 errors

CAST-T (text version)

Analogous to the CAST-P the CAST-T uses equivalent verbal labels. Verbal labels denote actions like step to the left, extend right/left arm laterally, or 180° rotation to the left with the left leg.

The protocol file looks just like the file illustrated in Table 1. One has just to substitute the pictures by verbal items.

Application of the CAST: Experiment in Motor Learning

Methods

First results of applying the tests to motor learning were obtained with an experiment involving the learning of a sequence of gymnastic skills (sample: N = 80). The purpose of this experiment was to investigate the effects of Rhythmic Verbal Cues (RVC) on motor performance and internal representations during initial learning (Angert, Bund, & Wiemeyer, 2009). In general rhythm is considered to have positive effects on motor imagery, motor performance and motor perception (Effenberg, 2005).

Based on existing evidence (Magill & Schoenfelder-Zohdi, 1996; Angert & Wiemeyer, 2001) we hypothesized that the effects of RVC on performance and cognitive representations when learning a dance sequence depend on the mode of instruction (Model Instruction [MI] versus Verbal Instruction [VI]). Because visual instruction compared to verbal instruction seems to promote a more differentiated motor imagery during initial learning, a more pronounced positive effect of rhythmic instruction is expected for the VI condition.

Participants: Eighty university students (40 women and 40 men) with no prior experience in dancing volunteered to participate in the experiment (age: M = 23.96 yrs, SD = 4.0; semesters: M = 2.67, SD = 2.80).

Procedure: According to a 2 x 2 quadratic experimental design with a Mode of Instruction factor (Model Instruction [MI] versus Verbal Instruction [VI]) and a Rhythm factor (Rhythmic Verbal Cues [RVC] versus no RVC) four experimental groups were examined: MI-plus-RVC, MI-only, VI-plus-RVC, and VI-only. Under the premise of gender balance, participants were randomly assigned to one of the four experimental groups.

The acquisition phase consisted of two acquisition sessions (AS) separated by an interval of one week. Each acquisition session was divided into three acquisition blocks (AB). Each

acquisition block was structured as follows: instruction phase – CAST – 5 practice trials (PT) without KR. Subjects performed this sequence three times per session. The first instruction phase consisted of six repetitions of the group-specific instruction whereas the second to sixth instruction phase included just two repetitions, respectively.

In the instruction phase the MI groups received a video presentation of an expert model performing the sequence of the gymnastic skills six times in the first and two times in the following instruction phases, respectively. Participants of the VI groups watched a power-point presentation on a computer screen providing a detailed verbal description of the gymnastic skill six times in the first and two times in the following phases , respectively. In addition, the MI-plus-RVC and VI-plus-RVC group received a rhythmic instruction as spoken rhythmic verbal cues (RVC) consisting of one- or two-word phrases such as 'vor – vor – seit-seit – stehn' (English: 'ahead – ahead – sideward-sideward – stand'; Landin, 1994). The RVC was added to the model and the verbal instruction during the fifth and sixth repetition of the instruction in the first instruction phase and during the second repetition in the second to sixth instruction phase, respectively.

Immediately after the instruction phase participants performed the instruction-related version of the CAST (MI groups: CAST-P, VI groups: CAST-T) followed by five practice trails (PT) without extrinsic feedback. The retention and transfer phase were conducted one day after the second acquisition session. During retention the participants performed the instruction-related CAST. As a transfer test the MI groups performed the CAST-T, whereas the VI groups completed the CAST-P.

Selected Results

The results concerning the performance score, the number of corrections and the time needed for deliberation during the reproduction of the movement sequence in the CAST are presented in Figures 7, 8, and 9, respectively. These parameters are the most important measures of overall performance, accuracy, and speed of the reconstruction of motor imagery.

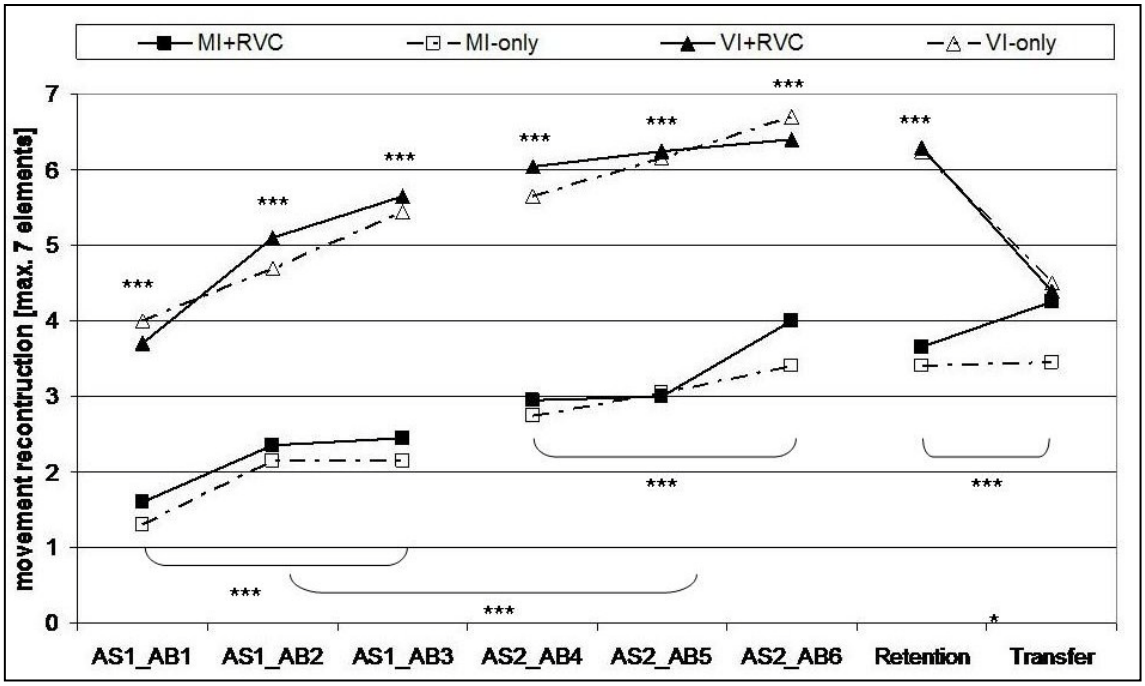

Figure 5. Performance score of the reproduction of the movement sequence in the CAST for the four experimental groups during acquisition, retention, and transfer phase (*p<.05; ***p<.001). Legend: AS – Acquisition session; AB – Acquisition block; MI – Model instruction; VI – Verbal instruction; RVC – Rhythmical verbal cues.

Acquisition phase data were analyzed in 2 (Mode of Instruction) x 2 (Rhythm) x 2 (Acquisition Session [AS]) x 3 (Acquisition Bock [AB]) ANOVAs, with repeated measures on the factors AS and AB (see Table 2).

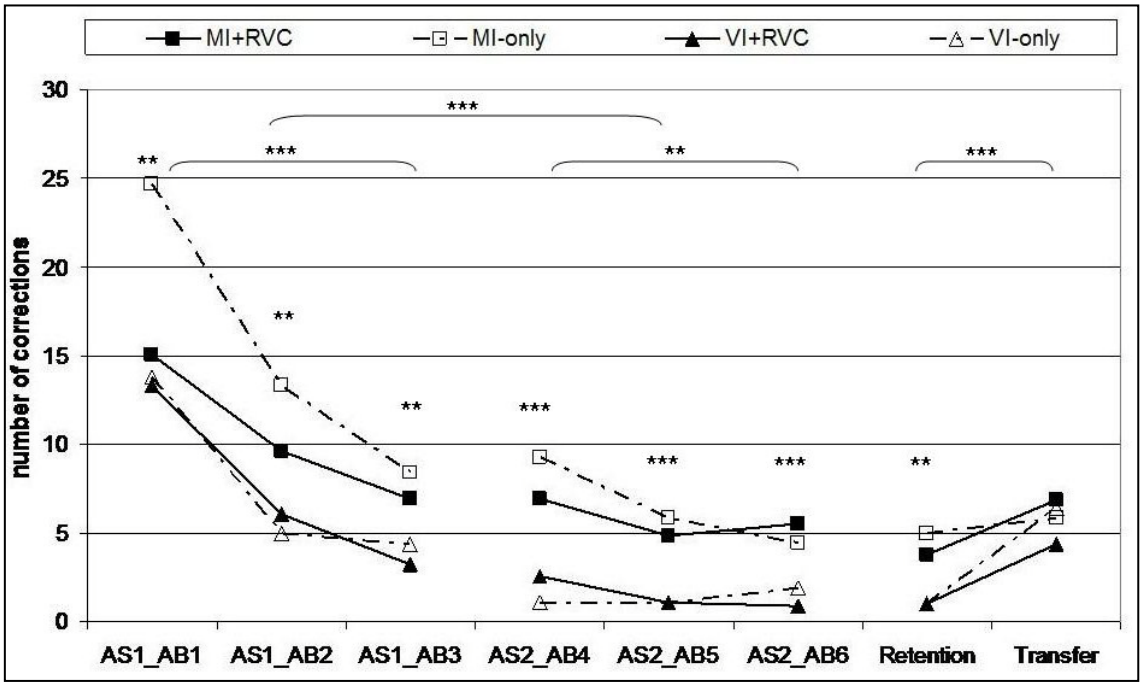

Figure 6. Number of corrections in the CAST for the four experimental groups during acquisition, retention, and transfer phase (**p<.01; ***p<.001).
Legend: AS – Acquisition session; AB – Acquisition block; MI – Model instruction; VI – Verbal instruction; RVC – Rhythmical verbal cues.

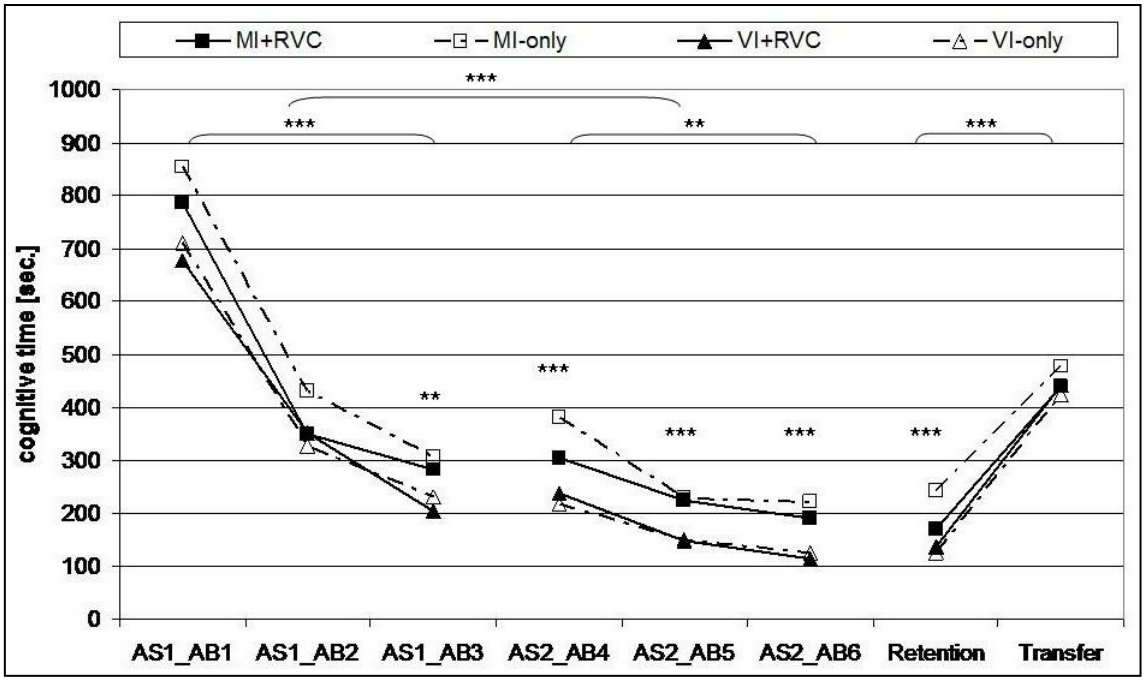

Figure 7. Time needed for deliberating in the CAST for the four experimental groups during acquisition, retention, and transfer phase (**p<.01; ***p<.001). Legend: AS – Acquisition session; AB – Acquisition block; MI – Model instruction; VI – Verbal instruction; RVC – Rhythmical verbal cues.

The reproduction of the movement sequence (Figure 5) improved during the acquisition phase in all groups, while both VI groups outperformed both MI groups.

Analysis of the number of corrections (Figure 6) revealed a significant improvement of all groups with the major improvement occurring in the first acquisition session. Again, both VI groups outperformed both MI groups in the acquisition phase.

Analysis of the time needed for deliberation (Figure 7) shows comparable results to the number of corrections, i.e., a significant improvement of all groups in the acquisition phase, particularly during the first acquisition session, and a significant Mode of Instruction effect in favour of the VI groups.

In addition 2 (gender) x 6 (acquisition blocks) ANOVAs were performed to test gender effects. Whereas no gender effects and no interactions of gender x acquisitions blocks were found for deliberation time and corrections ($Fs_{1,78} \leq 1.24$), a significant gender effect in favour of the women was found for the correct number of elements ($F_{1,78} = 5.01$; $p = .028$; $\eta^2 = .060$).

Table 2. Selected results of ANOVA (acquisition phase). Legend: MI – mode of instruction; AS – acquisition session; AB – acquisition blocks.

Factor	No. of correct elements			No. of Corrections			Cognitive time [s]		
	F	η^2	ε	F	η^2	E	F	η^2	ε
Treatment									
MI	81.31#	0.52	1.03	26.09#	0.26	0.59	10.46	0.12	0.37
Rhythm (R)	0.28			2.10			0.87		
MI x R	0.07			2.05			0.59		
Repeated measures									
AS	84.01 #	0.53	1.05	93.00#	0.55	1.11	231.85#	0.75	1.75
AB	53.64#[1]	0.41	0.84	42.71#[2]	0.36	0.75	241.11#[3]	0.76	1.78
AS x AB	5.74+[4]	0.07	0.27	21.91#[5]	0.22	0.54	82.01#[6]	0.52	1.04

* p<.05; + p<.01; # p<.001

Retention and transfer phase data were analyzed in 2 (Mode of Instruction) x 2 (Rhythm) ANOVAs (see Table 3).

Table 3. Results of ANOVA (retention and transfer phase). Legend: MI – mode of instruction.

Factor	No. of correct elements			No. of Corrections			Cognitive time [s]		
	F	η^2	ε	F	η^2	ε	F	η^2	ε
Retention phase									
MI	50.57 #	0.40	0.82	12.03 #	0.14	0.41	16.47 #	0.18	0.47
Rhythm (R)	0.15			0.41			2.51		
MI x R	0.07			0.41			5.11 *	0.06	0.26
Transfer phase									
MI	2.10			0.45			0.32		
Rhythm (R)	0.71			0.13			0.04		
MI x R	1.18			1.13			0.36		

* p<.05; + p<.01; # p<.001

The significant Mode of Instruction effect for reproduction of the movement sequence, number

[1] $\varepsilon_{\text{Huynh-Feldt}} = .858$ ($\varepsilon_{\text{Greenhous-Geisser}} > .75$)

[2] $\varepsilon_{\text{Greenhous-Geisser}} = .717$

[3] $\varepsilon_{\text{Huynh-Feldt}} = .902$ ($\varepsilon_{\text{Greenhous-Geisser}} > .75$)

[4] $\varepsilon_{\text{Huynh-Feldt}} = .917$ ($\varepsilon_{\text{Greenhous-Geisser}} > .75$)

[5] $\varepsilon_{\text{Greenhous-Geisser}} = .716$

[6] $\varepsilon_{\text{Huynh-Feldt}} = .804$ ($\varepsilon_{\text{Greenhous-Geisser}} > .75$)

of corrections and time needed for deliberation in favour of the VI groups still existed in the retention test (see Figures 6 to 8).

Furthermore, there was a significant Mode of Instruction x Rhythm interaction, which was caused by the significantly shorter deliberation time of the MI-plus-RVC group compared to the MI-only group. There is no significant difference between the VI groups.

The specificity of the prescriptive knowledge was tested in the transfer test by switching to the non-instruction-related version of the CAST. Analysis detected no significant effect of Mode of Instruction and Rhythm for reproduction of the movement sequence, number of corrections and time needed for deliberation.

2 (Mode of Instruction) x 2 (Rhythm) x 2 (measuring time [MT]) ANOVAs with repeated measures on the factor MT (see Table 4) yielded a significant main effect of MT for reproduction of the movement sequence from retention to transfer test, which was caused by the VI groups whose performance declined significantly while the model groups performed on the same level (Figure 5).

Analysis of number of corrections and time needed for deliberation revealed significant main effects for Measuring Time indicating an increase in the number of corrections and a longer time for deliberation in the transfer test from retention to transfer test (see Figures 7 and 8).

Table 4. Selected results of ANOVA for effects of treatment and test specificity. Legend: MI – mode of instruction; MT – Measuring Time.

Factor	**No. of correct elements**			**No. of Corrections**			**Cognitive time [s]**		
	F	η^2	ε	F	η^2	E	F	η^2	ε
Main effects									
MI	22.26#	0.23	0.54	5.35*	0.07	0.27	3.63		
Rhythm (R)	0.50			0.36			0.54		
MT	16.34#	0.18	0.46	17.06 #	0.18	0.47	146.93 #	0.66	1.39
Interactions									
MI x R	0.60			0.22			1.71		
MI x MT	33.57#	0.31	0.66	2.47			1.16		
R x MT	0.29			0.01			0.19		
MI x R x MT	0.89			1.90			0.10		

* p<.05; + p<.01; # p<.001

Again 2 (gender) x 2 (retention & transfer block) ANOVAs were performed to test gender effects. Whereas no gender effects and no interactions of gender x retention/transfer blocks were found for deliberation time and corrections ($Fs_{1,78} \leq 1.5$), a significant gender effect in favour of the women was found for the correct number of elements ($F_{1,78} = 4.48$; $p = .037$; $\eta^2 = .054$).

Discussion

The CAST clearly showed that all test scores gradually improved during acquisition. However, rate of improvement differed between groups and tests:

- The performance score increased from about 4 to 6.5 elements in the MI groups and from 1.5 to 4 in the VI groups.
- Numbers of corrections decreased from 15/25 to 5/7 in the MI groups and from 14 to 1 in the VI groups.
- Cognitive time decreased from 800 to 200 s in the MI groups and from 700 to 100 s in the VI groups.

Whereas the performance score results could have been obtained with a traditional test, corrections and cognitive time are unique to the CAST, i.e. a dramatic speeding up by factor 4 to 7 and a substantial gain in correct choice by factor 3 to 14. All measures show a clear superiority of the VI groups performing the text version of the CAST.

In the retention phase all measures were stable. Therefore the CAST documents strong learning effects.

However, in the transfer test where participants of the MI groups switched to the CAST-T version and the VI groups had to perform the CAST-P version a differential picture emerged: Whereas cognitive time and corrections increased in all groups, only the VI group showed a dramatic decrease in the number of elements. The transfer score of the VI group was well above the retention score of the MI group. The MI group showed a slightly better performance corresponding to the initial acquisition scores of the VI group. This result can be considered as a hint to a selective cross-modal transfer from verbal to visual representation.

However, the missing correspondence of CAST data and performance scores indicates that the two tests were not equivalent. The CAST-P version seems to be more difficult than the CAST-T version.

Furthermore, the CAST allowed us to detect a positive learning effect of rhythm on cognitive time in the MI group. Rhythmic instruction supported a faster reconstruction of the CAST-P elements without impairing precision.

The CAST also revealed gender differences in favour of women concerning the correct selection of movement elements. At a first glance, this seems to be in contradiction to the well-known disadvantages of women. There are several possible explanations. Keeping in mind that gender differences in spatial abilities are task-specific and women are superior in spatial memory (e.g., Ecuyer-Dab & Robert, 2004) the CAST tasks may have required this kind of memory, for example, recalling the positions of arms and legs. A second possible reason may be the different domain-specific perceptual expertise with compository sports deemed female like dance, rhythmic gymnastics etc. (Calvo-Merino, Glaser, Grèzes, Passingham, & Haggard, 2005; Mennesson, 2009).

There are, however, still considerable restrictions. The CAST just assesses symbolic representations of actions and the correct order and (rough) timing of actions. The detailed structure of motor imagery concerning exact timing und tuning of actions cannot be measured, as well as the kinaesthetic components.

Conclusion

The CAST offers new options for assessing the visual and verbal components of motor imagery. The procedure of (re)constructing these components can be studied in much more detail. Therefore beyond the results of the test we can also analyse duration of parts of the task, cognitive and motor components of the tasks, order of completion, and the structure of

corrections. As a consequence we gain much more information about motor imagery as compared to the existing test procedures.

The proposed results show that the developed CAST versions were able to detect the expected dynamics of motor imagery and, at least partly, instruction-related differences. An interesting finding is the facilitating effect of RVC in the MI group concerning deliberation time. Therefore a much more detailed analysis of motor imagery was possible compared to a simple procedure using conventional tests.

A next step may be to improve equivalence of the two versions and to develop more demanding tests for motor imagery. The existing tests provide verbal or visual items to select. In a way, this procedure requires that the participants recognise the particular item and its correct order within all items. It would be much more demanding to force the participant to actively reconstruct key postures of the movement using, for instance, a real or virtual puppet and to reconstruct the movement based on these postures, just like keyframe animations. This procedure means a shift from recognition to more demanding recall tests.

References

Angert, R., Bund, A., & Wiemeyer, J. (2009). Rhythmic verbal instruction and motor learning. In A. Baria, E.H. Nabli, M. Madani, A. Essiyedali, M. Aragon, & A.E. Quartassi (Eds.) Meeting new challenges and bridging cultural gaps in sport and exercises psychology. Proceedings of the 12th World Congress of Sport Psychology, International Society of Sport Psychology (ISSP). Marrakesh, Marocco.

Angert, R., & Wiemeyer, J. (2001). Der Einfluss rhythmischen Sprechens auf das Erlernen einer gymnastischen Bewegung [The effect of rhythmic speech on the learning of a gymnastic movement]. In J. R. Nitsch & H. Allmer (Eds.), Denken - Sprechen - Bewegen [Thinking – Speaking – Moving] (pp. 186-192). Köln: bps.

Calvo-Merino, B., Glaser, D., Grèzes, J., Passingham, D., & Haggard, P. (2005). Seeing what you can do: the dancers brain. In J. Birringer & J. Fenger (Eds.), Tanz im Kopf [Dance in the head] (pp. 201-209). Münster: LIT Verlag.

Dalenoort, G.J. (1990). Towards a general theory of representation. Report "Mind and Brain", No. 31. Bielefeld: ZiF.

Daugs, R., Blischke, K., Olivier, N. & Marschall, F. (1989). Beiträge zum visuomotorischen Lernen im Sport [Contributions to visual-motor learning in sport]. Schorndorf: Hofmann.

Ecuyer-Dab, I. & Robert, M. (2004). Have sex differences in spatial ability evolved from male competition for mating and female concern for survival? *Cognition, 91*, 221–257.

Effenberg, A. O. (2005). Movement Sonification: Effects on Perception and Action. *IEEE Multimedia, Special Issue on Interactive Sonification, 12*(2), 53-59.

Farah, M.J. (1984). The neurological basis of mental imagery: A componential analysis. *Cognition, 18*, 245–272.

Gröben, B. (1997). Wirkdimensionen verbaler Instruktionen [Effect dimensions of verbal instructions]. In E. Loosch, & M. Tamme (Eds.), Motorik – Struktur und Funktion [Motor activity – Structure and Function] (pp. 236-240). Hamburg: Czwalina.

Hikosaka, O., Nakamura, K., Sakai, K. & Nakahara, H. (2002). Central mechanisms of motor skill learning. *Current Opinion in Neurobiology, 12*, 217-222.

Hoyek, N., Cahmpely, S., Collet, C., Fargier, P. & Guillot, A. (2009). Age and gender-related differences in the temporal congruence development between motor imagery and motor performance. *Learning and Individual Differences, 19*, 555–560.

Karageorghis, C. & Priest, D.-L. (2008). Music in Sport and Exercise: An Update on Research and Application. *The Sport Journal, 11* (3).

Kosslyn, S.M., Digirolamo, G.J., Thompson, W.L., & Alpert, N.M. (1998). Mental rotation of objects versus hands: Neural mechanisms revealed by positron emission tomography. *Psychophysiology, 35*, 151–161.

Kovacs, A. & Shea, C. H. (2006). The coding of movement sequences. *Journal of Sport & Exercise Psychology. Supplement, 28*, 104-105.

Landin, D. (1994). The role of verbal cues in skill learning. *Quest, 46*, 299-313.

Linn, M.C. & Petersen, A.C. (1985). Emergence and characterisation of sex differences in spatial ability: A meta-analysis. *Child Development, 56*(6), 1479-1498.

Magill, R. A., & Schoenfelder-Zohdi, B. (1996). A visual Model and knowledge of performance as source of information for learning a rhythmic gymnastics skill *International Journal of Sport Psychology, 27*, 7-22.

Marr, D. (1982). *Vision. A computational investigation into the human representation and processing of visual information*. New York: W. H. Freeman.

Mennesson, C. (2009). Being a man in dance: Socialization modes and gender identities. *Sport in Society, 12*(2), 174–195.

Müller, H. (1995). *Kognition und motorisches Lernen* [Cognition and Motor Learning]. Bonn: Holos.

Munzert, J., Lorey, B., & Zentgraf, K. (2009). Cognitive motor processes: The role of motor imagery in the study of motor representations. Brain Research Reviews, 60, 306-326.

Panzer, S., Büsch, D., Shea, C.H., Mühlbauer, T., Naundorf, F., & Krüger, M. (2007). Dominanz visuell-räumlicher Codierung beim Lernen von Bewegungssequenzen. [Dominance of visual-spatial coding when learning movement sequences] *Zeitschrift für Sportpsychologie* [Magazine of Sports Psychology], *14*(3), 123-129.

Park, J.-H. & Shea, C. H. (2005). Sequence learning: Response structure and effector transfer. *The Quarterly Journal of Experimental Psychology, 58A*, 387-419.

Rockmann, U. (1998). Illustration „Große Körperwelle“. Retrieved March 2, 2006, from http://www.uni-oldenburg.de/sport/bww2/Expmente/ onl_exp/kwelle/KW.html

Schack, T. (2001). On the structure of movement representations – Basic assumptions and methodical approach. *Motor Control and Learning in Sport Science,* 1-12.

Schack, T., Kneehans, E., & Lander, H.-J. (2001). Ein methodischer Zugang zur strukturdimensionalen Analyse mentaler Repräsentationen. [A methodic approach to the structure-dimensional analysis of mental representations] In J. R. Nitsch & H. Allmer (Eds.), Denken – Sprechen – Bewegen [Motor activity – Structure and Function] (pp. 144-147). Köln: bps.

Schack, T. & Mechsner, F. (2006). Representation of motor skills in human long-term-memory. *Neuroscience Letters, 391*, 77-81.

Schmidt, R.A. (1975). A schema theory of discrete motor skill learning. *Psychological Review 82*, 225-260.

Schmidt, R.A. & Lee, T.D. (2005). Motor control and learning: A behavioral emphasis (4th edition). Champaign, Ill: Human Kinetics.

Shepard, R.N. & Metzler, J. (1971). Mental rotation of three-dimensional objects. *Science, 171*(3972), 701-703.

Voyer, D., Voyer, S. & Bryden, M.P. (1995). Magnitude of sex differences in spatial abilities: A meta-analysis and consideration of critical variables. *Psychological Bulletin, 117*(2), 250-270.

Wiemeyer, J. (1994). *Interne Bewegungsrepräsentation.* [Internal representations of movements] Köln: bps.

Wiemeyer, J. (2001a). Bewußte Bewegungsrepräsentation – Komponenten, Zusammenhänge und Lerndynamik. [Conscious motor representations – components, relations, and learning dynamics] In J.R. Nitsch & H. Allmer (Eds.), Denken – Sprechen – Bewegen [Motor activity – Structure and Function] (pp. 131-137). Köln: bps.

Wiemeyer, J. (2001b). Conscious representations of movement: Structure and assessment. *Motor Control and Learning in Sport Science*, 1-12.

Zimmer, A.C., & Körndle, H. (1988). A model for hierarchically ordered schemata in the control of skilled action. *Gestalt Theory 10*, 85-102.

Mathematical and Computer Model of Sport Archery Bow and Arrow Interaction

Ihor Zanevskyy

Casimir Pulaski Technical University in Radom, Poland

Abstract

The aim of the research was to summarize a mathematical model of bow and arrow interaction in the vertical plane and to develop an appropriated computer model. A bow was modeled as a non-deformed riser and hinged to it two non-deformed limbs with Archimedean springs. Their stiffness as well, as an elasticity of a string was taken into account in a linear approach. An asymmetric bow scheme was considered. A stabilizer system was modeled as a construction of multi-rod cantilever flexible bars fixed to the riser. An arrow was modeled as a rod hinged to the string in a nock point. A mathematical model of bow and arrow interaction was created using Lagrange method as a system of ten differential equations and initial conditions. Correspondent Cauchy problem was solved using Runge-Kutta method and NDSolve programs from Mathematica package. The initial conditions were determined as solution of a static problem based on the bow model in a drawn situation. Correspondent system of non-linear algebraic equations were solved using Newton method with FindRoot program. The model shown its possibility to study main kinematical and kinetic parameters of bow and arrow interaction in the vertical plane. Results of modeling was presented in graphs.

KEYWORDS: ARCHERY, BOW, STABILIZER, ARROW, MODELING

Introduction

An archery sport bow consists of three main parts. They are a riser, limbs, and string (Figure A in Appendix 1). Additionally, there are few stabilizers (from one to five rods) and a sight mounted on the riser. An archery arrow consists of a shaft with a head, fletching, and a nock (Figure A2). A nock point on a string and a rest and a clicker in a central part of a riser serve to state an arrow position relatively a bow.

A bow and an arrow during their interaction are in a common space motion. Their displacements in the vertical plane (exactly to say, in projection to the vertical plane) and their dimensions are commensurable quantities. Their displacements in the lateral direction are significantly smaller. Therefore, it is reasonably to consider bow and arrow interaction in the vertical plane separately from the lateral motion.

The first attempt to the problem of archery bow modeling was done by Hickman (1937) with his model of a limb as a non-deformed rod hinged to a riser by an Archimedean spring. Marlow (1982) developed the model taking into account elasticity of a string. Kooi and Sparenberg (1980) developed a flexible bar model of a limb. Ohsima & Ohtsuki (2002) investigated static and dynamics of Japanese bow which is not traditionally equipped with a

stabilizer. An arrow was modeled as a mass concentrated in a nock point of a string.

Zanevskyy (2006) considered an arrow as a rod and took into consideration an asymmetry bow scheme and an angular displacement of a riser in the vertical plane relatively a grip point. Zanevskyy (2008) worked out a model of bow stabilization in the vertical plane. Park (2010) studded compound archery bow dynamics in the vertical plane assuming symmetrical deformations of limbs and ignoring stretching of a string. Zanevskyy & Zanevska (2009) developed a model of a multi-rod stabilizer as a system of cantilever flexible bars and studded their influence on the bow and arrow dynamics in the vertical plane.

Papers on a complex mathematical and computer model of a modern sport bow and arrow interaction in the vertical plane has not been published. The aim of the research was to summarize a mathematical model of bow and arrow interaction in the vertical plane and to develop an appropriated computer model.

Methods

Static model of a bow was created using methods of Engineering Mechanics. Correspondent system of non-linear algebraic equations was solved using Newton method. Dynamic model of bow and arrow common motion was created using Lagrange method. Correspondent Cauchy problem as a system of differential equations with initial conditions was solved using Runge-Kutta method. Calculations were done using FindRoot and NDSolve programs from Mathematica computer package.

Results

A bow was modeled as a non-deformed riser and hinged to it two non-deformed limbs with Archimedean springs. Their stiffness as well, as an elasticity of a string was taken into account in a linear approach. An asymmetric bow scheme was considered. A stabilizer system was modeled as a construction of multi-rod cantilever flexible bars fixed to the riser. An arrow was modeled as a rod hinged to the string in a nock point.

Two models were considered. The first one was a dynamic model of described bow and arrow interaction (internal ballistics of the arrow). The second one was a static model of a bow in a drawn situation as an initial position of the system.

Dynamic model

Mathematical model of bow and arrow interaction during their common motion in the vertical plane was presented as a system of Lagrange's equations regarding the generalized coordinates: ξ_A, η_A are longitudinal and transverse displacements of the arrow nock point A (Figure 1); ψ is an arrow's attitude angle relatively its longitudinal movement; κ is an angular displacement of a riser (and a stabilizer uni-bar too) which is measured from the axis $O\eta$ counterclockwise; θ_U, θ_L are virtual angles of upper and lower limbs respectively; q_c, q_b are displacements (as function of time) of free ends of the central and an upper stabilizer rods caused with a bend; q_ν, q_τ are bend displacements of a free end of a side stabilizer rod in ν and τ directions respectively (Figure 2). The first of them (ν) is a normal component to the rod axis as a displacement in the vertical plane upward when side rods lay in the same plane as a central rod $(\alpha = 0)$ or outside a bow when side rods are inclined $(\alpha \neq 0)$. The second component (τ) is a displacement normal to the vertical plane of the rod inside a bow.

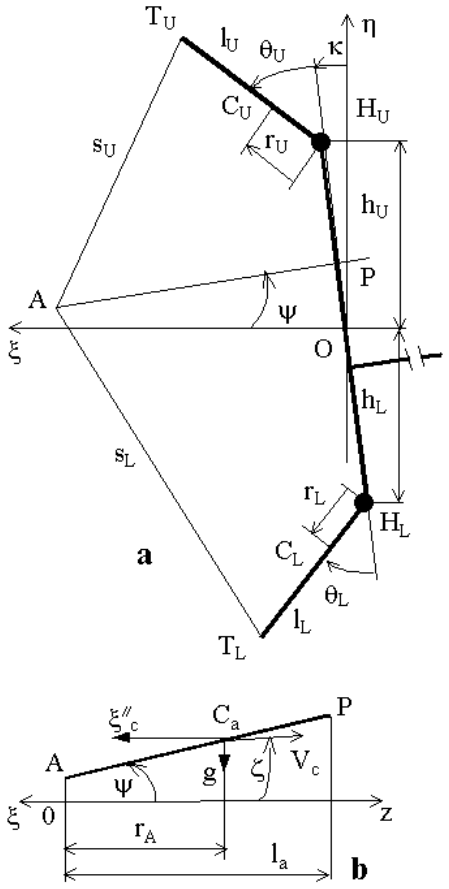

Figure 1. Dynamic scheme of a bow model (a); scheme model of an arrow (b).

The Lagrange's equations are:

$$\left\{\begin{matrix} I_H + I_U + I_L + m_U h_U^2 + m_L h_L^2 + I_V + m_V\left(x_V^2 + y_V^2\right) \\ + I_{cm} + I_{dm} + I_{bm} + I_{cM} + I_{dM} + I_{bM} \end{matrix}\right\}\ddot{\kappa}$$

$$+ m_U r_U h_U\left[b_1\left(\ddot{\theta}_U + 2\ddot{\kappa}\right) - b_2\left(\ddot{\theta}_U + \ddot{\kappa}\right)^2\right] -$$

$$m_L r_L h_L\left[b_3\left(\ddot{\theta}_L - 2\ddot{\kappa}\right) - b_4\left(\ddot{\theta}_L - \ddot{\kappa}\right)^2\right] + I_U\ddot{\theta}_U - I_L\ddot{\theta}_L$$

$$+ 2m_d\left(Q_{\nu m}\ddot{q}_\nu + Q_{\tau m}\ddot{q}_\tau\right) + 2M_d\left(Q_{\nu M}\ddot{q}_\nu + Q_{\tau M}\ddot{q}_\tau\right) +$$

$$\left(m_c Q_{cm} + M_c Q_{cM}\right)\ddot{q}_c + \left(m_b Q_{bm} + M_b Q_{bM}\right)\ddot{q}_b +$$

$$e_U\left[S_2\left(b_1 l_U + h_U\right) - S_1 b_2 l_U\right] - e_L\left[S_4\left(b_3 l_L + h_L\right) + S_3 b_4 l_L\right] = 0;$$

$$I_U\left(\ddot{\theta}_U + \ddot{\kappa}\right) + m_U r_U h_U b_1\ddot{\kappa} + c_U\left(\theta_U + \varphi_U\right) + e_U l_U\left(S_{U\xi} b_1 - S_{U\eta} b_2\right) = 0;$$

$$I_L\left(\ddot{\theta}_L - \ddot{\kappa}\right) - m_L r_L h_L b_3\ddot{\kappa} + c_L\left(\theta_L + \varphi_L\right) + e_L l_L\left(S_{L\xi} b_3 + S_{L\eta} b_4\right) = 0;$$

$$\left(\frac{33}{140}m_c + M_c\right)\ddot{q}_c + \left(m_c Q_{cm} + M_c Q_{cM}\right)\ddot{\kappa} + c_c q_c = 0;$$

$$\left(\frac{33}{140}m_d + M_d\right)\ddot{q}_\nu + \left(m_d Q_{\nu m} + M_d Q_{\nu M}\right)\ddot{\kappa} + c_d q_\nu = 0;$$

$$\left(\frac{33}{140}m_d + M_d\right)\ddot{q}_\tau + \left(m_d Q_{\tau m} + M_d Q_{\tau M}\right)\ddot{\kappa} + c_d q_\tau = 0;$$

$$\left(\frac{33}{140}m_b + M_b\right)\ddot{q}_b + \left(m_b Q_{bm} + M_b Q_{bM}\right)\ddot{\kappa} + c_b q_b = 0;$$

$$\left(m_A + m_a\right)\ddot{\xi}_A - e_U S_{U\xi} - e_L S_{L\xi} = 0;$$

$$\left(m_A + m_a\right)\ddot{\eta}_A + m_a r_A\ddot{\psi} + m_a g - e_U S_{U\eta} - e_L S_{L\eta} = 0;$$

$$I_A\ddot{\psi} + m_a r_A\left(\ddot{\eta}_A + \ddot{\xi}_A\psi + g\right) = 0, \qquad (1)$$

where $I_{cm} = m_c\left(\frac{l_c^2}{3} + x_V^2 + y_V^2 - y_V l_c\right)$; $Q_{cm} = \frac{11}{40}l_c - \frac{3}{4}y_V$; $I_{cM} = M_c\left[x_V^2 + \left(l_c - y_V\right)^2\right]$;

$Q_{cM} = l_c - y_V$; $I_{bm} = m_b\left(x_b^2 + y_b^2 + l_b r_b + \frac{1}{3}l_b^2\right)$; $Q_{bm} = \frac{3}{8}r_b + \frac{11}{40}l_b$; $r_b = x_b\sin\gamma - y_b\cos\gamma$;

$I_{bM} = M_b\left(x_b^2 + y_b^2 + 2l_b r_b + l_b^2\right)$; $Q_{bM} = r_b + l_b$;

$$I_{dm} = 2m_d\left[x_V^2 + y_V^2 + l_d\left(y_V\cos\alpha\cos\beta - x_V\sin\alpha\right) + \frac{1}{3}l_d^2\left(\sin^2\alpha + \cos^2\alpha\cos^2\beta\right)\right];$$

$$I_{dM} = 2M_d\left[\left(x_V - l_d\sin\alpha\right)^2 + \left(y_V + l_d\cos\alpha\cos\beta\right)^2\right];$$

$$Q_{\nu m} = \frac{3}{8}\left(x_V\sin\alpha\cos\beta - y_V\cos\alpha\right) - \frac{11}{40}l_d\cos\beta;\ Q_{\tau m} = \left(\frac{3}{8}x_V - \frac{11}{40}l_d\sin\alpha\right)\sin\beta;$$

$Q_{\nu M} = x_V\sin\alpha\cos\beta - y_V\cos\alpha - l_d\cos\beta$; $Q_{\tau M} = \left(x_V - l_d\sin\alpha\right)\sin\beta$;

$$e_U = \frac{f\left(s_U - S_U\right)}{s_U S_U};\ e_L = \frac{f\left(s_L - S_L\right)}{s_L S_L};\ s_U = \sqrt{S_1^2 + S_2^2};\ s_L = \sqrt{S_3^2 + S_4^2};$$

$S_1 = h_U + l_U b_1 - \eta_A$; $S_2 = h_U\kappa + l_U b_2 - \xi_A$; $S_3 = h_L + l_L b_3 + \eta_A$; $S_4 = h_L\kappa - l_L b_4 + \xi_A$;

$b_1 = \cos\left(\theta_U + \kappa\right)$; $b_2 = \sin\left(\theta_U + \kappa\right)$; $b_3 = \cos\left(\theta_L - \kappa\right)$; $b_4 = \sin\left(\theta_L - \kappa\right)$; l_U, l_L are limbs' lengths; s_U, s_L are lengths of string branches in the drawn bow situation; S_U, S_L are lengths of the branches of a free string; h_U, h_L are virtual lengths of the riser, i.e. the distances from the pivot point (O) to the points of virtual flexible elements of limbs; c_U, c_L are stiffness of the limbs; l_a is a length of an arrow (and drawn distance too); f is a parameter of stiffness of a string; $m_A = \frac{1}{3}m_s$ is mass of a string pinned to the nock point; m_s is mass of a string; m_a is mass of an arrow; r_A is a distances of center of mass of the arrow to the nock point; I_H is a moment of inertia of a riser relatively the pivot point; m_U, m_L are mass of limbs with added mass of a string $\left(\frac{1}{3}m_s\right)$ pinned to tips; I_U, I_L are moments of inertia of limbs relatively their joints to the riser with addition the same part of string mass; r_U, r_L are distances of centers of mass of limbs to their joints; g is gravity acceleration; x_V, y_V are coordinates of a common

point of projection to the plane of symmetry of axes of all the three stabilizer rods; l_c is length of the central rod; m_c is mass of the central rod; M_c is mass of a load concentrated at a free end of the rod; c_c is a stiffness of the central rod relatively a normal force at a free end; m_d is mass of each the side rod; M_d is mass of a load concentrated at a free end of the side rod; l_d is length of the side rod; c_d is a stiffness of the side rod relatively a normal force at a free end; m_V and I_V are mass and moment of inertia of the uni-bar and a bar-extender relatively their common center of mass with coordinates x_V, y_V; x_b, y_b are coordinates of a point where an upper stabilizer rod is fixed to a riser; γ is an angle of upper rod incline to a central rod axis; l_b is a length of the an upper rod; m_b is mass of the upper rod; M_b is mass of a load concentrated at a free end of the upper rod; c_b is a stiffness of the upper rod relatively a normal force at a free end. The subdivides "U" and "L" mark corresponding the upper and lower limbs.

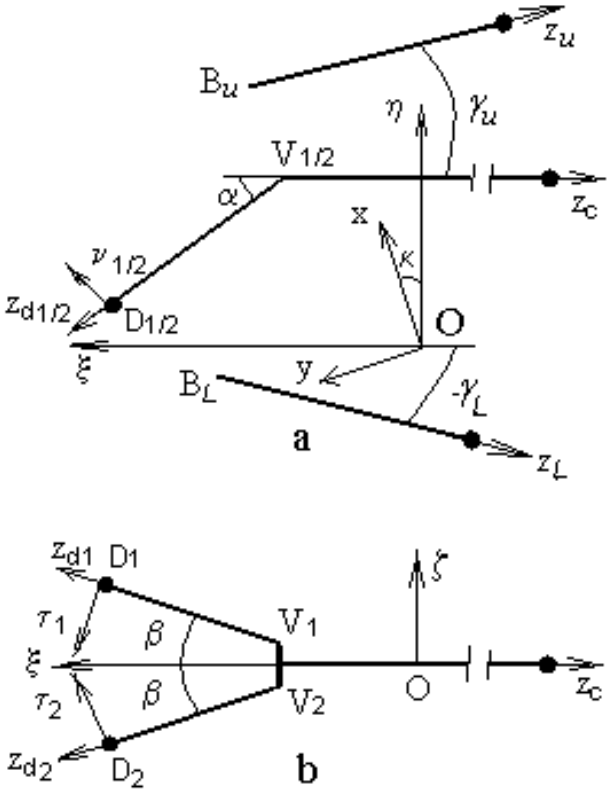

Figure 2. Scheme model of stabilizer rods in the vertical plane (a) and its sight in the transverse plane (b).

Initial conditions of the problem are:

$$t=0,\xi_A=\xi_{A0};\eta_A=\eta_{A0};\theta_U=\theta_{U0};$$
$$\theta_L=\theta_{L0};\kappa=0;\psi=\psi_0;q_c=0;q_\nu=0;$$
$$q_\tau=0;\dot{\xi}_A=0;\dot{\eta}_A=0;\dot{\theta}_U=0;\dot{\theta}_L=0;$$
$$\dot{\kappa}=0;\dot{\psi}=0;\dot{q}_c=0;\dot{q}_\nu=0;\dot{q}_\tau=0, \quad (2)$$

where constants η_{A0}, θ_{U0}, θ_{L0} are solutions of the static problem (see the next subsection "Static model"). Zero values of derivations correspond the manner of the sport archer technique, i.e. breathing is stopped and a pose is motionless.

The model of an upper stabilizer rod was used to model a behavior of a sight.

Verification of the model was done during modeling of a modern sport bow example with parameters presented in Table.

Solving a static problem, we have got: $\eta_{A0} = 43$ mm; $\theta_{U0} = 0{,}766$; $\theta_{L0} = 0{,}794$. The rest point situates at the coordinate $\eta_{P0} = 43$ mm.

Table 1. Bow and arrow parameters (example).

No	Designation	Dimension	Data
1	l_U, l_L	mm	531
2	m_U, m_L	kg	0.107
3	I_U, I_L	kg*cm^2	68.2
4	r_U, r_L	mm	228
5	c_U, c_L	Nm	69.1
6	φ_U	rad	0.605
7	φ_L	rad	0.608
8	h_U, h_L	mm	342
9	I_H	kg*cm^2	2130
10	S_U	cm	78
11	S_L	cm	84
12	f	N	25515
13	m_s	g	6.9
14	l_a	mm	783
15	m_a	g	22,4
16	I_A	kg*cm^2	73.6
17	r_A	mm	510
18	m_c	kg	0.193
19	m_b	kg	0.088
20	m_d	kg	0.065
21	x_V	mm	-107

22	y_V	mm	-142
23	x_b	mm	221
24	y_b	mm	-18
25	m_V	kg	0.119
26	I_V	kg*cm^2	21.0
27	c_c	Nm^{-1}	485
28	c_b	Nm^{-1}	833
29	c_d	Nm^{-1}	1170
30	l_c	mm	760
31	l_b	mm	420
32	l_d	mm	250
33	α_{max}	rad	0.297
34	β_{max}	rad	0.617
35	γ	rad	0.157
36	M_c	kg	0.043
37	M_b	kg	0.037
38	M_d	kg	0.028

NDSolve program from Mathematica package was applied to solve the system (1) with initial conditions (2). The text of the program with parameters of a modern sport bow measured in SI units is presented in Appendix 2.

The end of the phase of the bow and arrow common motion occurs just the longitudinal acceleration of the nock point equals zero: $\ddot{\xi}_A = 0$ (Figure 3). Negative values of the acceleration depend on the opposite direction of the ξ - axis (see Figure 1).

Static model

It is possible to consider a static model to study a bow and arrow at the drawing situation. In a static problem, we can assume only two external forces, which act to the handle and to the string, i.e. the forces acting corresponding in a pivot point and in a nock point. A mathematical model of the bow at the drawn situation is (Figure 4):

$$\begin{aligned}
&\xi_A = l_U \sin\theta_U + s_U \sin\gamma_U; \quad \xi_A = l_L \sin\theta_L + s_L \sin\gamma_L;\\
&\eta_A = h_U + l_U \cos\theta_U - s_U \cos\gamma_U; \; c_U(\theta_U + \varphi_U) = F_U l_U \sin(\theta_U + \gamma_U);\\
&\eta_A = s_L \cos\gamma_L - l_L \cos\theta_L - h_L; \quad c_L(\theta_L + \varphi_L) = F_L l_L \sin(\theta_L + \gamma_L);\\
&F_\xi = -F_U \sin\gamma_U - F_L \sin\gamma_L; \quad F_\eta = F_U \cos\gamma_U - F_L \cos\gamma_L;\\
&F_U = f\frac{s_U - S_U}{S_U}; \; F_L = f\frac{s_L - S_L}{S_L}; \; tg\phi = \frac{F_\eta}{F_\xi}; \; tg\phi = \frac{\eta_A}{\xi_A},
\end{aligned} \tag{3}$$

where F_U, F_L are forces of the string branches; F_ξ, F_η are projections of the drawn force (acted at a nock point A) to the axis of co-ordinates.

FindRoot program from Mathematica package was used to solve the system (3). The text of the program concerning a bow in the drawn situation (Nowak *et al*., 2008) is presented in Appendix 2.

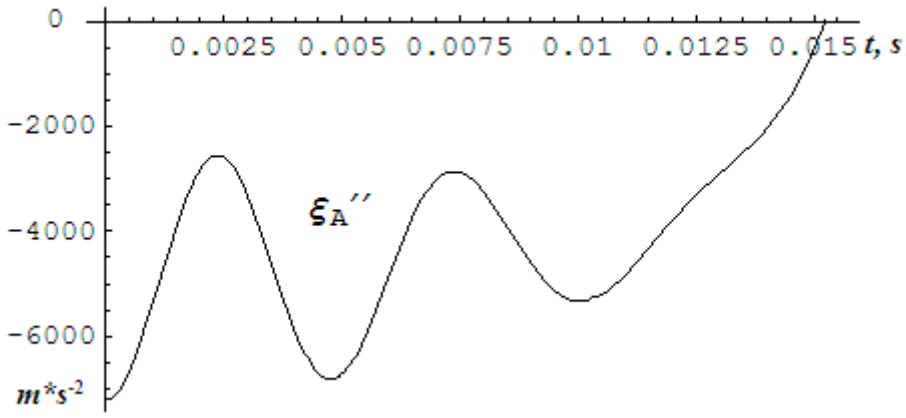

Figure 3. Dynamic scheme model (a); scheme model of an arrow (b).

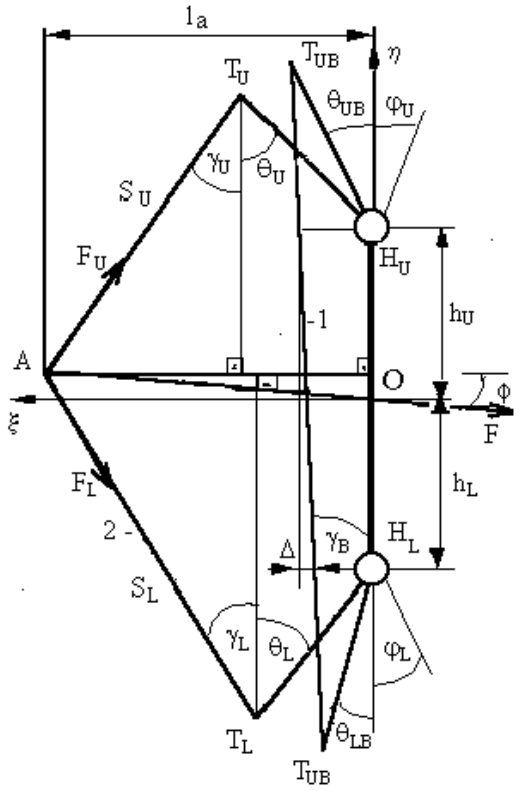

Figure 4. Scheme model of a braced (1) and a drawn (2) bow.

Discussion

The mathematical and computer model took into account main features of the archer bow and arrow interaction in the vertical plane. It allows to get parameters of the arrow kinematics during bow and arrow common motion: a function of the arrow longitudinal movement vs. time (Figure 5), nock point locus (Figure 6), an attitude angle and an angle of attack of the arrow (Figure 7), and its launch velocity.

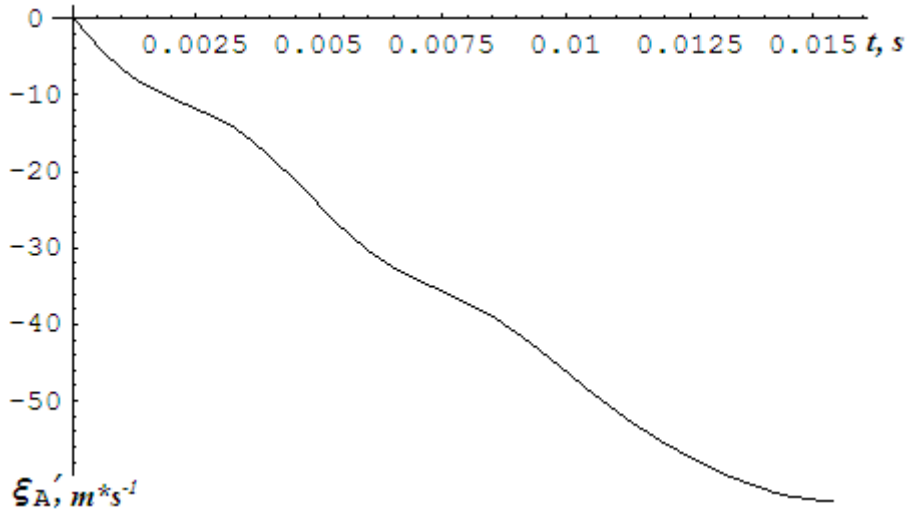

Figure 5. Arrow longitudinal speed vs. time: negative values of the acceleration depend on the ξ - axis direction (see Figure 1).

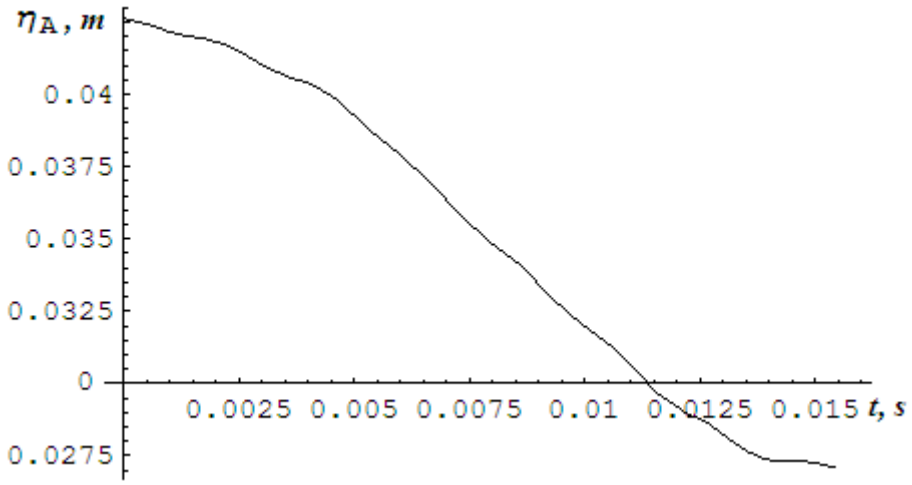

Figure 6. Nock point locus plot.

The model allows to get bow kinematical parameters: riser angular displacement vs. time (Figure 8), limbs' angles (Figure 9), string branches displacement and stretching, stabilizer rods' displacement and bending (Figures 10 and 11). Time of bow and arrow common movement (0.0153 s) was determined too.

The model describe bow and arrow interaction as an intensive vibration. There are near seven circles of oscillation of an arrow's angle of attack (see Figure 7) and an angular displacement of a riser (see Figure 8).

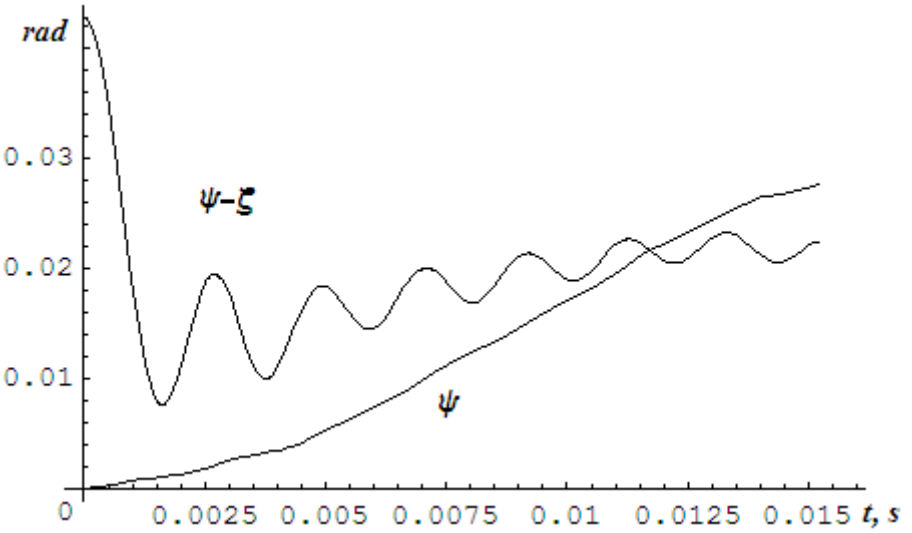

Figure 7. An attitude angle (ψ) and an angle of attack $(\psi - \zeta)$ of the arrow.

Because a symmetrical position of side rods regarding the vertical plane, a bow and arrow interaction do not share their common motion in a lateral direction.

The model allows to get bow kinetic parameters: a force accelerated an arrow, a bending moment between a limb and a riser, forces stretched string branches (especially, their pick values), a recoiled force acting from a grip to an archer hand (Figure 12). Because an archer does not hold a grip but set it, negative values of the recoiled force are plotted with an interrupted line.

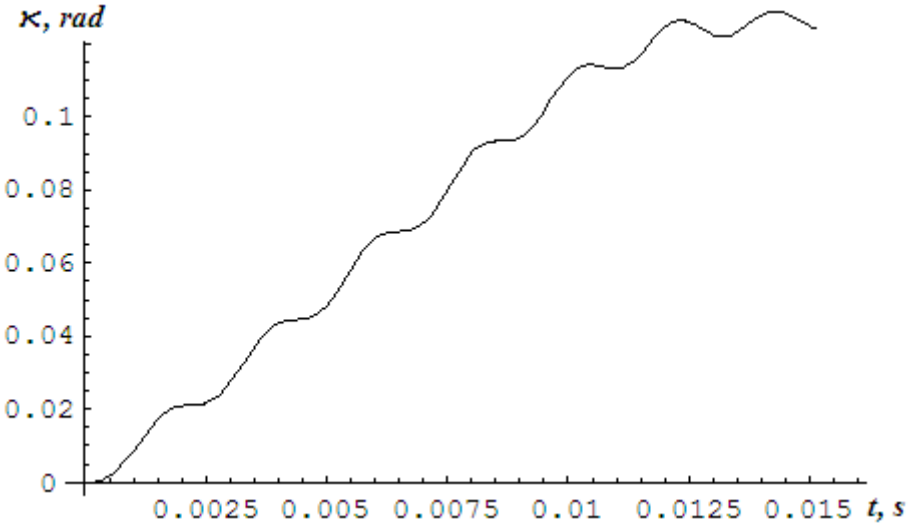

Figure 8. Riser angular displacement vs. time.

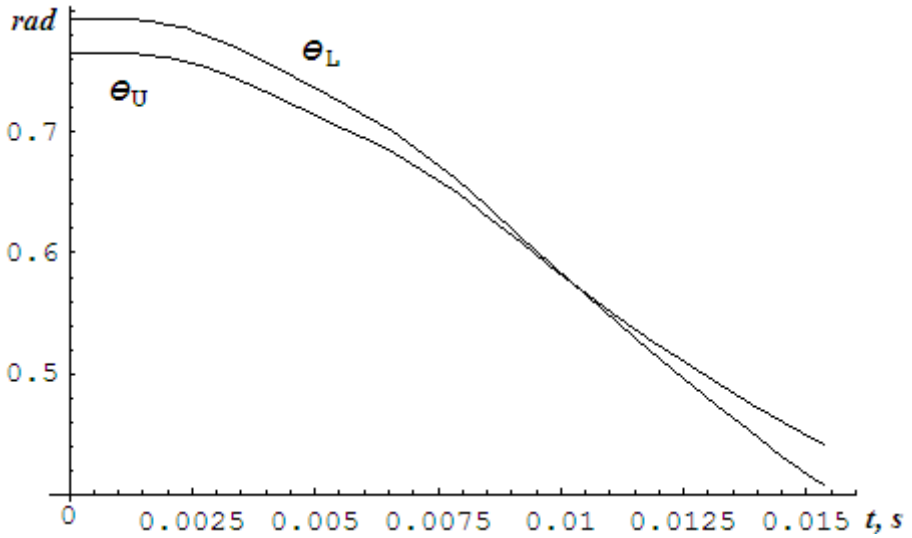

Figure 9. Upper and lower limb angles.

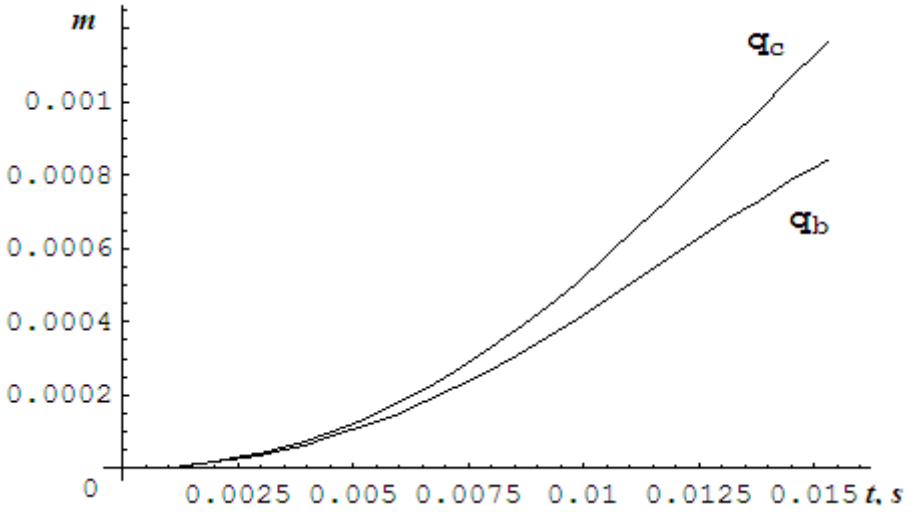

Figure 10. Displacements of free ends of the central (q_c) and an upper (q_b) stabilizer rods caused with a bend.

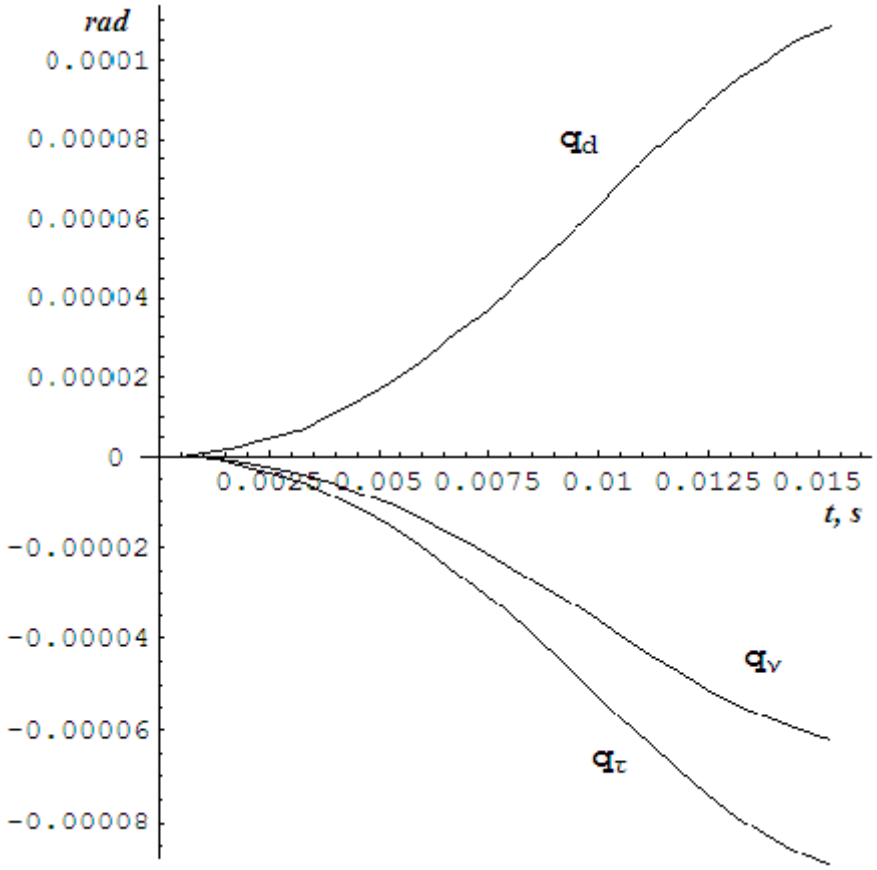

Figure 11. Bend displacement of a free end of a side stabilizer rod (q_d) and its projections to the normal (q_v) and tangent (q_τ) directions respectively.

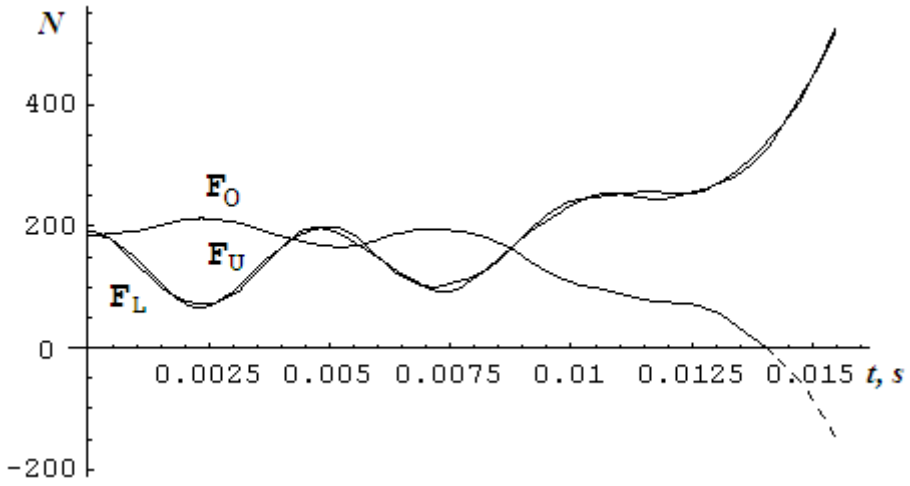

Figure 12. A recoiled force acting from a grip to an archer hand (F_O) and forces stretching string branches.

There were three clear oscillation circles in the longitudinal acceleration of an arrow (see Figure 3), in the string stretching forces, and the recoil force (see Figure 12). The same oscillations were observed in a soft form for a longitudinal speed of and arrow (see Figure 5),

for a nock point locus (see Figure 6), and for virtual angles of limbs (see Figure 9).

Conclusions

The mathematical and computer model presented in this paper took into account main features of the archer bow and arrow interaction in the vertical plane. This makes possible to calculate parameters of the arrow kinematics and kinetics during bow and arrow common motion.

Regarding to the dynamic models of the long English bow (Kooi and Sparenberg, 1980; Marlow, 1982) and traditional Japanese bow (Ohsima & Ohtsuki, 2002), the model proposed in this paper took into account an angular movement of a riser (therefore a whole bow too). As a development of the early published works on dynamics of the archery bow stabilizing (Zanevskyy, 2006, 2008; Zanevskyy & Zanevska, 2009), the upper and lower stabilizer rods were modeled. The model of this multi-rod stabilizer system could be applied to the compound archery bow dynamic model that has been derived by Park (2010).

Acknowledgements

The research was partly supported by Polish Ministry of Science and Higher Education, Research Grant No 2814/58/P.

References

FITA Beginner's Manual. 2010. http://www.archery.org (Publications/Bookstore).

Hickman, C. N. (1937). Dynamics of a bow and arrow. *Journal of Applied Physics*, *8*, 404–409.

Kooi, B. W. & Sparenberg J. A. (1980). On the static deformation of a bow. *Journal of Engineering Mathematics 14*(1), *27-45*.

Marlow, W. C. (1981). Bow and arrow dynamics. *American Journal of Physics*, *49*(4), 320–333.

Nowak, S., Zanevska, L. & Zanevskyy, I. (2008). Mathematics computer systems in archery bow modeling. Proceedings of International conference on Sports Science and Sports Engineering, Nanjing, 1, 17-22.

Ohsima, S. & Ohtsuki, A. (2002). Simulation of the shape and dynamics of Japanese bow – Application of large deflection theory. The Book of the 4th International Conference on Engineering of Sport, Kioto, 102-107.

Park, J. L. (2009). Compound-archery-bow nocking-point locus in the vertical plane. Proc. IMechE, Part P: *Journal of Sports Engineering and Technology, 224*(4), 141–153.

Zanevskyy, I. (2006). Bow tuning in the vertical plane. *Sports Engineering, 9*, 77-86.

Zanevskyy, I. (2008). Modeling and computer simulation of bow stabilization in the vertical plane. *International Journal of Sports Science and Engineering, 2*(1), 3-14.

Zanevskyy, I. & Zanevska, L. (2009). Model of a three-rod stabilizer for the sport archery bow. *Sports Science of Ukraine, 7*(1), 20-42 (in Ukrainian).

Appendix 1

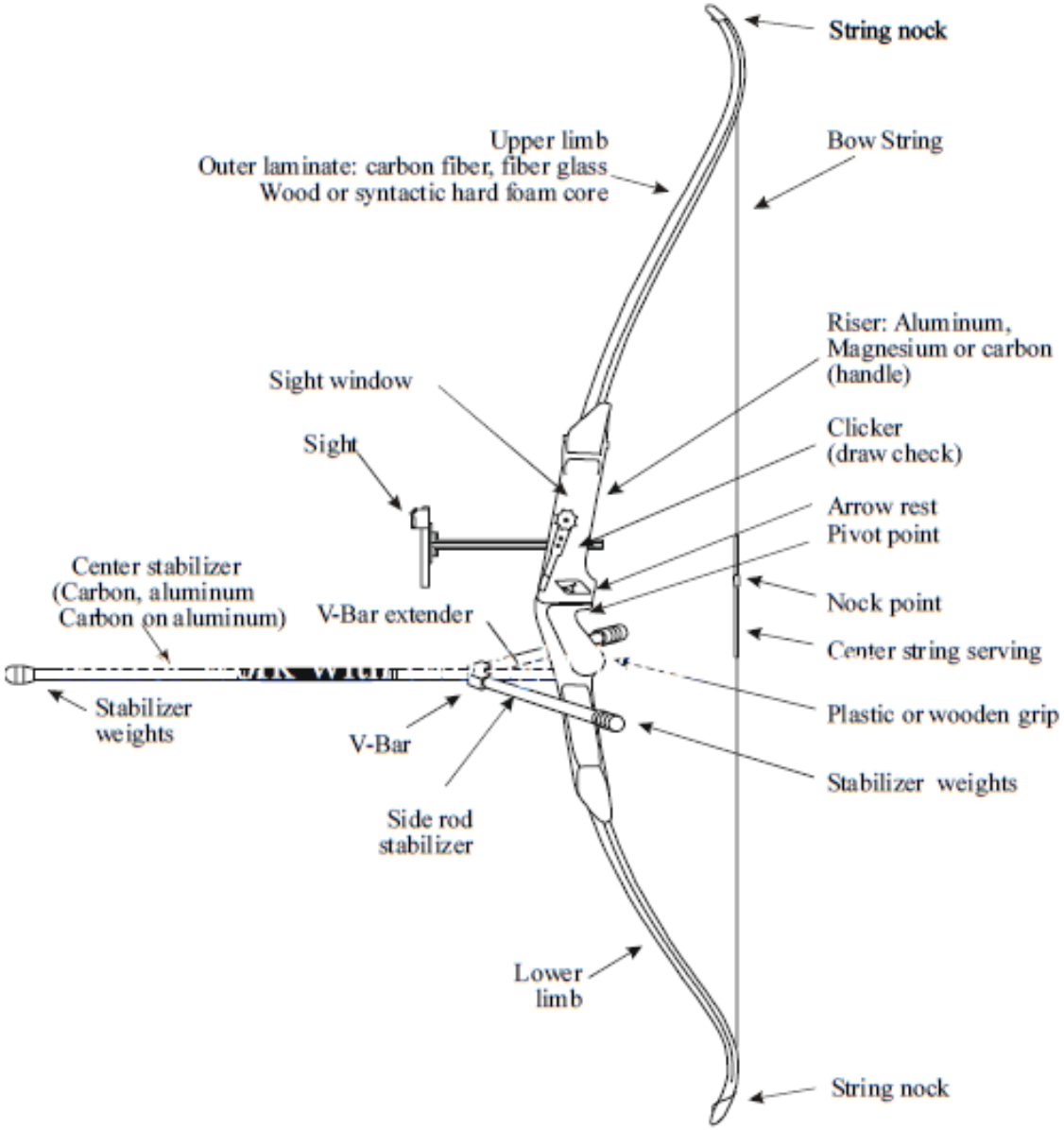

Figure A1. Sport archery bow in the vertical plane (FITA, 2010).

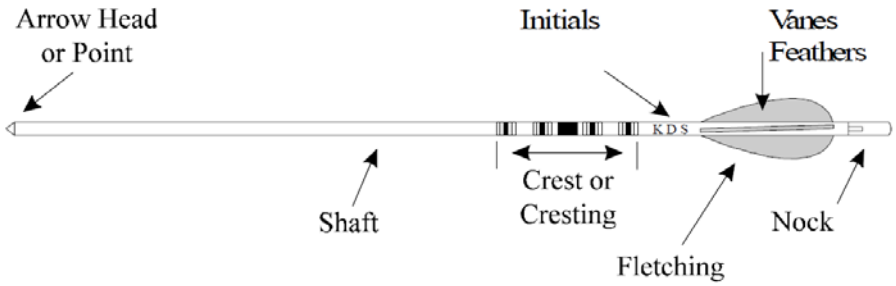

Figure A2. Sport archery arrow (FITA, 2010).

Appendix 2

A. 2. 1. Mathematica computer program on bow and arrow dynamics

```
ξA0 = 0.7576; ηA0 = 0.0426237; θU0 = 0.765512; θL0 = 0.794188;
mA = 0.0023; mU = 0.107; mL = 0.107; rU = 0.228; rL = 0.228;
lU = 0.531; lL = 0.531; hU = 0.342; hL = 0.342; SU = 0.780;
SL = 0.840; f = 25515; IU = 0.00682; IL = 0.00682; IH = 0.213;
cU = 69.1; cL = 69.1; φU = 0.604672; φL = 0.607552;
IA = 0.00736; ma = 0.0224; rA = 0.5103; la = 0.783;
ηP0 = 0.0426237; g = 9.81; ξH0 = 0.009366; ηH0 = 0.001062;
xb = 0.221; yb = -0.018; xV = -0.107; yV = -0.142;
mc = 0.193; cc = 485; lc = .76; mb = 0.088; cb = 833; lb = .42;
md = 0.065; cd = 1170; ld = .25; α = .297; β = .617; χ = .157;
Mc = .043; Mb = .037; Md = .028; Mv = .119; Iv = .0021;
Icm = mc * (lc^2 / 3 + xV^2 + yV^2 - lc * yV);
IcM = Mc * (lc^2 + xV^2 + yV^2 - 2 * lc * yV);
Qcm = .5 * (.55 * lc - .75 * yV); QcM = lc - yV;
rb = xb * Sin[χ] - yb * Cos[χ];
Ibm = mb * (lb^2 / 3 + xb^2 + yb^2 + lb * rb);
IbM = Mb * (lb^2 + xb^2 + yb^2 + 2 * lb * rb);
Qbm = .5 * (.55 * lc + .75 * rb); QbM = lc + rb;

Idm = 2 * md * (xV^2 + yV^2 + (yV * Cos[α] * Cos[β] - xV * Sin[α]) * ld
        *((Sin[α])^2 + (Cos[α])^2 * (Cos[β])^2) * ld^2 / 3);

IdM = 2 * Md * ((xV - ld * Sin[α])^2 + (yV + ld * Cos[α] * Cos[β])^2);
Qνm = .5 *((.75 * (xV * Sin[α] * Cos[β] - yV * Cos[α])
    - .55 * ld * Cos[β]));
Qτm = .5 * ((.75 * xV - .55 * ld * Sin[α]) * Sin[β]);
QνM = xV * Sin[α] * Cos[β] - yV * Cos[α] - ld * Cos[β];
QτM = (xV - ld * Sin[α]) * Sin[β];
ψ0 = (ηP0 - ηA0) / la;
ζ = -ArcTan[(ηA'[t] + rA * ψ'[t]) / ξA'[t]];
```

$$s_U = \sqrt{S_{U\eta}^2 + S_{U\xi}^2}\ ;\ s_L = \sqrt{S_{L\eta}^2 + S_{L\xi}^2}\ ;\ e_U = \frac{f * (s_U - S_U)}{s_U * S_U}\ ;$$

$$e_L = \frac{f * (s_L - S_L)}{s_L * S_L}\ ;$$

$$S_{U\eta} = h_U + l_U * b_1 - \eta_A[t]\ ;\ S_{U\xi} = h_U * \kappa[t] + l_U * b_2 - \xi_A[t]\ ;$$

$$S_{L\eta} = -h_L - l_L * b_3 - \eta_A[t]\ ;\ S_{L\xi} = -h_L * \kappa[t] + l_L * b_4 - \xi_A[t]\ ;$$

$$b_1 = \text{Cos}[\kappa[t] + \theta_U[t]]\ ;\ b_2 = \text{Sin}[\kappa[t] + \theta_U[t]]\ ;$$

$$b_3 = \text{Cos}[-\kappa[t] + \theta_L[t]]\ ;$$

$$b_4 = \text{Sin}[-\kappa[t] + \theta_L[t]]\ ;$$

$$\text{system} = \{(m_A + m_a) * \xi_A''[t] - e_U * S_{U\xi} - e_L * S_{L\xi} == 0,$$

$$(m_A + m_a) * \eta_A''[t] + m_a * r_A * \psi''[t] + m_a * g - e_U * S_{U\eta} - e_L * S_{L\eta} == 0,$$

$$I_A * \psi''[t] + m_a * r_A * (\xi_A''[t] * \psi[t] + g + \eta_A''[t]) == 0,$$

$$I_U * (\theta_U''[t] + \kappa''[t]) + m_U * r_U * h_U * b_1 * \kappa''[t] + c_U * (\theta_U[t] + \varphi_U) +$$
$$e_U * l_U * (S_{U\xi} * b_1 - S_{U\eta} * b_2) == 0,$$

$$I_L * (\theta_L''[t] - \kappa''[t]) - m_L * r_L * h_L * b_3 * \kappa''[t] + c_L * (\theta_L[t] + \varphi_L) +$$
$$e_L * l_L * (S_{L\xi} * b_3 + S_{L\eta} * b_4) == 0,$$

$$(I_H + I_U + I_L + m_U * h_U^2 + m_L * h_L^2 + Icm + IcM + Idm + IdM + Ibm +$$
$$IbM + Iv + Mv * (x_V^2 + y_V^2)) * \kappa''[t] + I_U * \theta_U''[t] -$$
$$I_L * \theta_L''[t] +$$
$$m_U * r_U * h_U * (b_1 * (\theta_U''[t] + 2 * \kappa''[t]) - b_2 * (\theta_U'[t] + \kappa'[t])^2)$$
$$- m_L * r_L * h_L * (b_3 * (\theta_L''[t] - 2 * \kappa''[t]) - b_4 * (\theta_L'[t] - \kappa'[t])^2)$$
$$+ (m_c * Qcm + Mc * QcM) * q_c''[t] + (m_b * Qbm + Mb * QbM) * q_b''[t] +$$
$$2 * ((m_d * Q\nu m + Md * Q\nu M) * q_\nu''[t] +$$
$$(m_d * Q\tau m + Md * Q\tau M) * q_\tau''[t]) +$$
$$e_U * (S_{U\xi} * (l_U * b_1 + h_U) - S_{U\eta} * l_U * b_2) -$$
$$e_L * (S_{L\xi} * (l_L * b_3 + h_L) + S_{L\eta} * l_L * b_4) == 0,$$

```
(Mc + mc * 33 / 140) * qc''[t] +
(mc * Qcm + Mc * QcM) * κ''[t] + cc * qc[t] == 0,
(Mb + mb * 33 / 140) * qb''[t] +
(mb * Qbm + Mb * QbM) * κ''[t] + cb * qb[t] == 0,
(Md + md * 33 / 140) * qν''[t] +
(md * Qνm + Md * QνM) * κ''[t] + cd * qν[t] == 0,
(Md + md * 33 / 140) * qτ''[t] +
(md * Qτm + Md * QτM) * κ''[t] + cd * qτ[t] == 0,

ξA[0] == ξA0, ηA[0] == ηA0, θL[0] == θL0, θU[0] == θU0, ψ[0] == ψ0,
 ψ'[0] == 0, κ[0] == 0, ξA'[0] == 0, ηA'[0] == 0, θL'[0] == 0,
 θU'[0] == 0, κ'[0] == 0, qc[0] == 0, qc'[0] == 0, qb[0] == 0,
 qb'[0] == 0, qν[0] == 0, qν'[0] == 0, qτ[0] == 0, qτ'[0] == 0};
t0 = 0; t1 = 0.01529;

solution = NDSolve[system,
    {ξA, ηA, ψ, θL, θU, κ, qc, qν, qτ, qb}, {t, t0, t1},
    Method → ExplicitRungeKutta]
```

A. 2. 2. Mathematica computer program on a bow in the drawn situation

```
In[1]:= hU = .342; hL = .342; lU = .531; lL = .531; cU = 69.084; cL = 69.084;
        sU0 = .78; sL0 = .84; φU = .604672; φL = .607552; ξA = .7576; f = 25515;
        FindRoot[{ξA == lU * Sin[θU] + sU * Sin[γU], ξA == lL * Sin[θL] + sL * Sin[γL],
          ηA == hU + lU * Cos[θU] - sU * Cos[γU], ηA == -hL - lL * Cos[θL] + sL * Cos[γL],
          cU * (θU + φU) == FU * lU * Sin[θU + γU], cL * (θL + φL) == FL * lL * Sin[θL + γL],
          -Fξ == FU * Sin[γU] + FL * Sin[γL], Fη == FU * Cos[γU] - FL * Cos[γL],
          FU == f * (sU - sU0) / sU0, FL == f * (sL - sL0) / sL0, Fη / Fξ == ηA / ξA},
        {θU, .8}, {θL, .8}, {γU, .5}, {γL, .5}, {FU, 200}, {FL, 200},
        {sU, .79}, {sL, .85}, {Fξ, 200}, {Fη, 10}, {ηA, .04}]

Out[3]= {θU → 0.765512, θL → 0.794188, γU → 0.518941, γL → 0.464122, FU → 185.83,
        FL → 191.65, sU → 0.785681, sL → 0.846309, Fξ → -177.954, Fη → -10.012,
        ηA → 0.0426237}
```

Designing an Acoustic Feedback System for On-Water Rowing Training

Nina Schaffert & Klaus Mattes

University of Hamburg

Abstract

Analysis of measured kinematic parameters is commonly used in competitive sports to optimize athletes' performance. The progress in technology offers new ways for displaying feedback information to athletes. In rowing, synchronous visual feedback is regularly used, but the presentation of acoustic information is a new and promising application for technique training and monitoring. This paper describes the prototype *Sofirow* as an online acoustic feedback system for on-water rowing training, developed in cooperation between the University of Hamburg and BeSB GmbH Berlin. *Sofirow* measures propulsive boat acceleration (MEMS sensor, up to 125Hz) and velocity (4Hz-GPS). Technical requirements concerned with the acoustic transformation (sonification) and its presentation. The associated software *Regatta* provides an analysis of the measured data. An intra-cyclic analysis of the boat's acceleration-time-trace investigated potential benefits for the time structure of the acceleration trace. Effects on boat motion were explored in an empirical investigation with the German junior national rowing team in 2009. The first significant results were encouraging and support the implementation of acoustic information regularly into training processes for elite athletes. *Sofirow* represents the rhythmic acceleration trace distinctly and audibly and thus, offers systematic monitoring and control of the boat motion in on-water technique training.

KEYWORDS: MEASUREMENT AND TRAINING SYSTEM, ACOUSTIC ONLINE FEEDBACK, MOVEMENT SONIFICATION, MOVEMENT OPTIMIZATION, ROWING

Introduction

Biomechanical analysis in on-water rowing dates back to 1860, describing typical kinematical patterns of the rowing movement [0]. Validity of information has not changed since then in contrast with the methods used for the analysis. To control the technique training in racing rowing, biomechanical measuring and feedback systems are used regularly in the German Rowing Association (DRV) as synchronous information which is displayed visually [0]. But visual observation is in principle limited by physiological capacities of the visual perception system whose effectiveness decreases with increasing movement intensities (stroke rates (sr) >30 strokes per minute). Furthermore, focus on the graphical display requires a specific position of the head as well as additional concentration and thus, it is attention consuming. In contrast, acoustic feedback (AF) offers a new and promising method to optimize the boat motion (BM) by taking advantage of auditory perception, which is particularly sensitive to temporal resolution. Furthermore, multiple attributes were perceivable at one time and athletes' focus of attention can be guided reliably to specific movement sections without occupying the sensory channel. In addition to existing devices, the prototype *Sofirow* (*So*nif*i*cation in *row*ing)

was developed as an online AF-system for on-water rowing training in cooperation between the University of Hamburg and the sound and vibration company BeSB GmbH Berlin. The technical requirements concerned the acoustic transformation (sonification) of the propulsive boat acceleration-time-trace (a_{boat} trace) to represent changes in BM differentiated and online as well as the presentation of the sound result and the effect analysis. It was assumed that AF has an effect particularly on the time structure of the recovery phase of the rowing cycle (rc). During the process of prototype development, primary focus was set on sonifying a_{boat} as well as its perceived functionality and aesthetics.

Methods

Sofirow measured and stored the kinematic parameter of BM during rowing: propulsive boat acceleration (a_{boat}) via a micro-electro-mechanical (MEMS) acceleration sensor (sample rate adjustable up to 125Hz; SMB380 Bosch Sensortec; ±2g: 256LSB/g) and boat velocity (v_{boat}) with GPS (4Hz; Navilock-550ERS ublox5; velocity: 0.1m/s; distance: 0.25% measuring error (2000m)). The a_{boat} trace was converted online into a sound sequence (max. delay of <100ms) and transmitted to the athletes in the boat as AF via loudspeaker and earplugs, optionally. The time for and duration of AF could be switched on and off by the scientist using remote-control and in agreement with the coach who could receive the acoustic transmission simultaneously with the athletes in the motorboat. Figure 1 showed *Sofirow* positioned on top of the boat.

Figure 1. The training and AF-system *Sofirow*.

The transformation of the a_{boat} trace, derived from physical parameters, was realized using the software Pure Data (Pd), which is software that crates interactive computer music. To convert the data into a meaningful sound result, the regularly used sonification method of Parameter Mapping [0] was chosen that mapped every data point to a tone on the MIDI-scale (electronic musical scale), related to tone pitch. In doing so, every whole number (integer) corresponded to a specific semitone. Middle C on the western musical tone scale represented the point of zero a_{boat}; positive and negative a_{boat} varied above and below this tone pitch. Thus, the algorithmic transformation of the data into an audible sound was realized as a direct modulation that produced movement-defined sound sequences as the outcome: tone pitch changed as a function of a_{boat} trace and represented qualitative changes in BM differentiated. Acoustic transmission proceeded via WLAN that enabled the remote-controlled turning-on and off as well as an online modulation of the sound in terms of tone pitch and volume. The data storage on a SD-card made it possible to analyze the effect of AF on BM as well as to re-sonify the data subsequently.

To investigate the data, the special software *Regatta* was developed which indicates the

essential details of external training load in different rowing specific analysis routines [0] [0]. For the effect analysis, a_{boat} trace was analyzed intra-cyclically by identifying twelve events inside the acceleration curve related to the phase structure of rc which was rhythmically divided into the two main phases: drive and recovery (or release). In doing so, zero points and local as well as global extreme values were calculated as points in time (t_1-t_{12}) (Figure 2). To analyze the time structure of the curve, the times between the points were calculated as time intervals (Δt_1-Δt_{10}). Furthermore, acceleration values (a_{boat1}-a_{boat12}) and acceleration integrals were defined.

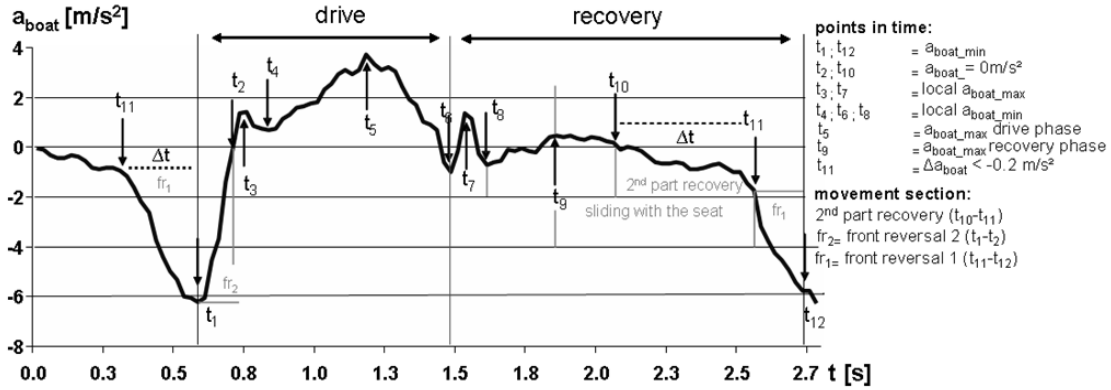

Figure 2. Characteristic intra-cyclical a_{boat} trace with the defined points in time defined according to the movement section.

The training device was tested with the German junior national rowing team (*N*=23) in small and big boats (six boats) in up to five training sessions during the preparation phase for the junior world championships. Sections without and with AF (alternating) over 30 rc each were considered for all boats and statistical compared using an ANOVA with repeated measures (level of statistical significance set at $p<0.05$). Investigation of a_{boat} trace intra-cyclically considered two sections without and with AF using the example of the junior men's eight (jm8+). Additionally, standardized questionnaires were taken to examine athletes' perception of AF (comprehensibility, correspondence with the rowing movement and attention-guidance for specific movement sections).

Results

The results showed statistically significant improvements in mean vboat for all boat categories during the sections with AF immediately after AF was switched on ($F2.38=36.6$; $p=0.00$) as well as significant reduction for the time between the events (time intervals) ($F1=94.54$; $p=0.00$) inside the acceleration curve. Furthermore, significant interaction between the different boat categories was found ($F11=2.03$; $p=0.03$). Figure 3 represents the single profiles of rc in which the reduction in Δt became evident for the second part of the recovery phase ("1" in Figure 3) as well as for the front reversal ("2" in Figure 3) and was audible in the acoustic mapping.

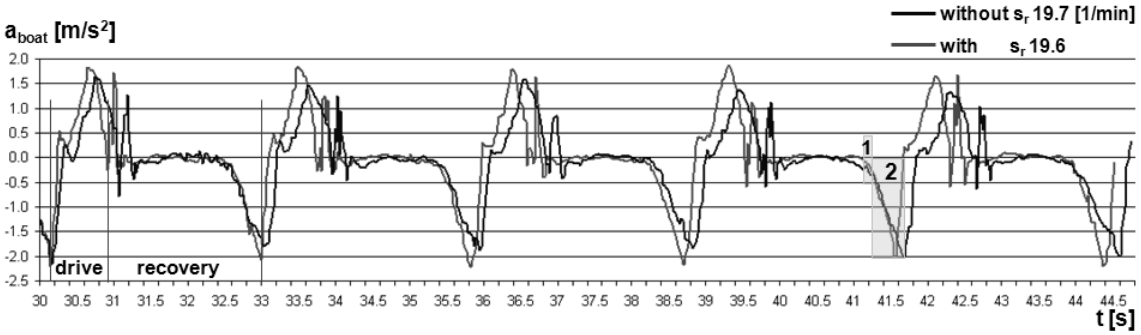

Figure 3. Single profiles of rc for the sections without and with AF in comparison using the example of jm8+; (classification of the drive and recovery phase=based on the section "with").

The section with AF differed from the section without AF in the sound sequence in terms of tone pitch and duration before the tone lowered ("1") as a result of a more carefully controlled movement of the athletes when sliding with the seat. Furthermore, the duration of negative a_{boat} ("2") was reduced as a result of starting the front reversal later. Therewith, initial assumptions were confirmed that AF can affect the time structure of a_{boat} trace at a comparable sr.

Questioning showed high acceptance among athletes (and their coaches). Characteristic phases of a_{boat} were perceived as changes in tone pitch and athletes could adjust their kinaesthesia in relation to the sound sequence. Additionally, imagination of the movement was supported which facilitated the guidance effect of AF to specific sections inside rc. As a result, control of the recovery phase in particular was improved.

Functionality of the sound sequence dominated over aesthetic aspects for the practical use of AF in the daily routine of on-water training sessions due to a direct and valid (pure) mapping of the inherent information. The presentation of AF was preferred using loudspeaker in order to perceive the natural soundscape of rowing in addition to, but not in isolation from, sounds athletes were used to hearing during rowing.

Discussion and Conclusion

Sofirow provides a differentiated acoustic mapping of a_{boat} trace with its characteristics in rowing and offers the possibility for transmitting the sound sequence as AF online (synchronized with the movement) to athletes and coaches. Besides that, it is possible to analyze the acceleration curve intra-cyclically by the use of software applications (*Regatta*) and subsequently to reveal by an investigation of the effects of AF. The sound sequence represented the rhythmical processing of a_{boat} trace distinctly and audibly. The a_{boat} trace is defined as a complex parameter with the combined effect of all internal and external forces acting on the system (boat and athletes), or, more specifically, as the reflection of overall effects of active forces as well as athletes' movements [0]. With that, different intensity steps (sr) and boat categories (big and small boats as well as sweep-oar rowing and sculling) show differing profiles of a_{boat} traces and so, differing acoustic profiles. That contributes to previous research in rowing biomechanics [0], [0] and complements the existing visual analysis of the rowing technique [0] for the audible domain.

Using the training-system *Sofirow* in on-water rowing training demonstrated the possibility for AF to affect mean v_{boat} as well as the a_{boat} trace intra-cyclically within a single stroke as well as a the stroke series. As hitherto assumed, interdependency existed as a result of an improved synchronization of the crew to explain the extension of the recovery phase in the section of

positive a_{boat} as well as the reduction of the intervals "1" and "2" in Figure 3. This effect resulted in a reduced time period in which the boat was decelerated, or in other words, the total area below the curve was smaller. Finally, v_{boat} increased which is commonly defined as the main goal in rowing races and on-water training by minimizing intra-cyclic variability [0]. But results showed also higher absolute amplitudes in a_{boat} (positively and negatively) during the section with AF. This was interpreted as an increased reaction to AF. To what extend the athletes' pulling force increased in addition, was not investigated in the present study, but should be addressed in future investigations. However, AF supported the feeling for synchronization and improved the coordination among the crew as an interpersonal rhythm. In the mid and big boat categories this yielded a common team rhythm which characteristically has compulsive and intoxicative effects.

The sound sequence provided enabled the athletes to receive information of movement patterns independently from their vision. In doing so, the presentation supported their perception of the boat run and thus, facilitated and improved its control. As a function of a_{boat} trace, AF was generated directly resulting from the motion of the whole system of boat and athletes, whose movements occurred in the minimum of time that is necessary for neuronal information acquisition and processing [0]. Online presentation of AF allowed the control of movement execution time-uncritical. Because of the direct coupling of tone pitch to changes in the a_{boat} trace, the content of information in the measured data became intelligible for the athletes, directly and intuitively.

With *Sofirow*, a training system is available that supports the control of the a_{boat} trace with a feedback signal provided through the sense of hearing in addition to existing sensory channels as well as to existing feedback systems. As a new approach it opens further possibilities for rhythmical training, a systematic control of BM in on-water technique training as well as for an acoustical training of specific race phases (start and/or 2000-m-race profile). Captured sonified data of the a_{boat} trace are stored as audio files (wav. format) and are available for a mental preparation for training session and/or competitions. Moreover, it offers acoustical comparisons of training sessions and race phases (such as the start phase for example).

In further studies, the questions that still remain open are to be clarified in terms of the practicability of AF in principle for control as well as for retention of information (number of training sessions, time structure as well as frequency of using AF) in on-water training sessions with and without AF for learning processes.

Acknowledgements

We would first like to thank the coaches and athletes of the German junior national rowing team and the German Rowing Association (DRV) for their cooperation. Many thanks as well go to the engineers of BeSB GmbH Berlin for developing the training and AF-system *Sofirow* and their technical support. Special thanks go to the German Federal Institute of Sport Science (BISp) for supporting the research project financially (IIA1-070802/09). We also want to thank Bruce Grainger for critically proof reading the manuscript.

References

Bachev, V., Tsvetkov, A. & Boichev, K. (1989). System for biomechanical study and simultaneous improving of the rowing cycle. In Tsarouchas, L., Terauds, J., Gowitzke, B.A. & Holt, L.E. (Eds.). Biomechanics in Sports V: Proc 5th Int. Symposium of Biomechanics in Sports, 245-255.

Mattes, K. & Böhmert, W. (1995). Biomechanisch gestütztes Feedbacktraining im Rennboot mit dem „Processor Coach System-3“ (PCS-3) [Biomechanically aided Feedback Training in the Racing Boat with the „Processor Coach System-3“ (PCS-3)]. In Krug, J. & Minow, H.-J.(Eds.), Sportliche Leistung und Techniktraining [Athletic Achievement and Technique Training]. St Augustin: Academia, 283-286.

Hermann, T. (2008). Taxonomy and Definitions for Sonification and Auditory Display. In Proc. 14th Int. Conference on Auditory Display (ICAD), Paris, France.

Mattes, K. & Schaffert N. (2010). A new measuring and on-water coaching device for rowing. *Journal of Human Sport and Exercise*; *5*(2), 226-239.

Accrow System. Retrieved June 1, 2011, from http://www.accrow.com.

Garland, S. (2005). An analysis of the pacing strategy adopted by elite competitors in 2000 m rowing. *Br J Sports Med*, *39*(1), 39-42.

Kleshnev V. (2010). Boat acceleration, temporal structure of the stroke cycle, and effectiveness in rowing. *J Sports Eng & Technol*, *224*(1), 63-74.

Nolte, V. (2011). (Ed.) Rowing faster. Serious Training for serious rowers. 2nd edition. Human Kinetics.

Baudouin, A. & Hawkins, D. (2004). Investigation of biomechanical factors affecting rowing performance. *J Biomech; 37*(7), 969-76.

Noth, J. (1991). Neurophysiological aspects of training of sport skills. In Daugs, R., Mechling, H., Blischke, K. & Olivier, N. (Eds.). Sportmotorisches Lernen und Techniktraining [Sport Motor-Driven Learning and Technique Training] (part 1). Schorndorf Hofmann, 184-190.

Net-Based Game Analysis by Means of the Software Tool *SOCCER*

Jürgen Perl[1] *& Daniel Memmert*[2]

[1]*D-55124 Mainz, Germany*

[2]*D-50933 German Sport University Cologne, Germany*

Abstract

Game analysis has become much easier by automatic position recording. However, the problem remains how to transfer the astronomic amount of available data to a selection of useful information. Our approach is based on two ideas: Data reduction and pattern recognition. In the first step, by means of SOCCER, the position data of the players of a team are reduced to those of tactical groups like offense or defence, followed by normalization, where the players' constellations on the playground are reduced to their geometric formations relative to their centroids – i.e. the playground-independent position patterns. In the second step, those patterns are learned by the self-organizing neural network DyCoN, resulting in a collection of formation clusters, each containing a variety of shapes of the corresponding formation type. Based on that information, game analysis with DyCoN and SOCCER works as follows: Along the time-axis, position data of interacting tactical groups are fed to the net, which recognizes the time-dependent corresponding formation types. A first quantitative analysis then results in frequency distributions of formation types. Recombination with the playground position information leads to a playground specific frequency distribution. And adding the time information finally allows for process and interaction oriented analyses. Moreover, SOCCER not only offers quantitative results but also qualitative ones like game animation and tactical analyses by use of additional semantic action valuation.

KEYWORDS: PATTERN ANALYSIS, FORMATION, STATISTICS, TRAJECTORY

Introduction

In the following, first results from a project are reported, which deals with net-based game analysis in soccer. The project is supported by the German Research Foundation (DFG, Project-No. ME 2678/3-2). Additional information is given in Perl (2008), Grunz, Memmert & Perl (2009), Memmert & Perl (2009-1, 2009-2) Grunz, Endler, Memmert & Perl (2011).

In the beginning of computer aided game analysis, about 35 years ago, interesting ideas were developed but could not got to work because of a lack of available data. Meanwhile, data acquisition has become much easier due to automatic position recording. The problem is to transfer the astronomic amount of available data to a selection of useful information.

Our approach is based on two ideas: Data reduction and pattern recognition.

(*Developed and © by Jürgen Perl, Mainz, Germany.)

The process is starting with position data preparation and pre-processing, which is done by means of the software tool *SOCCER*[*], followed by three steps of analyses:

In the first step, *SOCCER* reduces the position data of the players of a team to those of tactical groups like offense or defence, followed by normalization, where the players' constellations on the playground are reduced to their geometric formations relative to their centroids – i.e. the playground-independent position patterns.

In the second step, those patterns are learned by the self-organizing neural network *DyCoN*[*], resulting in a collection of formation clusters, each containing a variety of shapes of the corresponding formation type.

Based on that information, game analysis with *DyCoN* and *SOCCER* works as follows:

Along the time-axis, position data of interacting tactical groups are fed to the net, which recognizes the time-dependent corresponding formation types.

A first quantitative analysis then results in frequency distributions of formation types. Recombination with the playground position information leads to a playground specific frequency distribution. And adding the time information finally allows for process and interaction oriented analyses.

Also qualitative analyses like semantic valuation and animation of game processes are supported by *SOCCER*.

In the third step, the trajectory analysis component of *DyCoN* enables tactical analyses of the game, including interaction and phase analyses. This way, in particular long term interaction patterns as well as hidden or creative tactical activities can be recognized and analyzed regarding success.

SOCCER-Based Data Reduction

In the first processing step the position data are transformed into pieces of information that can be used for statistic, pattern and tactic analyses.

The main idea is to transform constellations of players into a pair of normalized formations and corresponding positions on the playground: As is shown in Figure 1, the position data of a group build time-dependent constellations, which can be departed into its position (i.e. centroid of the constellation) and its characteristic formation (i.e. the normalization of the constellation relative to its centroid).

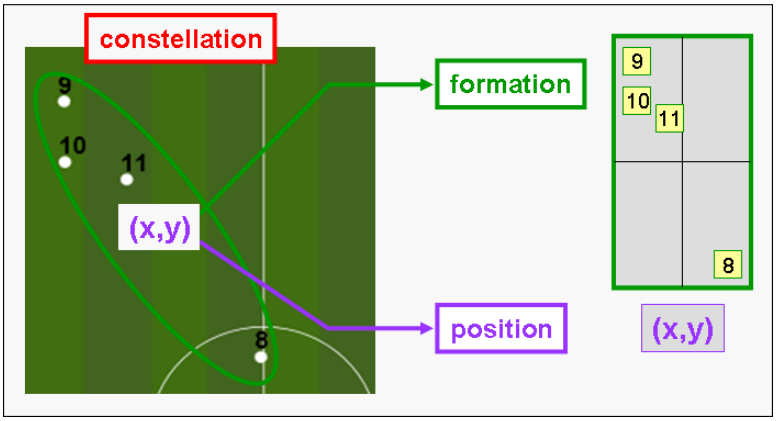

Figure 1. Departing a constellation into its position (centroid) and its characteristic formation.

To this purpose, SOCCER offers an interface for loading players' position data and selecting interesting tactical groups for normalization (see Figure 2). The normalized data are transferred to a file or a database.

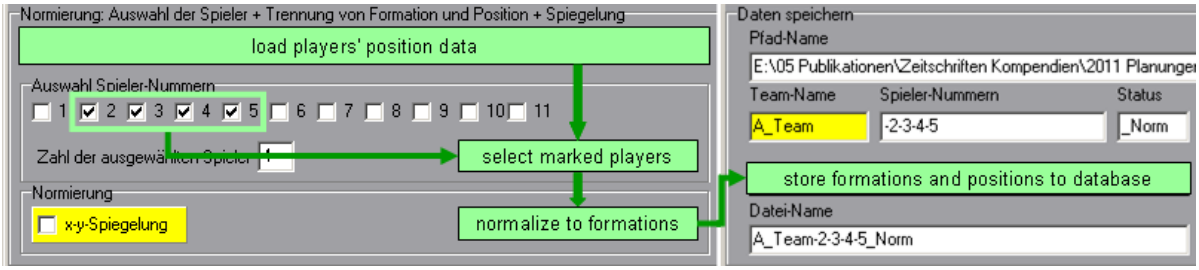

Figure 2. *SOCCER* data pre-processing interface.

Obviously, the number of characteristic formations (about 10) is much less than that of possible constellation (about 5400 per half-time). Therefore this reduction allows a much better pattern analysis of tactical group behaviour without loss of information, because the real game process can be reconstructed using the stored time-series of positions.

DyCoN-Based Pattern Analysis

By means of the self-organizing neural network *DyCoN*, the different types of formations are recognized and grouped into clusters, which in Figure 3 are presented using different colours. Within each type-representing cluster the different neurons (coloured small squares) represent different shapes of the corresponding type, as is exemplarily shown by 4 shapes of the defence formation "line".

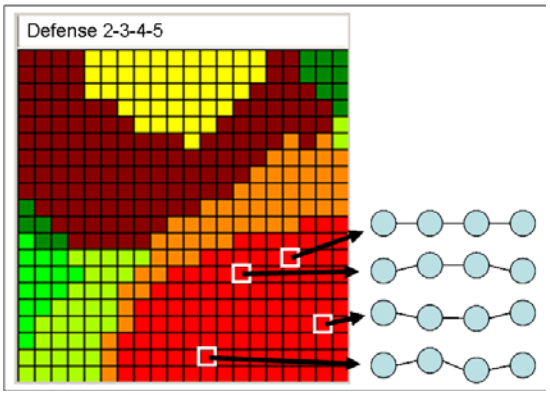

Figure 3. Trained DyCoN showing coloured clusters of formations, the neurons of which represent different shapes of the corresponding formation type.

If formation data are input to the trained net, the type (and the particular shape) is recognized by the net and now can be re-combined to the corresponding position and time data, resulting in a significantly reduced presentation of the game and its processes, nevertheless preserving all important information.

Those time-series of formation types and positions allow for a lot of analyses from space- or time-oriented distributions over success in interactions up to tactical aspects process of phases.

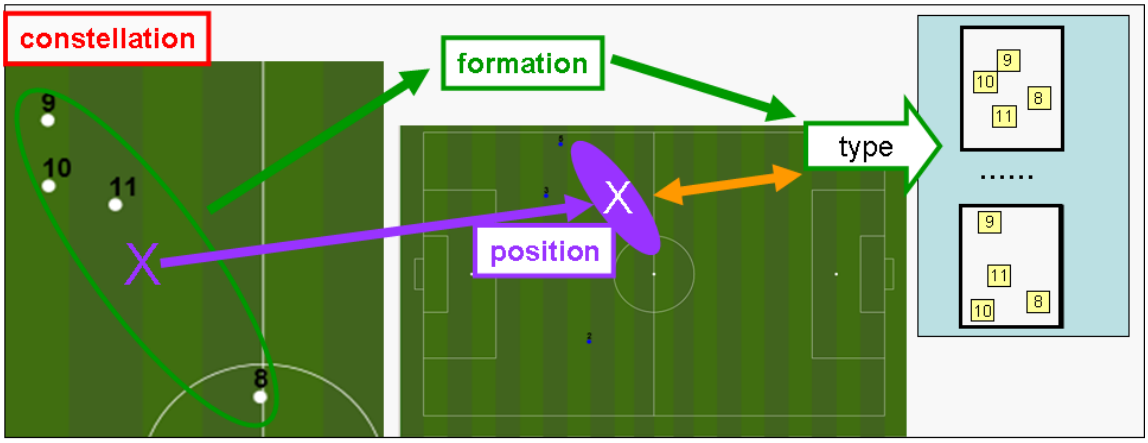

Figure 4. Net-based recognition of formation types and re-combination with position and time information.

The condensed game information from above can be used for generating a game protocol like presented in Figure 5, where time, formation type and position is completed by a manual semantic valuation.

time	type	position	action / result
…			
HT1 34:15	7	(45,23)	pass / successful
…			

Figure 5. Automatically generated game protocol manually completed by semantic valuations (yellow column).

Those protocol data then build the basis for the actual game analysis, as will be discussed in the following.

SOCCER-based Game Analysis

Game analysis in the following will roughly be distinct into three phases: Distribution analysis deals with space- and time-specific frequencies of formations as well as frequencies of corresponding interactions. Process analysis is oriented in the dynamics of the game, dealing in particular with simulation and animation of processes corresponding to formations. Tactics analysis deals with the game as a whole in order to recognize specific group behaviour and success of interaction processes.

Distribution Analyses

The distribution analysis presented in Figure 6 demonstrates a typical situation: Team A attacks in the formation of type 4, team B reacts with a defence formation of type 3. The distribution matrix shows that this particular interaction happened 523 times (i.e. at 523 seconds) in the regarding half-time.

In general, the matrix provides the distributions of formations of the teams as well as those of the respective interactions.

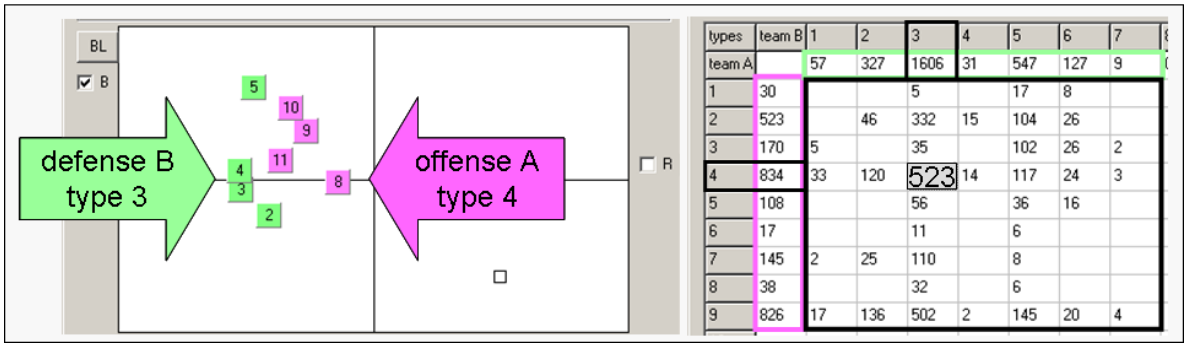

types	team B	1	2	3	4	5	6	7
team A		57	327	1606	31	547	127	9
1	30			5		17	8	
2	523		46	332	15	104	26	
3	170	5		35		102	26	2
4	834	33	120	523	14	117	24	3
5	108			56		36	16	
6	17			11		6		
7	145	2	25	110		8		
8	38			32		6		
9	826	17	136	502	2	145	20	4

Figure 6. Distribution matrix of formation types and interactions.

The distribution matrix of *SOCCER* is interactive – i.e. clicking one of the entries shows the distribution of the corresponding events on the grids of the playground (which can be arranged arbitrarily). Figure 7 shows how the 132 interactions 'defence type 3 vs. offense type 1' (green highlight) are distributed on the playground. Clicking one of the grid fields (blue highlight) shows the distribution of the remaining entries in that area.

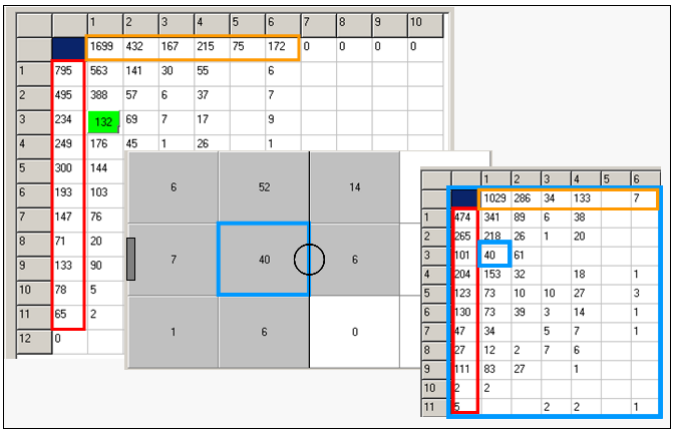

Figure 7. Interactive presentation shows distributions of formation interactions.

Statistical analysis is helpful for a first recognition of normal and of seldom or striking situations. In order to recognize the role they play in the game process, statistical analysis can be combined with animated process analysis:

Process Analysis

Clicking one of the entries of the distribution matrix also shows a list of all processes where that interaction took part. In Figure 8 the clicked interaction (green highlight) activates a list of 14 processes, the 8th of which took part in minute 23 from second 1374 to 1384 (violet highlight). Also this sequence can be activated resulting in an animation of the motion of the teams' centroids on the ground.

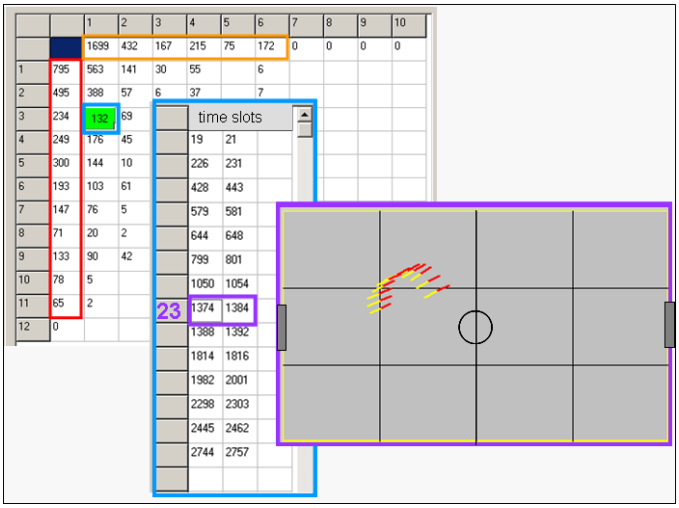

Figure 8. Interactive presentation: Number of interactions (green highlight) → list of processes with selected process (violet highlight) → sequence of teams' centroids.

Combined Quantitative and Qualitative Analysis

As has been mentioned above (see Figure 5), the formation data can be completed by semantic ones like technical or tactical aspects and success. In the following two examples demonstrate the valuation of success by means of *SOCCER*:

In the first example the success of a single player, depending on his tactical position and his action in the context of the current formation, is valuated. In Figure 9 the blue highlights mark the selected team (ITA), player (number 10) and formation (number 2, which is shown in the left most graphic together with the moving direction) as well as the selected action (number 6 of 13) and the selected tactical position (number 9 of 9). The graphic on the right hand side shows that there were 27 events in that situation, 24 of which were successful.

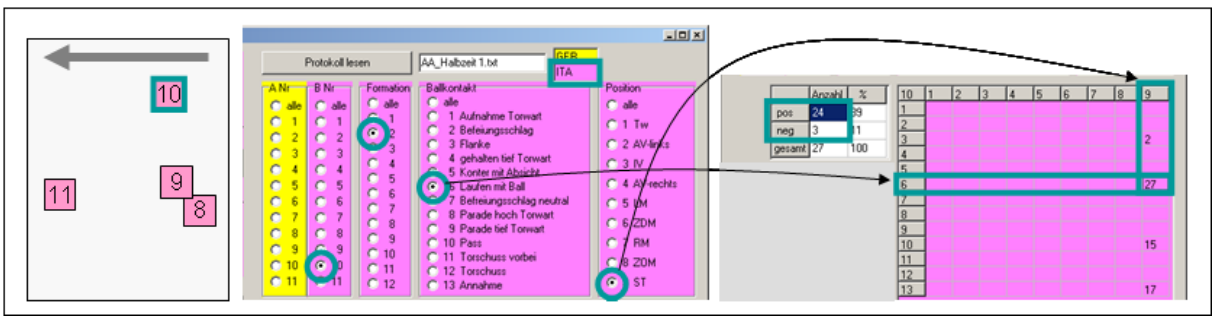

Figure 9. Tables for selecting team, formation, player, tactical position, and action with resulting information about player's success.

The second example deals with valuating the success of the team in a given formation interaction. Figure 10 shows from left to right the number of valuated interactions of a team, followed by the negative ones in absolute numbers and as percentages. Concentrating on the right graphic it seems that team A has serious problem in the interaction of formation 3 vs. formation 3. However, the absolute numbers are very small, reducing the importance significantly. Also '5 vs. 5' is negative but does not seem very important, while '5 vs. 2' seems to be a significant weakness, although the percentage of negative results is only 16.

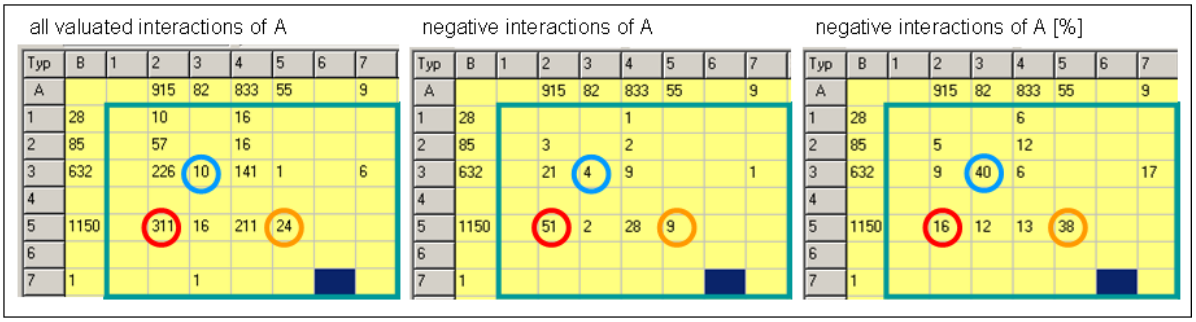

Typ	B	1	2	3	4	5	6	7
A			915	82	833	55		9
1	28		10		16			
2	85		57		16			
3	632		226	10	141	1		6
4								
5	1150		311	16	211	24		
6								
7	1			1				

Typ	B	1	2	3	4	5	6	7
A			915	82	833	55		9
1	28				1			
2	85		3		2			
3	632		21	4	9			1
4								
5	1150		51	2	28	9		
6								
7	1							

Typ	B	1	2	3	4	5	6	7
A			915	82	833	55		9
1	28				6			
2	85		5		12			
3	632		9	40	6			17
4								
5	1150		16	12	13	38		
6								
7	1							

Figure 10: Matrices of valuated team success in the context of formation interaction.

Note, that the presented kinds of analysis are just examples, which can arbitrarily be completed if the valuation data are once available.

Net-based Tactics Analysis

A last kind of analysis that is provided by *SOCCER* is the net-based trajectory analysis. The idea is that at each point in time the formations of tactical groups are identified and therefore can be encoded by a corresponding number respectively colour. In Figure 11 the net has identified 10 offense formations, which are coloured from violet (1) to dark grey (10). In the left graphics it is shown, how team A and team B change their formations during the 60 seconds of the 16th minute – i.e. the process trajectories of teams A and B in minute 16. In the same way the trajectories can be shown for the whole game or, as has been done in Figure 11, for a particularly interesting part of one half-time (here minute 15 to 30): The selected part shows that the trajectory behaviours of A and B are quite different, possibly reflecting different tactical concepts.

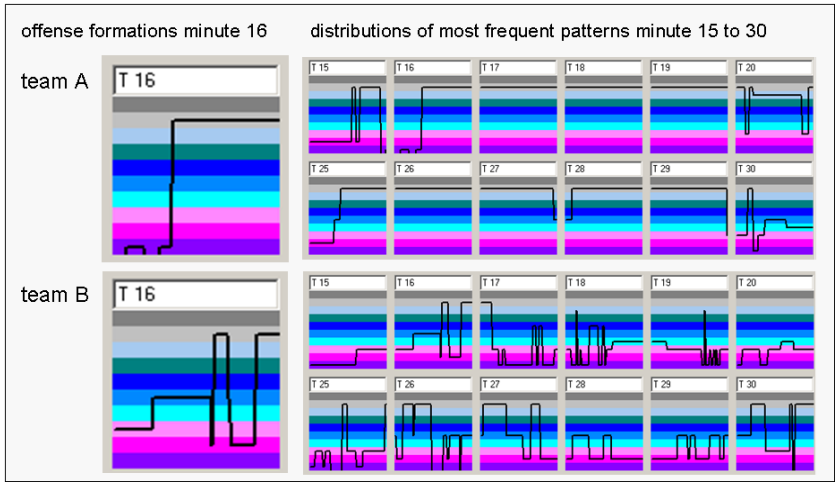

Figure 11. Process trajectories based on the time-series of formation types.

If and how much such trajectories really tell about tactics obviously depends on the tactical quality of the teams and has to be judged by experts like trainers.

Conclusion and Outlook

The aim of the distribution was to demonstrate what kinds of game analyses are possible if combining net-based pattern analysis with conventional statistic methods, as is symbolized in Figure 12:

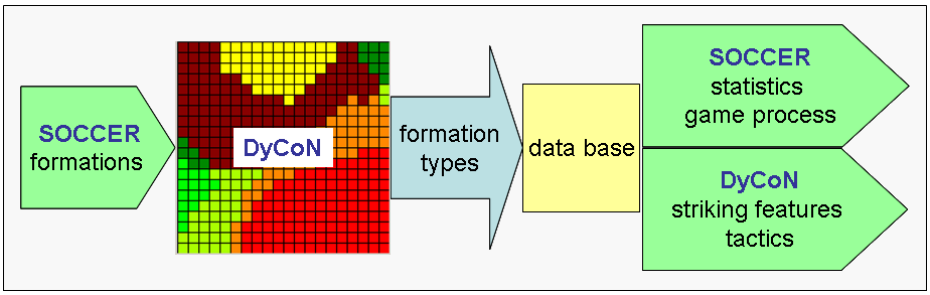

Figure 12. The concept of SOCCER: Combining net-based pattern recognition with statistical methods.

The results are encouraging and promise to be helpful in order to run successfully the above mentioned project as well as in getting new ideas and results for further and improved game analysis approaches.

References

Perl, J. (2008). Modelling. In P. Dabnichki & A. Baca (Eds.), Computers in Sport (pp. 121–160). Wit Press.

Grunz A., Memmert D. & Perl J. (2009). Analysis and Simulation of Actions in Games by Means of Special Self-Organizing Maps. In International Journal of Computer Science in Sport, *8*(1), 22-37.

Memmert, D. & Perl, J. (2009-1). Game Creativity Analysis by Means of Neural Networks. Journal of Sport Science, *27*, 139–149.

Memmert, D. & Perl, J. (2009-2). Analysis and simulation of creativity learning by means of artificial neural networks. *Human Movement Science*, *28*, 263-282.

Grunz, A., Endler, S. Memmert, D. & Perl, J. (to appear 2011). Netz-gestützte Konstellations-Analyse im Fußball [Net-based constellation analysis in soccer]. Darmstadt, Workshop on Computer Science in Sport 2010.

PerPot DoMo: Antagonistic Meta-Model Processing two Concurrent Load Flows

Jürgen Perl[1] *& Mark Pfeiffer*[2]

[1]*D-55124 Mainz, Germany*

[2]*Technical University of Munich, D-55099 Mainz, Germany*

Abstract

The antagonistic meta-model PerPot has been developed in order to simulate the interaction of load and performance in physiologic processes – which has been done successfully in a lot of applications. There are, however, a lot of cases where neither the restriction to just one type of load nor the transformation of two or more load flows to one abstract substitute represents practice satisfyingly. Two very well-known examples are given by the load pairs [speed and slope] in case of running and [volume and intensity] in case of long term training.In order to meet those demands the PerPot concept has been extended to PerPot DoMo, the concept and the tool of which are briefly introduced, followed by some first results of how it works. Although the model approach seems to be rather simple, it turns out that the simu-lation quality is surprisingly high and allows good predictions in short term as well as in long term activities.

KEYWORDS: LOAD, PERFORMANCE, FATIGUE, RECOVERY, DELAY, SIMULATION

Introduction

The basic methodical concept of PerPot is that of reducing complexity. In the case of training load effects, antagonism seems to be the central aspects, where fatigue and recovery are triggered by the same input, together resulting in a change of performance. In order to deal with two load flows effecting one common performance potential the PerPot concept has been extended without changing that basic methodical idea of most possible simplicity.

The results are encouraging. They show that the effect of even quite different types of load can be simulated and used for long time training scheduling.

PerPot DoMo: The concept

PerPot DoMo is based on PerPot, where "DoMo" means "***Do***uble ***Mo***del", reflecting the approach of combining two exemplars of PerPot to one new model, which is able to process two concurrent load flows.

PerPot basics

As is presented in Perl (2008-2), the meta-model PerPot describes physiological adaptation on an abstract level as an antagonistic process, as is shown in Figure 1: A load input flow is

feeding identically a strain potential as well as a response potential. From the response potential the performance potential is increased by a positive flow, while the strain potential reduces it by a negative flow. All flows show specific delays modelling the time that components of the modelled system need to react.

Additional components and effects like overflow, reserve and atrophy are described in detail in Perl (2005), (2008-1) and (2008-2).

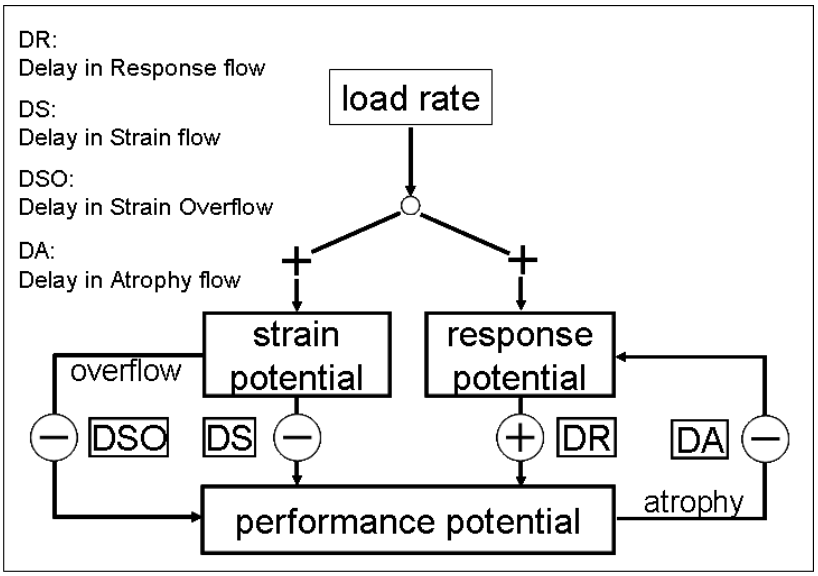

Figure 1. Basic PerPot structure with flows and delays.

One main goal of such a model is to predict future performance development in order to optimize current load management. Figure 2 demonstrates the corresponding two phases of model use: In the calibration phase the model is adjusted to the athlete by estimating the model parameters like delays, starting values, or base load. In the prediction phase those parameters are used for simulation, where the performance development is calculated depending on a given load profile. In particular in order to check simulation precision, such a simulation can be done compared to given original performance values, as has been done in Figure 2.

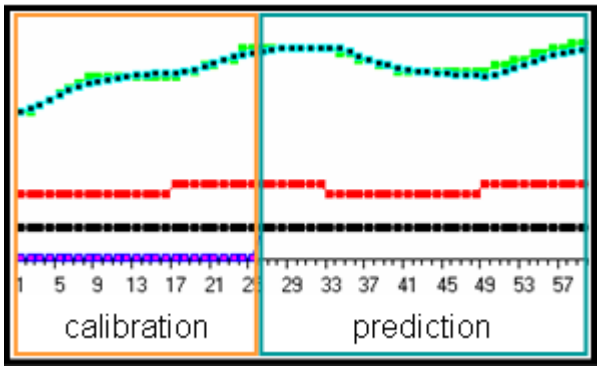

Figure 2. Simulation with calibration phase (violet area) and prediction phase, load profile (red), original performance (green), and simulated performance (blue).

So far, PerPot works really satisfying – as long as the number of load flows is restricted to just one (see Perl & Endler (2006), Pfeiffer (2008), Pfeiffer & Perl (2009), Perl (2010)). Very often, however, in reality there are more than one concurrent load inputs like for example

biking, running and swimming load in triathlon or volume and intensity in general. First ideas in this direction led to a so-called matrix model, which distributes n types of load to m types of performance – and is much to complex for practical use.

A much simpler idea, which however covers a lot of major problems, is to model the effect of two concurrent load flows on just one common performance output:

PerPot DoMo extension

In addition to a usual PerPot a parallel second PerPot component is simulating the effect of the second load flow. The performance values of both models are combined to the final performance output of PerPot DoMo.

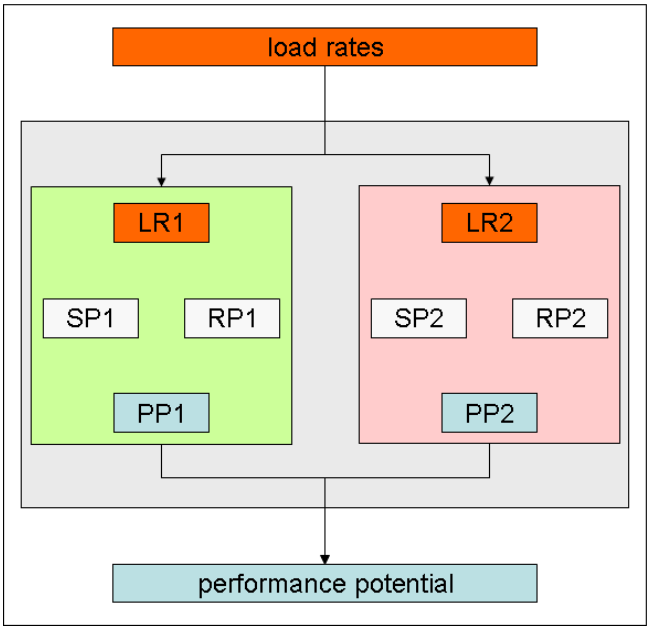

Figure 3. PerPot DoMo with two PerPot components (light green and light red), two load inputs and one performance output.

Although this approach looks quite simple (and in fact is), the problems lie in detail, in particular in estimating the appropriate parameters of the concurrent dynamics. I.e. calibration becomes a serious problem. In order to support model development as well as original data analyses, a special software tool has been developed which briefly is presented in the following section.

PerPot DoMo Tool

Besides others, the PerPot Domo Tool offers the following functionality (compare the marked areas in Figure 4):

- Selection of the profiles to be presented (A)
- Selection of the profile to be manipulated manually (B)
- Profile modification by linear transformation (C)
- Monitoring (D)
- Selection of the time ranges for calibration, simulation, and deviation measuring (E)

Figure 4. User interface of the PerPot DoMo Tool with marked areas, which are explained in the text. The colours of the curves in the graphic window identify the different time series: Red: load 1, brown: load 2, green: original performance, blue: simulated performance.

In particular, the scroll bars below the graphic window of the interface allow for departing the calibration time range from the simulation and the deviation measuring time ranges, which enables simulated or original prediction (also see Figure 2): The original data range from time unit 1 to 159 (the position of the monitor window). The data from the first 84 time units are used for calibration: The resulting parameters are used for the simulated prediction of the already known performance values, which are simulated with a deviation of 4.14%. An original prediction is calculated from unit 160 to unit 300, where manually added load profiles generate a simulated performance profile based on the calibration parameters.

First results

In a first step, the model was checked by means of simulated validation – i.e. generated load profiles together with given model parameters were used to simulate performance profiles. Generated load and simulated performance then were input to the calibration to measure the precision of parameter estimation and performance approximation.

In a second step, original test data were used to check prediction precision in an analogous way.

Generated data

The idea was to check how combinations of different types of load profiles influence the

performance and how precise can calibration and simulation work. Figure 5 shows a collection of 4 examples, each measured including and excluding the starting area. As expected, it turns out that a combination with constant load (test 2) or stochastic noise load (test 4) can be analyzed most precisely, while off-phase overlays (test 1) or overlays with quite different oscillation frequencies (test 3) show slightly lower precision.

To sum up, calibration with estimating parameters and approximating performance worked satisfyingly with generated data.

Moreover, the balancing out process during the starting phase almost always causes high deviations without giving significant information about the overall precision. Neglecting this phase normally results in much lower deviation values.

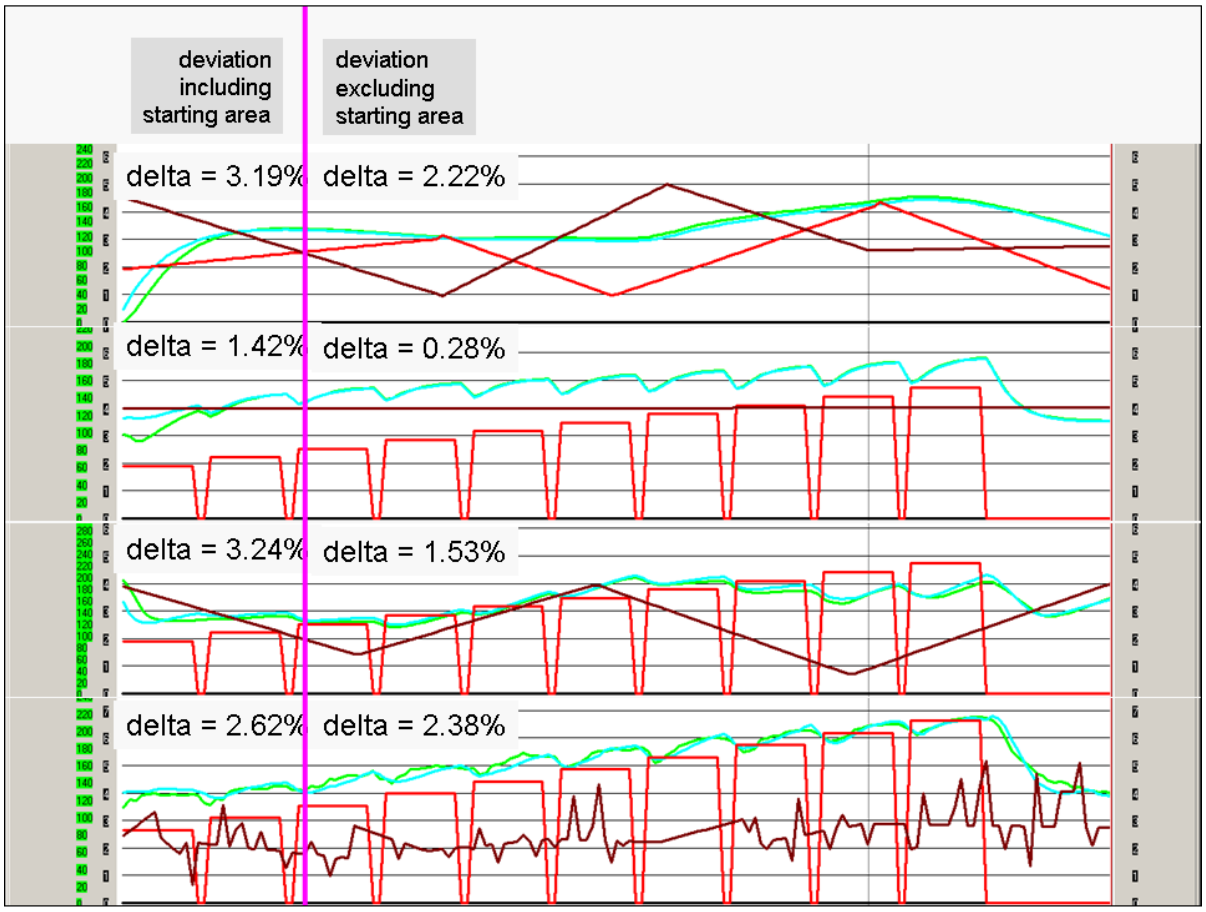

Figure 5. Four tests with given parameters, generated load profiles (red and brown) and simulated performance (green) together with a calibration-based performance approximation (blue). Deviation values are measured including (left) and excluding (right) the starting area of balancing out processes.

These results were encouraging to run tests with original data, which also worked satisfyingly and will be demonstrated by one exemplary case study from swimming.

Original test data

The data exemplarily used here stem from training units of a top swimmer. Figure 6 in the upper graphic shows the original values, where the red curve means load-*volume*, the brown one means load-*intensity* and the green one means performance, measured by a special swim test (semi-tethered incremental test). The time unit is "day", the time range of the test is 128

days.

Although there was a serious gap without any performance data available, the calibration worked comparably well and resulted in a simulated performance profile (blue curve) with a deviation of only 5.90 %.

Corresponding to the test from Figures 2 an 4, the test now was departed in three areas: The first area, ranging from unit 1 to unit 89 was used for a reduced calibration (yellow box in the lower graphic of Figure 6), the results of which where used for a simulated prediction in the second area (blue box) with a surprisingly good result of only 4.49 % deviation. Finally, in addition to the original data, the third area (violet box) was provided with generated load data, on which a performance profile was predicted by simulation (blue curve).

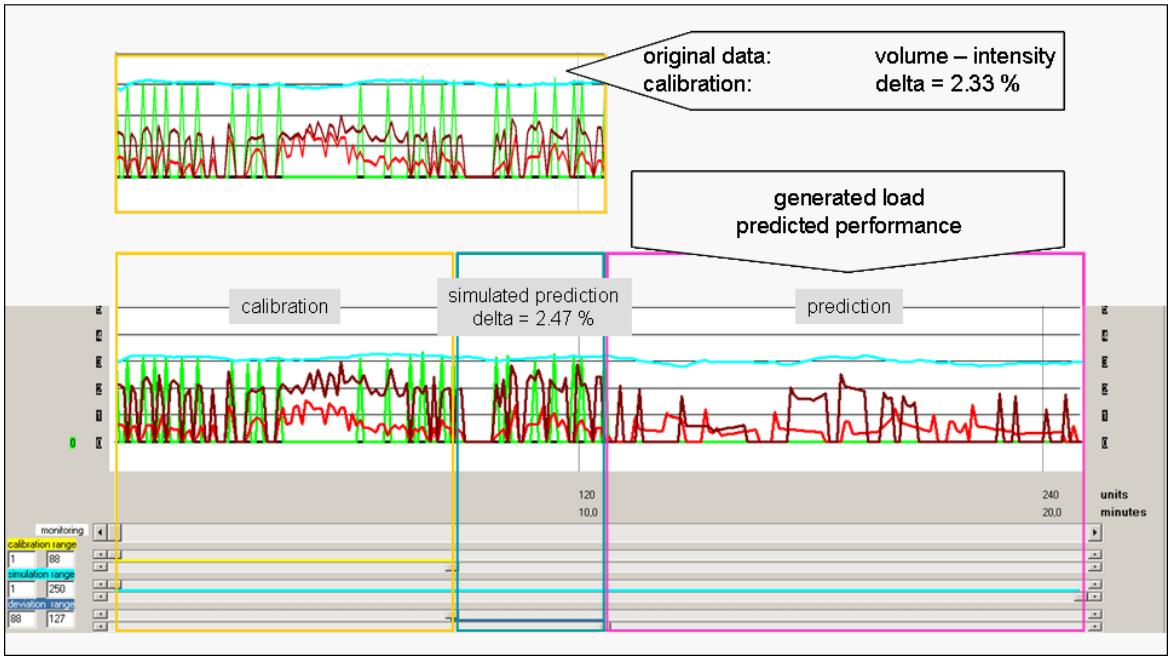

Figure 6. Original data calibration (upper graphic) and calibration-based prediction (lower graphic).

Of course, one cannot say how good such a prediction is before checking it in practice (which is the reason for the approach of simulated validation from above). However, it can at least be checked, how consistent such a prediction is by means of cross-checking with a second calibration. This means that the generated load profiles together with the predicted performance profile are input to a calibration, which then produces a simulated performance profile. At least, the predicted and the newly simulated performance profile should be rather similar.

The result can be taken from Figure 7: The new calibration changes the internal parameters a little bit, which can be seen from minimal differences of the corresponding load values, caused by the modified relation between load 1 and 2 in the prediction area compared to the area of original data.

Independent of this problem it seems to be a surprisingly good result that the deviation of 1,21 % between prediction (lower graphic, green curve) and new simulation (blue curve) is even significantly smaller than that of the original calibration (see Figure 6).

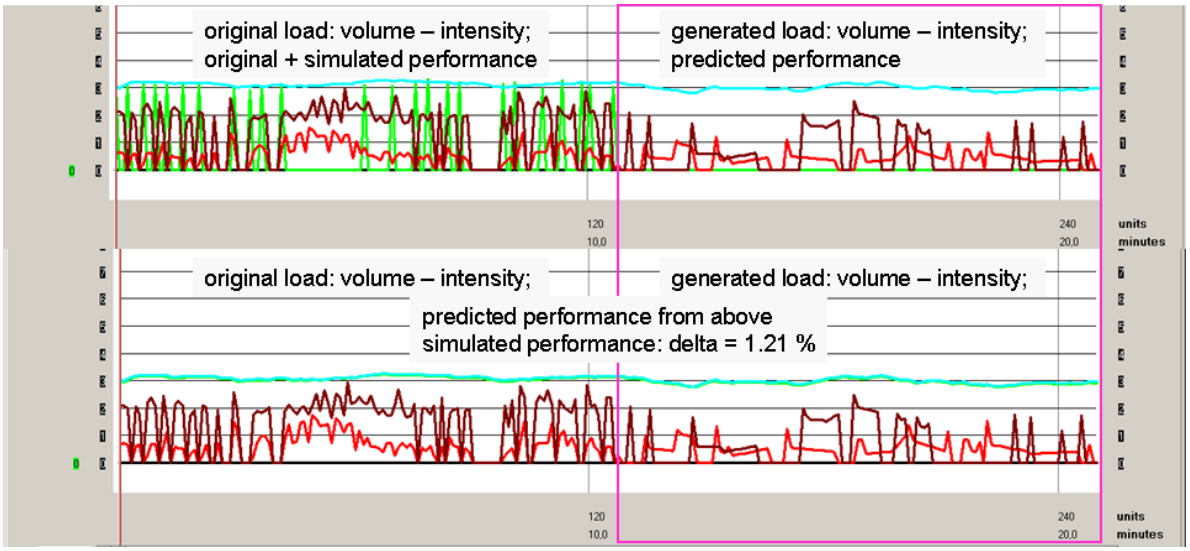

Figure 7. Simulated and predicted performance compared to the result of a prediction check: Upper graphic: predicted performance (blue curve); lower graphic: predicted performance as original data (green curve) compared to simulated performance (blue curve).Note that because of the extremely small deviation the green and the blue curve are rather difficult to distinct.

Finally, a last minute result demonstrates that even types of load which are not actually physiological ones, can be used. The following example combines the speed load profile with the incline profile of the road, the results of which can be seen in Figure 8, where the deviation of the simulated heart rate profile is only 1.88 % - despite the fact that inclines (brown curve) and speed (red curve) are sometimes in-phase and sometimes anti-phase.

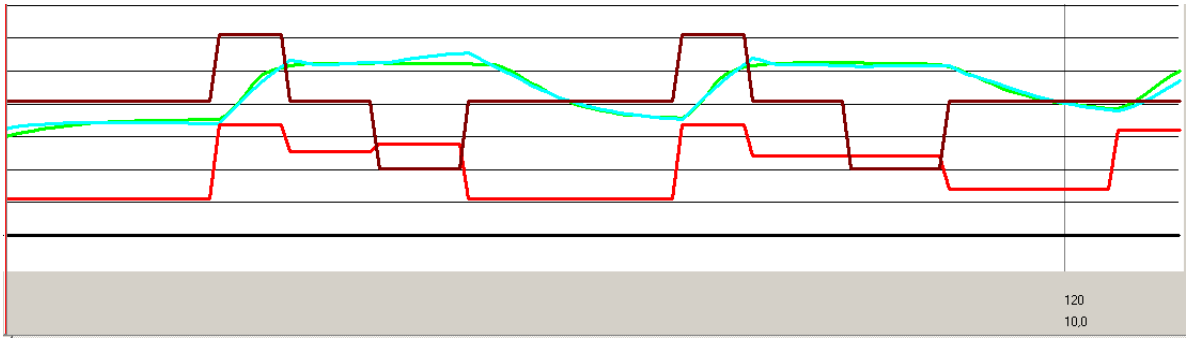

Figure 8: Speed (red) and incline (brown) profiles driving heart rate (original values: green; simulated values: blue).

It seems that the last result opens new ways of predicting the effect of load considering contextual conditions like road profile or weather as well.

Conclusion and Outlook

The results show that the double load model works with acceptable precision. Improved data preparation as well as model tuning are necessary to avoid systematic problems like missing or badly sized data. In particular it turned out that types of load like intensity might be too

abstract for the introduced model-based handling – i.e. volume and intensity could miss the necessary semantic symmetry to be handled with a symmetric model like PerPot DoMo.

Therefore a next step of model development could be to better map the load types to specifically corresponding model components. A first concept of a special Volume-Intensity-Model is currently being designed.

References

Perl, J. (2004). PerPot – a meta-model and software tool for analysis and optimisation of load-performance-interaction. In *International Journal of Performance Analysis of Sport*, *4*(2), 61-73.

Perl, J. (2005). Dynamic Simulation of Performance Development: Prediction and Optimal Scheduling. In International Journal of Computer Science in Sport, *4*(2), 28-37.

Perl, J. & Endler, S. (2006). Training- and Contest-Scheduling in Endurance Sports by Means of Course Profiles and PerPot-Based Analysis. In *International Journal of Computer Science in Sport*, *5*(2), 42-46.

Perl, J. (2008-1). Modelling. In P. Dabnichki & A. Baca (Eds.), Computers in Sport (pp.121-160). Wit Press.

Perl, J. (2008-2). Physiologic Adaptation by Means of Antagonistic Dynamics. In M. Khosrow-Pour (Ed.), Encyclopaedia of Information Science and Technology (2nd ed.), VI, 3086-3092.

Pfeiffer, M. (2008). Modeling the Relationship between Training and Performance - A Comparison of Two Antagonistic Concepts. In *International Journal of Computer Science in Sport*, *7*(2), 13-32.

Pfeiffer, M. & Perl, J. (2009). Simulative Trainingswirkungsanalyse bei einem Fahrradergometertraining mittels antagonistischer Modelle [Simulative training effect analysis in ergometer biking by means of antagonistic models]. In Lames, Augste, Cordes, Dreckmann, Görsdorf & Siegle (Eds.), Schriften der Deutschen Vereinigung für Sportwissenschaft [Scripts of the German Association of Sport Science], Part 189, 41-51.

Perl, J. (2010). Trainingswirkungsanalyse: Planung und Optimierung mithilfe des antagonistischen Metamodells PerPot [Training Effect Analysis: Scheduling and Optimization by means of the Antagonistic Meta-Model PerPot]. Zeitschrift für Angewandte Trainingswissenschaft [Journal of Applied Training Science], 2/09, 117-127.

Endler, S. & Perl, J. (to appear 2011). Leistungsoptimierung beim Marathon mit sportinformatischen Modellen [Performance Optimization in Marathon by means of Models from Computer Science in Sport]. Darmstadt, Workshop on Computer Science in Sport, 2010.

Letter to the Editor

Perspectives on Exergaming

Robin R. Mellecker[1], Richard Coshott[2]

[1] Institute of Human Performance, University of Hong Kong, Pokfulam, Hong Kong, SAR China

[2] Gamercize, Southampton, United Kingdom

Exergaming, or active gaming, is a concept of combining video games and exercise and the advancement in this innovative technology has given rise to a unique industry sector, which requires a multi-disciplinary approach between the fitness and video game industry. The sector has quickly become the fastest growing and most popular segment of the games for health market. The relationship between the video game and fitness industry appear to be unlikely partners in this collaboration but this growing sector is estimated to be worth US$6.4 billion (Doner A, Goldstein D, & Loughran J, 2008). The companies, organizations and individuals that make up the industry originate, in the most part, from either the video gaming or fitness industry, bringing with them their own language, ways of thinking and objectives. For these reasons, the exergaming sector contains its own inherent confusion, misrepresentation and mixed messages. The confusion within the exergaming sector is not limited internally within the two distinct industries that drive the market. Recent media reports suggest that the confusion within the industry and between experts may be impacting the dissemination of research findings and subsequently advances in the development of active games for health.

Currently, research findings are reported in disparate journals and social media is used as an information highway to convey user experiences and observations from experts in the field. Inevitably this leads to a disconnect in publications, mixed messages from the industry, disjointed reports in the news media and limited collaborative opportunities to build on current research findings. Sadly the information disseminated to the public is not always linked to evidence based research, systematic observations from the individuals delivering the programs or the end user. Consequently what is currently known about exergaming is misrepresented. An example of the mixed messages communicated to the public can be found by reading the media reports from a study investigating the energy expenditure of exergaming (Graves L, Stratton G, Ridgers ND, & NT, 2007). Most recently, two distinctly different conclusions on active video gaming were reported by the same news organization (BBC News, 2007a, BBC News, 2007b). One report suggested that active gaming results in “energy expenditure to a level which could help lose weight” (BBC News, 2007a) whilst the second report advised readers that participation in active gaming is “not of high enough intensity to contribute towards the daily recommended moderate and vigorous levels of exercise” (BBC News, 2007b). What may be most surprising is that these articles were written in a two month time frame. While it is easy for those with knowledge about exergaming research to distinguish the subtle difference between the two reports, the public remains misinformed and confused about the effectiveness of exergaming. Subsequently, efforts to understand the possible effects of using exergaming to improve health and attempts to improve and build evidence based research are being hampered.

Despite the confusion there is growing evidence to support the benefits associated with exergaming (Lange BS et al., 2010; Lange BS, Flynn SM, & Rizzo, 2009; Saposnik G et al., 2010, Staiano & Calvert 2011). However, evidence to support the use of exergaming technology to increase physical activity levels over the long term and subsequently decrease the diseases associated with an inactive lifestyle are scarce (Daley A, 2009; Foley L & Maddison R, 2010). When discussing the efficacy of exergaming technology in reference to tackling the obesity epidemic, Pate (2008) previously reported that although findings on energy expenditure of active gaming are important these studies provide "only a drop in the bucket of research that will be needed to learn how we can increase physical activity and reduce obesity..." and further noted that the research focus should be driven towards finding ways to "take this strategy to the population level." Surprisingly many of the questions needed to ascertain whether exergaming is viable to improve health at a population level remain unanswered.

The push to discover the effects of using exergaming on health is admirable but it is evident from current research that much more is to be learned and there may be a need to revisit the words by Pate (2008) in future efforts to investigate exergaming and the effect on health. Many interventions seem to be introduced without evidence based research to support the efficacy of the trials. Intervention studies have failed to investigate the use of exergaming long enough to determine whether play will be adhered to for a significant length of time (Foley L & Maddison R, 2010). Furthermore, it is possible that some of the evidence required to implement successful intervention strategies is available from the individuals delivering exergaming programs. Recent appeals by the World Health Organization (WHO) highlight the urgent need for international collaboration and innovative prevention and intervention strategies to halt the rapidly increasing trend in global obesity. Given the recent call for action, the economic downturn and limited financial resources it may be time to re-focus efforts in building an evidence base and expand international efforts to support innovative research to ensure that the messages conveyed are consistent and informed.

Future efforts to explore the basic principles of intervention implementation, improved communication and national and international collaborations within the exergaming community may be required to advance the development of exergaming technology, build a foundation of evidenced based research and improve the efficacy of active gaming interventions. The recent introduction of international journals dedicated to games for health research is clearly much needed and will undoubtedly be welcomed by an international audience of researchers, developers, individuals delivering exergaming programs and ultimately the end user.

References

BBC News. (2007a). Computer games 'burn up calories'. Retrieved from http://news.bbc.co.uk/1/hi/health/6376637.stm

BBC News. (2007b). Wii players need to exercise too. Retrieved from http://news.bbc.co.uk/1/hi/health/7155342.stm

Daley A. (2009). Can exergaming contribute to improving physical activity levels and health outcomes in children? *Pediatrics 124*, 763-761.

Doner A, Goldstein D, & Loughran J. (2008). Health e-Games market report: status and opportunities (pp. 57-93): Physic Ventures.

Entertainment Software Association. (2008). Essential facts about the computer and video game industry Retrieved August 18, 2011, from http://www.theesa.com/facts/pdfs/ESA_EF_2008.pdf.

Foley L, & Maddison R. (2010). Use of active video games to increase physical activity in children: A (virtual) reality? *Pediatric Exercise Science, 22*, 7-20.

Graves L, Stratton G, Ridgers ND, & NT, C. (2007). Comparison of energy expenditure in adolescents when playing new generation and sedentary computer games: cross sectional study. *BMJ, 335*, 1282-1284.

Lange BS, Flynn SM, Chang CY, Liang W, Chieng CL, Si Y, et al. (2010). Development of an interactive stepping game to reduce falls in the elderly. Paper presented at the 8th International Conference Disability, Virtual Reality & Associated Technologies Viña del Mar/Valparaíso, Chile.

Lange BS, Flynn SM, & Rizzo, A. (2009). Initial usability assessment of off-the-shelf video game consoles for clinical game-based motor rehabilitation. *Physical Therapy Reviews, 14*, 355–363.

Pate RR. (2008). Physically active video gaming an effective strategy for obesity prevention? *Archives of Pediatric and Adolescent Medicine, 162*, 895-896.

Saposnik G, Teasell R, Mamdani M, Hall J, McIlroy W, Cheung D, et al. (2010). Stroke Outcome Research Canada (SORCan) Working Group. Effectiveness of virtual reality using Wii gaming technology in stroke rehabilitation: a pilot randomized clinical trial and proof of principle. *Stroke, 41*, 1477–1484.

Staiano AE, Calvert S. (2011). Exergames for physical education courses: Physical, social, and cognitive benefits. *Child Development Perspectives, 5*, 93-98.